Summer 5-2012

Analysis of Street Drugs Using Comprehensive Two Dimensional Gas Chromatography Coupled with Time of Flight Mass-Spectrometry

Brian B. Barnes
Seton Hall University

Analysis of Street Drugs using Comprehensive Two Dimensional Gas Chromatography coupled

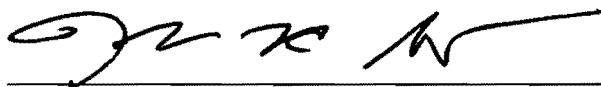with Time of Flight Mass Spectrometry

BY

Brian B. Barnes

DISSERTATION

Submitted to the Department of Chemistry and Biochemistry at Seton Hall University in partial

fulfillment of the requirements for the degree of Doctor of Philosophy.

May, 2012

We certify that we have read this dissertation and that in our opinion it is adequate to scientific scope and quality as a dissertation for the degree of Doctor of Philosophy.
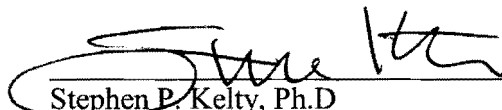
APPROVED

Nicholas H. Snow, Ph.D
Research Mentor

Yuri V. Kazakevich, Ph.D
Member of the Dissertation Committee

Joseph T. Maloy, Ph.D
Member of the Dissertation Committee

Stephen P. Kelty, Ph.D
Chair, Department of Chemistry and Biochemistry

LIST OF FIGURES

PAGE

LIST OF TABLES   PAGE

ABSTRACT

Drug abuse has become a more prevalent problem even as governments and law enforcement officials have enacted restrictions of the use, possession, distribution, and sale of these substances. Within the last 10 years, a new class of drugs known as designer drugs have appeared around the world. They are usually conventional drugs that have been chemically modified to avoid the restrictions placed on them by law enforcement personal and to increase the euphoric effect. During the course of this work two designer drugs, salvinorin A and Yaba, were studied.

Gas chromatography-mass spectrometry(GC-MS) has been used by forensic scientists with great success and is one of the standard techniques for the analysis of drugs of abuse. The instrument is designed to separate a complex mixture and then identify its components. Since its inception, improvements have been made to the GC-MS in order increase its detection capability, speed, sensitivity, accuracy, and precision. A technique that meets these criteria is Comprehensive Two Dimensional Gas Chromatography Time of Flight Mass Spectrometry(GCxGC-ToFMS). It uses two columns, each having different dimensions and different stationary phases to perform orthogonal separations. 'Comprehensive' means that the entire sample is separated on both columns. 'Orthogonal' means that the sample is separated by two independent mechanisms without interference. This was primary instrument used in this work.

When drug samples arrive in forensic laboratories they are usually contained in some type of aqeuous matrix. In order to perform instrumental analysis on them, the drugs must

be extracted from the matrix. Two extraction techniques performed in this work: solid phase microextraction(SPME) and liquid-liquid extraction(LLE). SPME is a simple and efficient technique that uses a polymer coated fiber to extract analytes from a complex or simple matrix. The technique was automated allowing improved repeatability for the SPME methods performed in comparison to LLE.

The analytical figures of merit obtained showed that SPME produced better precision, higher recoveries, and detection limits at least two orders of magnitude lower than LLE. The orthogonal separation and rapid, full-scan capability of the GCxGC-ToFMS identified several impurities and degradation products following the analysis of both drugs. It is believed that this work can be very beneficial to law enforcement officials for the identification of drug trafficking patterns and development of effective regulations prohibiting the sale and use of these substances.

TABLE OF CONTENTS

CHAPTER 1 – THEORY OF EXTRACTION TECHNIQUES PERFORMED AND THEORY AND INTRODUCTION TO COMPREHENSIVE TWO DIMENSIONAL GAS CHROMATOGRAPHY TIME OF FLIGHT MASS SPECTROMETRY

CHAPTER 2 – MATERIALS AND METHODS

2.2 – METHODS

CHAPTER 3 – CHROMATOGRAPHIC PERFORMANCE OF SECOND DIMENSION IN GCXGC USING GROB TEST MIXTURE

CHAPTER 4 – ANALYSIS OF COCAINE IN MONEY, WATER, AND URINE

\

CHAPTER 1 – THEORY AND USE OF EXTRACTION TECHNIQUES PERFORMED AND INTRODUCTION TO COMPREHENSIVE TWO DIMENSIONAL GAS CHROMATOGRAPHY TIME OF FLIGHT MASS SPECTROMETRY

The use of gas chromatography coupled with mass spectrometry(GC-MS) is critical for the analysis of illicit drugs in the field of forensic science. The technique provides accurate and precise qualitative and quantitative information that can be used by law enforcement officials to determine a suspect's guilt or innocence, identify drug trafficking patterns, and generate specific chemical profiles for the drugs analyzed. These drugs are typically contained in complex biological matrices and require extraction prior to instrumental analysis. In this work, three common extraction techniques were used in conjunction with a very sensitive analytical technique known as comprehensive two dimensional gas chromatography time of flight mass spectrometry(GCxGC-ToFMS). This chapter will discuss theory and use of each extraction technique as well as the theory of two dimensional separations in gas chromatography and its use with time of flight mass spectrometry.

1.1 Extraction Techniques

One of the most critical requirements in gas chromatography, is that the samples to be analyzed must be volatile in order for them to be detected. One method where this can be is achieved is a process called extraction which also serves to clean-up the sample by removing non-volatile components that may cause damage when injected into the instrument. The basic premise of extraction is based on equilibrium between a solid or liquid matrix containing the analyte to be extracted and an extraction medium that bears a different polarity than the matrix[1, 2]. This equilibrium can be summed-up by Equation 1-1:

$$[A]_{matrix} \rightleftharpoons [A]_{medium} \qquad \text{(Equation 1-1)}$$

where the equilibrium constant expression is shown in Equation 1-2:

$$K_C = \frac{[A]_{medium}}{[A]_{matrix}} \equiv K_D \qquad \text{(Equation 1-2)}$$

For all extraction techniques, the concentration equilibrium constant is often referred to as the distribution constant, K_D, and can be used to assess the completeness of the extraction of the analyte. When $K_D < 1$, a majority of the analyte has not been extracted and remains in the matrix. When $K_D > 1$, a majority of the analyte has been extracted from the matrix and is contained in the extraction medium indicating a more complete extraction where $K_D \gg 1$ indicates the possibility of exhaustive extraction. Since equilibrium is assumed when K_D is used, the percent recovery of an analyte is used to assess the completeness of an extraction.

The percent recovery is a similar to the K_D value, but it is *not* the same. The percent recovery is an experimental value determined by comparing a known concentration of an analyte spiked into a matrix to the concentration of the analyte determined after extraction. The method used to calculate the %recovery is described in Chapter 2. The K_D value is a constant that has been verified for numerous analytes under standard conditions (1 atm, 25°C, and pH 7)[1]. The K_D and %recovery are affected by the type of medium used, temperature, and the pH which can affect the completeness of an extraction and cause matrix effects. Matrix effects are the result of interactions between the sample matrix and the analyte resulting in low recovery of the analyte and are common in all extraction techniques.

The pH of the matrix determines what form the analyte is in upon its extraction and is based on the respective pKa of the analyte. Since weak acids and weak bases undergo partial dissociation

in aqeuous matrices according to the reactions shown in Equations 1-3 and 1-4, the pH of the matrix must often be adjusted in order to ensure that the analyte is in its non-ionized form prior to extraction.

For weak acids, $HA + H_2O \rightleftharpoons H_3O^+ + A^-$ (Equation 1-3)

For weak bases, $B + H_2O \rightleftharpoons BH^+ + OH^-$ (Equation 1-4)
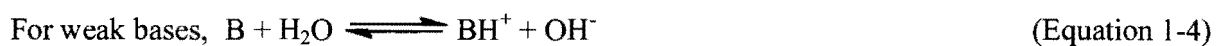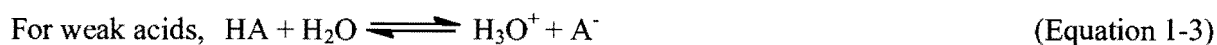
The pH of the matrix is only adjusted during the extraction of weak acids and weak bases. Neutral compounds, such as salvinorin A, do not contain any readily ionizable groups in their structure, thus the pH of the matrix generally has little effect on the extraction of these compounds. The rule of thumb is that the pH of the matrix is adjusted to be at least two pH units away from the pKa of the analyte in order to prevent ionization[2]. For acidic analytes, the pH is typically adjusted to be lower than the pKa. For basic analytes, the pH is typically adjusted to be higher than the pKa. Further, pKa values are determined based on the type of ionizable functional groups present in their structure[3]. These values are derived from the equilibrium constant expressions dictated by the reactions shown in Equations 1-3 and 1-4. During this work, all of the drugs studied were either weak bases or neutral compounds. Their respective pKa values are shown in Table 1-1.

The second major factor affecting any extraction is the temperature at which the extraction is performed in that it affects the Gibbs free-energy, ΔG, of the extraction. This relationship is expressed in Equation 1-5.

$\Delta G = -RT \ln Q$ [4, 5] (Equation 1-5)

Q is the called the reaction quotient and is similar to K_D in that it reflects the completeness of an extraction. However, these two values are not the same. As stated previously, K_D is only valid

Drug	pKa
methamphetamine	10.4
MDMA	10.3
ketamine	6.46
caffeine	10.4
Salvinorin A	neutral
cocaine	8.97

Table 1-1 – Table of pKa values for drugs analyzed. Values were determined using ACD/Labs PhysChem Suite.

under standard conditions. Equation 1-5 shows that the temperature varies inversely with the natural log of the reaction quotient. It also shows how ΔG varies with temperature. Thus, at temperatures below 25°C, ln Q is high, therefore Q > 1 indicating a larger concentration of analyte in the extraction medium. This ultimately results in a more negative value for ΔG and more favorable extraction. When the temperature is higher than 25°C, ln Q is low, therefore Q < 1 indicating a larger concentration of analyte in the matrix. This ultimately results in a more positive ΔG value and less favorable extraction. Thus, the temperature of the reaction affects the thermodynamic spontaneity of the extraction.

Aside from affecting the ΔG of the system, the temperature also affects two other thermodynamic parameters, the enthalpy, ΔH, and the entropy, ΔS. The enthalpy of the system reflects the amount of heat flow from the system and is directly proportional to the temperature[4, 5]. Therefore, as the temperature of the system is increased, the kinetic energy of the matrix increases, allowing the system to absorb more heat from the surroundings making it more endothermic and ΔH more positive. This also increases the kinetic energy of the analyte resulting in an increase of its solubility in the extraction medium. The entropy, ΔS, reflects the measure of disorder present in a system and is inversely proportional to the temperature[4]. For a reversible system, such as an extraction, the entropy is always greater than zero. Therefore, as the temperature (and the kinetic energy) of the analyte are increased, the entropy becomes less positive as the disorder of the system increases. In SPME, there is both an extraction and a concentration process occurring. During the extraction process, the disorder of the system increases as the analyte is removed from the matrix due to an increase in its kinetic energy.

During the concentration process, the disorder of the system decreases as the analyte is absorbed into the SPME fiber due to a decrease in the kinetic energy of the analyte. Although the entropy of the system may be less than zero during the extraction process, the decrease in entropy during the concentration process results in a more positive value ultimately resulting in an equilibrium in which the net result of the entropy is greater than zero. All three of these thermodynamic parameters and the temperature of the system are related by the Gibbs Energy Equation shown in Equation 1-6:

$$\Delta G = \Delta H - T\Delta S \qquad\qquad\qquad\qquad (\text{Equation 1-6})$$

Thus, an increase in temperature, increases ΔH, making it more positive, and decreases ΔS, making less positive. The final result is that ΔG becomes more negative, indicating a more spontaneous reaction, with an increase in temperature.

A third factor that can affect an extraction is the amount of agitation applied on the vessel containing the sample and the extraction medium. Increasing the amount of agitation of the vessel only serves to increase the amount of analyte dissolved in the extraction medium thereby resulting in a faster extraction and higher analyte recovery[1]. Thus, increasing agitation only results in faster kinetics during the extraction, it is does not affect the K_D value or the solubility of the analyte. An example is the use of ultrasonication assisted extraction(UAE) in conjunction with another extraction technique such as solid-liquid extraction which will be discussed further in a later section.

The last major factor that affects all extractions is the type of the extraction medium. For the purposes of this thesis, the extraction medium was either a liquid or a polymer coated fiber. The

most critical requirement for the analyte is that it must be soluble in both the chosen extraction medium and well as the matrix in order to ensure an efficient extraction[1, 2, 6]. The solubility of an analyte in a particular matrix and extraction medium is driven by the intermolecular forces between the analyte, matrix, and extraction medium.

In this thesis, several drugs were spiked into deionized water and urine samples where the solubility of the drugs in each matrix was driven by hydrogen bonding and induced dipole interactions. The dominant intermolecular force between most drugs and water was hydrogen bonding which readily occurs between molecules containing hydrogen with a single covalent bond to an electronegative atom such as oxygen or nitrogen[3]. This results in a partial negative charge on the oxygen or nitrogen atom and a partial positive charge on the hydrogen atom allowing the hydrogen to form a bond with hydroxyl groups or primary amines on other moelcules. In water, this process readily occurs forming an extensive network.

When a drug containing a hydroxyl or primary amine functional group is brought in contact with water, the drug dissolves as it is incorporated into the hydrogen bonding network of water[3]. This also occurs when the drug brought in contact to urine, however due the presence of salts, fats, and proteins, the more dominant intermolecular force between the drugs and urine are dipole-dipole and induced dipole interactions[7]. Dipole-dipole interactions form by the same mechanism as hydrogen bonds, however the interactions between the molecules do not involve hydrogen and are most commonly observed in carbonyl groups[3]. This property allows the oxygen to readily interact with a positive ion resulting in the dissolution of the drug in the urine.

The solubility of the drug is also greatly influenced by the difference in polarity due to the strength of the Van der Waals forces between the drug and the matrix or extraction medium[7-10]. These forces are present between all molecules and are considered to be one of the weakest types of intermolecular forces, however they can appear to be a dominant force when the polarity between the drug and matrix or extraction medium are similar resulting in greater solubility for the drug[3]. This is especially true in liquid-liquid extraction which will be discussed in the following section. The factors discussed above are the critical factors affecting most extraction techniques. The next sections will discuss the extraction techniques performed in this work as well as the critcal factors that were observed to be specific to each one.

1.1.1 Liquid-Liquid Extraction(LLE)

In this work, liquid-liquid extraction was performed on both cocaine and Salvinorin A. In LLE, the extraction medium used is a liquid solvent immiscible in the sample matrix and having similar polarity as the analyte to be extracted[1, 2, 6]. The equilibrium expression and corresponding expression for the distribution constant are expressed in Equations 1-1 and 1-2, respectively. When liquid-liquid extraction is performed, two immiscible liquid layers are observed. One layer is the sample matrix, the other layer is the extraction solvent. When the two layers are mixed and then allowed to separate, the analyte distributes itself between the two layers depending on the K_D value. A schematic of the technique is shown in Figure 1-1 and is compared to schematics of the other extraction techniques performed in this work. It must be noted that the polarity of the matrix and the analyte must be considered when selecting the proper extraction solvent in order to ensure an efficient extraction. As stated previously, the polarity of the analyte and extraction solvent must be similar in order to maximize the Van der

Waals forces between them and ensure a high analyte recovery. Further, the polarity of the

matrix and the extraction solvent must also be different thereby producing weak Van der Waals

forces between them and ensuring immisciblity[1, 2, 6].

Aside from the factors described above that can affect the efficiency of the extraction, liquid-

liquid extraction is also affected by the volume of the extraction solvent used[1, 2, 6]. The mass

of analyte recovered after extraction is directly proportional to volume of extraction solvent and

also dictates maximum mass of analyte that can be extracted. This is known as the saturation

point or solubility limit of the analyte in a particular extraction solvent and can be changed by

changing the volume of solvent added. Therefore, the efficiency of LLE is independent of the

volume or nature of the liquid matrix used and should not affect the concentration of analyte

extracted. If the mass of analyte recovered changes in response to a change in the volume of

liquid matrix used, it is a good indication of variability occurring during the extraction. This

effect is common when extracting analytes from very complex matrices such as urine[7-10]. This

point will be discussed further in later chapters as it pertains to each drug.

A

Organic
Layer

Aqueous
Layer

● = solute

$[\text{solute}]_{org} \rightleftharpoons [\text{solute}]_{aq}$

$$K_D = \frac{[solute]_{aq}}{[solute]_{org}}$$

B

Water
bath

solvent

matrix

solute

$[\text{solute}]_{solv} \rightleftharpoons [\text{solute}]_{matrix}$

$$K_D = \frac{[solute]_{matrix}}{[solute]_{solv}}$$

C

Polymer
Fiber

Stir Bar

$[\text{solute}]_{fiber} \rightleftharpoons [\text{solute}]_{matrix}$

$$K_D = \frac{[solute]_{matrix}}{[solute]_{fiber}}$$
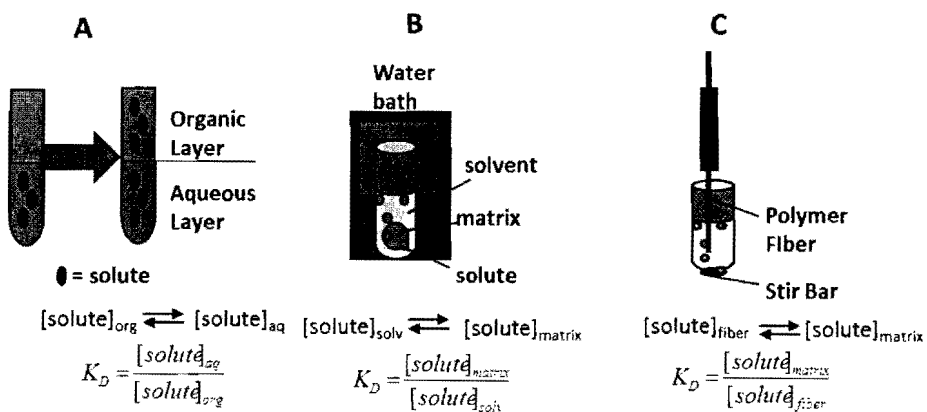
**Figure 1-1 – Set-up of Extraction Techniques Performed
(A) LLE (B) UAE (C) SPME**

24

LLE based procedures are often tedious, requiring many steps and taking many hours to perform a single extraction. One goal of any extraction technique is to minimize the number of steps it takes to perform thereby reducing chances for sample loss and contamination[1]. However, sample loss is inevitable in LLE. Each time the sample is transferred to another vial, filtered, dried, extracted in a separatory funnel, etc., small amounts of the sample are lost. This can be a major problem especially with analyzing the sample using an instrument with a high sensitivity, such as GCxGC-ToFMS. In GC, the magnitude of the signal produced by the detector is proportional to the mass of the sample introduced into the instrument[11]. Therefore, sample loss lowers the %recovery of sample and can also skew the calibration curve for a sample by generating a lower linear range than what appears on the calibration. In order to alleviate these problems, the chemical and physical properties of the analyte to be extracted must be considered to in order to develop a method with the absolute minimum number of steps necessary to perform the extraction and minimize the amount of sample loss.

1.1.2 Ultrasonication Assisted Extraction(UAE)

UAE is often used in conjunction with either solid-liquid extraction and liquid-liquid extraction. The experimental set-up used for this technique in this work is compared to LLE and SPME in Figure 1-1. During this process, the sample, contained in a vial (matrix plus the analyte) is placed into a water bath that is subjected to ultrasonic vibrations at room temperature[1, 12]. The vibrations cause the formation of bubbles in the water that absorb the energy produced by the vibrations until they implode[1, 12]. This causes a release of the absorbed energy which is distributed uniformly throughout the volume of water in the bath. This process is known as cavitation. Some of the energy produced by cavitation is transferred to the sample upon collision with the wall of the vial causing the matrix to break-up and release the analyte. The most critical

factors of UAE is the volume of water used in the water bath which is proportional to energy

distribution as the result of cavitation[12]. The means that less energy is transferred to the

sample resulting in less break-up of the matrix and a lower concentration of analyte free to be

extracted. The level of water used in the bath should be the same as the liquid level of sample to

achieve the best results using UAE[12]. In this work, UAE was used for the extraction of cocaine

from the money samples and the extraction of Salvinorin A from both urine and *S.divinorum*

leaves.

1.1.3 Solid Phase Microextraction(SPME)

Solid Phase Microextraction(SPME) was invented in 1990 as a "solventless extraction"

technique and is credited to the work of Pawliszyn[1, 13, 14]. The technique uses a polymer

coated fiber to extract the desired analytes from the sample matrix instead of using a liquid

extraction solvent. The fiber is either directly immersed in the sample or is exposed to the

headspace of the sample depending on the volatility of the analytes[13, 14]. Samples containing

volatile analytes are extracted using headspace SPME while less volatile analytes are extracted

using direct immersion SPME. For this research, direct immersion SPME was used to extract

each drug from the water and urine samples. The experimental set-up for SPME is compared to

both LLE and UAE in Figure 1-1. During SPME, analytes are absorbed into the fiber at room

temperature by the agitating a vial containing the sample at a constant speed. After typically

between 30 minutes to one hour, the fiber is inserted into the GC inlet. The high temperature of

the inlet provides the driving force to desorb the analytes from the fiber sweeping them into the

column for separation.

The critical factors that affect the extraction of the analytes into the fiber are the type of polymer coating on the fiber, the thickness of the coating, the extraction temperature, the agitation speed, and the extraction time[1, 13-18]. These are also the factors changed during SPME method development. The main factors that affect desorption of the analytes from the fiber is the time the fiber is exposed once inside the GC inlet, the temperature of the GC inlet, and the diameter of the glass sleeve. The desorption time of the fiber may also be changed during method development in order to prevent carryover. This term is used when analytes or matrix components fail to completely desorb from the fiber following a single extraction and are detected following subsequent extractions. This is a common problem when performing quantitative analysis with SPME often resulting in skewed calibration curves and non-repeatable data.

The polymer coating of the fiber is one of the most critical factors for when selecting the necessary SPME fiber to extract certain analytes. The polarity of the fiber should be similar to that of the analytes to be extracted, but should also be different than that of the sample matrix to ensure that the analytes and not the matrix components are extracted into the fiber. It should be noted that some of the matrix may be absorbed into the fiber, however the due to the difference in polarity between the fiber and sample matrix, this concentration is small compared to the concentration of the extracted analyte and is often neglible. A greater concern when performing direct immersion SPME, is the contamination of the fiber upon exposure to complex matrices such as urine. For example, urine contains a multitude of components such as salts, fats, proteins, etc. which usually are absorbed by most polymer coatings for SPME fibers, so repeated exposure of the fiber to urine can cause the polymer coating to degrade and lose its capacity for adsorbing the desired analytes. Further, the fiber is also sensitive to extremely acidic and basic

pHs and will degrade upon exposure to them[16-18]. The importance of pH adjustment as it applies to extracting acidic and basic analytes was previously discussed.

Another factor that is important when selecting the proper fiber is the thickness of the polymer coating. The rule of thumb is that fibers with a thicker coating are used for headspace SPME for the extraction and desorption of volatile analytes whereas polymers with a thinner coating are used for direct immersion SPME for the extraction and desorption of less volatile analytes[1, 13, 14]. Since volatile analytes typically evaporate quickly, a thicker fiber coating is used in order to reduce sample loss during extraction. Further, the matrix present when headspace SPME is performed is typically a solid or viscous matrix which could potentially damage or contaminate the fiber if direct contact between it and the matrix is allowed[13, 14]. For direct immersion SPME, the analytes are normally less volatile and are contained within the matrix thereby preventing the sample loss that frequently occurs during headspace SPME. In this case, direct contact between the matrix and the fiber is required for extraction of these analytes. Thus, a thinner polymer coating is used in order to prevent contamination of the fiber during extraction. During this work, the thickness of the fiber coating was between 60 μm and 65 μm, which was the only commercially available thickness for the fiber coating used for the research[17]. Figure 1-2 shows a chart developed by Pawliszyn for fiber selection[1, 13].

The chart suggests that the two most critical properties of the analyte that must be considered are it volatility and polarity. On the x-axis, polarity increases from left to right. On the y-axis, the volatility increases from bottom to top. For example, salvinorin A is a very polar, nonvolatile
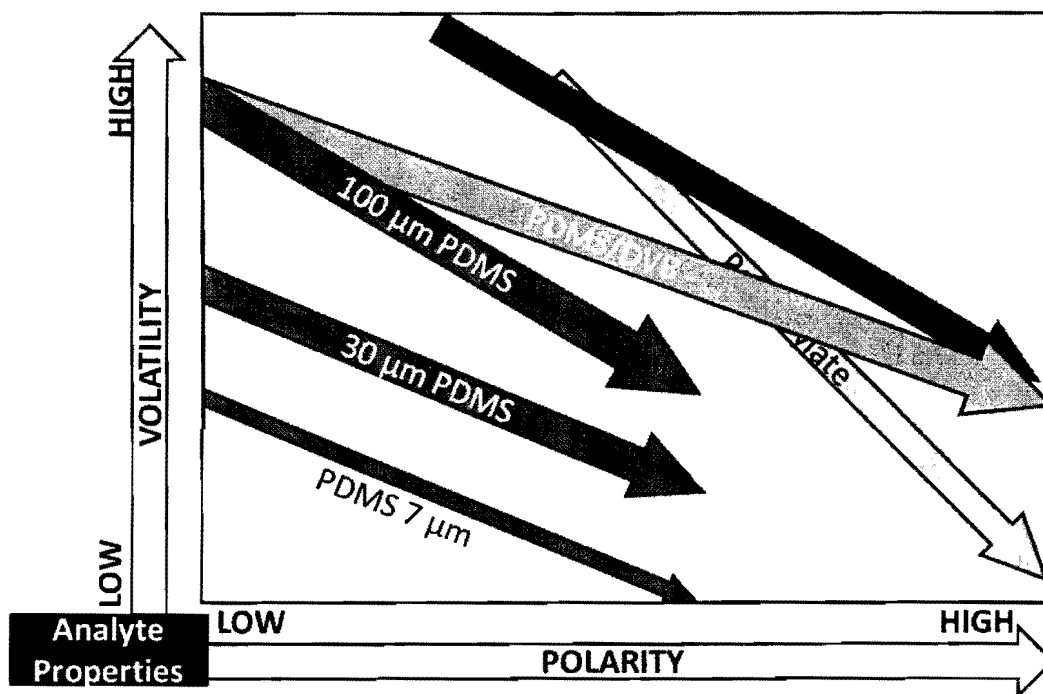
Figure 1-2 – SPME Fiber Coating Selection Chart. Figure adapted from
Pawliszyn, J. SPME: Theory and Practice. Wiley-WCH. New York. 1997.

compound which places the compound on the far right (most polar region) and the bottom (least volatile region) of the chart. Therefore, the proper fiber coating to use for SPME of salvinorin A is polyacryalate. This same criteria was also applied in order to select the fiber coating used for the extraction of the remaining drugs discussed in this thesis.

Two factors that are closely related and important in SPME method development are the temperature and agitation speed at which the extraction is carried out. Prior to extraction, the sample is incubated at the same temperature and speed at which the extraction is carried out in order to bring the sample to equilibrium[13]. For SPME, increasing the agitation speed increases the speed of absorption of the analytes into the fibers. In this work, the agitation speed was not changed from the pre-determined speed setting of the software of the autosampler for all SPME experiments in order to prevent damaging the fiber. At higher temperatures, the kinetic energy and enthalpy of the analyte increase ultimately resulting in a more favorable, endothermic reaction thereby making extraction more favorable for SPME[4, 13]. However, the temperature and speed need only be high enough to agitate the analytes to be extracted without allowing them to escape the sample matrix and also to maintain repeatability of the SPME method[13, 14].

The main parameter that is adjusted during SPME method development and optimization is the extraction time which is directly proportional to the peak area of the extracted analyte. A plot of the peak area versus extraction time is generated in order to determine the optimum extraction time. Figure 1-3 shows an example of a typical extraction time curve for SPME.
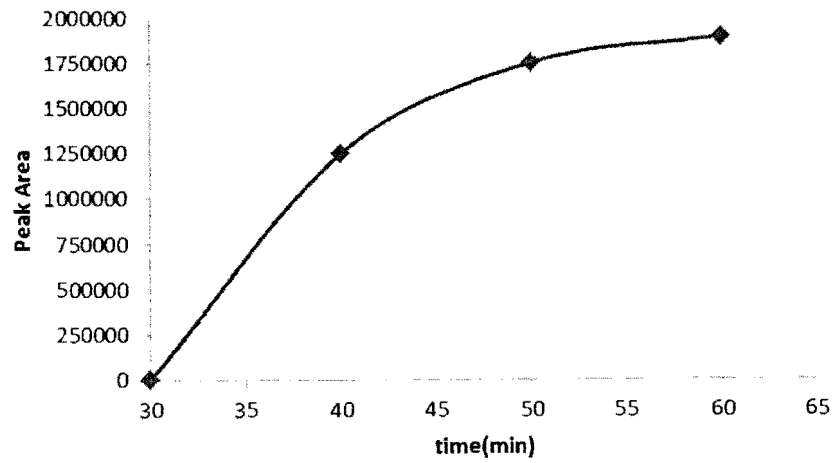
Figure 1-3 – SPME extraction time analysis curve

The curve in Figure 1-3 shows an increase of the analyte peak area with extraction time until an extraction time of 40 minutes is reached. Since the peak area remains constant after this point, it represents the optimum extraction time for this analyte. This is the maximum peak area corresponding to the extraction of a specific concentration of an analyte. After this point, increasing the extraction time will have no effect on the peak area of the analyte extracted.

As previously stated, a frequent challenge observed with SPME is carryover of the analyte or matrix components on the fiber. This can be eliminated by baking out the fiber between each extraction or by ensuring a complete desorption. During this work, the temperatures used were well-within the operational temperature limits for the fiber recommended by the vendor[17]. Although the breakdown of the fiber appeared to be minimal, it may have ultimately resulted in shortening the lifetime of the fiber. The specific experimental conditions for SPME of the Salvinorin A, cocaine, and Yaba will be discussed in Chapter 2.

1.2 Basic Chromatographic Theory

Following the extraction of analytes from a matrix, they are typically analyzed using a chromatographic technique such as gas chromatography or liquid chromatography. For the purposes of this thesis, only gas chromatography and multidimensional gas chromatography will be discussed. Since comprehensive two dimensional gas chromatography was primarily used for the extent of this research, a thorough discussion of the theory and necessary instrumentation will comprise a majority of this section. However, the initial part of this section will discuss the basic principle and also provide a historical overview of gas chromatography leading into a discussion of the principles and mechanisms governing separations performed using two

columns. This will provide the solid foundation necessary for the understanding of multidimensional gas chromatography.

1.2.1 Definition of the mobile and stationary phase in capillary GC

Like extraction, gas chromatography is based on the partitioning of analytes between two phases: a mobile phase and stationary phase. Prior to discussing the separation process that occurs on a typical GC column, is it imperative to develop clear definitions of the mobile phase and stationary phase. In gas chromatography, the mobile phase is a light, inert gas called the "carrier gas" which moves the analytes through the column[11, 19]. The three most common gases used for the mobile phase in GC are hydrogen, nitrogen, and helium. In the this work, helium was used as the carrier gas due its inert behavior making it safer than hydrogen and its lower molecular weight making capable of faster analyses than nitrogen. Martin and Synge proposed that the higher diffusivities of solutes in gas would result in faster partitioning of the analytes between the two phases, more efficient columns, and shorter separation times[20]. The work demonstrated that gas could be used as a mobile phase and was further supported by the work of James and Martin in 1952. In this paper, the use of passing an inert gas through a steel column packed with activated carbon in order to separate a homologous series of fatty acids was discussed [21].

The work of Martin, Synge, and James was further developed by van Deemter who is credited with the development of "rate theory"[22]. The theory incorporates both kinetic and mass transfer effects into the "plate theory" developed by Craig[23]. van Deemter established that the inherent "band broadening" of peaks traveling through the column is dependent upon three factors: eddy diffusion(A-term), longitudinal diffusion(B-term), and the resistance to mass

33

transfer(C-term)[22]. It should be noted that the C-term is comprised of two terms, the resistance

to mass transfer in the stationary phase, C_s, and in the mobile phase, C_m. Equation 1-7 shows the

standard and extended forms of the van Deemter equation relating these three factors to the plate

height, H, and the average linear velocity, $\bar{\mu}$:

$$H = 2\lambda d_p + \frac{2\gamma D_m}{\bar{\mu}} + \left(\frac{\omega d_c^2 \bar{\mu}}{D_m} + \frac{R d_f^2 \bar{\mu}}{D_s} \right) = A + \frac{B}{\mu} + (C_s + C_m)\bar{\mu}$$ (Equation 1-7)

In Equation 1-7, $2\lambda d_p$, $\frac{2\gamma D_m}{\bar{\mu}}$, $\frac{\omega d_c^2 \bar{\mu}}{D_m}$, and $\frac{R d_f^2 \bar{\mu}}{D_s}$ correspond to the A, B, C_s, and C_m terms,

respectively. A graphical representation of the van Deemter equation is shown in Figure 1-4 for

nitrogen, helium, and hydrogen. The optimal linear velocity of the column is located at the

lowest point on the curve which often corresponds to the point at which each of the three factors

are minimized[22, 26]. Thus, based on the shape of the curves, helium has the widest range for

the average linear velocity, but smallest increase in the plate height.

Golay applied the work of van Deemter to his study of capillary columns in 1957[24, 25]. It was

observed the use of capillary columns, instead of packed columns, resulted in GC separations

with both higher efficiencies and shorter diffusion time. This was due to the narrow internal

diameter of capillary columns thereby allowing for separations to be achieved using columns

with longer length ranging between 10 meters and 60 meters. However, the narrow internal

diameter prevented the use of packed columns used previously by James, Martin, Synge, and van

Deemter. Thus, Golay observed that the A-term of the van Deemter equation was zero when

applied to capillary columns. Equation 1-8 shows extended Golay equation which is similar to

Equation 1-7 in which the main difference is that the A-term has been eliminated:
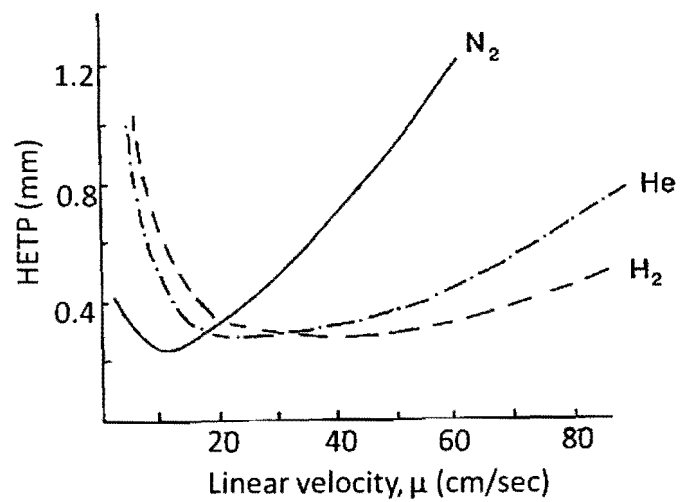
Figure 1-4 – Typical van Deemter plots for common carrier gases
used in GC systems. Taken from McNair, H.; Miller, J.
Basic Gas Chromatography. John Wiley and Sons, Inc. New York. 1998.

$$H = \frac{2D_G}{\overline{\mu}} + \frac{2kd_f^2\overline{\mu}}{3(1+k)^2 D_s} + \frac{(1+6k+11k^2)r_C^2\overline{\mu}}{24(1+k)^2 D_G} = \frac{B}{\overline{\mu}} + (C_s + C_m)\overline{\mu} \qquad \text{(Equation 1-8)}$$

In Equation 1-8, $\dfrac{2D_G}{\overline{\mu}}$, $\dfrac{2kd_f^2\overline{\mu}}{3(1+k)^2 D_s}$, and $\dfrac{(1+6k+11k^2)r_C^2\overline{\mu}}{24(1+k)^2 D_G}$ correspond to the B, C_s, and C_m

terms, respectively. In the second column of GCxGC, the average linear velocity and the

resistance to mass transfer are critical to analyte retention and will be discussed further in

Chapter 3. The expressions for the C-terms are more complex in Equation 1-7 and Equation 1-8

suggesting that the resistance to mass transfer is more complex in capillary columns. A thorough

examination of these equations is beyond the scope this thesis and is available in the

literature[22-26].

The stationary phase in GC may either be a liquid coating on the inside walls of the column or

solid particles packed inside the column[11, 19, 26]. The type of stationary phase is dependent

upon the type of separation being performed. As stated above, due the narrow diameter of

capillary columns, the liquid coating is used as the stationary phase instead of packing the

column with solid particles. The typical range for the internal diameter and film thickness for

capillary columns varies between 0.10 mm to 0.530 mm and 0.10 μm to 1.0 μm, respectively[11,

26]. The general rule is that more volatile analytes require a thicker film in order for them to be

retained on the column, whereas less volatile analytes require a thinner film for retention on the

column[11, 19, 26].

1.2.2. One column separations and the definition of retention

As stated previously, analytes injected onto a GC column are partitioned between the mobile

phase and the stationary phase which is expressed by Equation 1-9:

$[A]_{MP} \rightleftharpoons [A]_{SP}$ (Equation 1-9)

The corresponding equilibrium constant, K, is expressed in Equation 1-10

$$K_C = \frac{[A]_{SP}}{[A]_{MP}}$$ (Equation 1-10)

In chromatography, the equilibrium constant is known as the partition coefficient and is very similar to the distribution constant used to describe an extraction. In GC, retention is proportional to the partition coefficient through Equation 1-11:

$K_C = k\beta$ where $\beta = \frac{r}{2d_f}$ [11, 19, 26] (Equation 1-11)

In the equation, k is the retention factor , β is the phase ratio, r is the internal radius of the capillary column, and d_f is the film thickness of the stationary phase. The equation for the phase ratio in Equation 1-11 is used for capillary columns and is equal to the ratio of analyte volume in the mobile phase to the analyte volume in the stationary phase. Since the partition coefficient in Equation 1-10 is the ratio of the analyte concentration in the stationary phase to the mobile phase, it is dependent on the ratio of the analyte volume in the mobile phase to the stationary phase. Therefore, this implies that the equation for the phase ratio in Equation 1-11 is derived from the definition of the partition coefficient in Equation 1-10.

Since the partition coefficient is a concentration ratio, the retention factor in Equation 1-11 is the ratio of the mass of an analyte in the stationary phase to the mass of an analyte in the mobile phase[27]. In GC, retention increases as the volatility of analytes in sample decrease. The volatility of each analyte is dependent on its respective boiling point and vapor pressure. These properties are related to each other by the Clasius-Claperyon Equation shown in Equation 1-12[3, 4, 27]:

$$\ln p^o = \frac{-\Delta H^o_{vap}}{2.3RT}$$ (Equation 1-12)

The equation shows that the vapor pressure of a liquid, p^o, increases exponentially as the boiling

point of the liquid, T, decreases[3, 4]. It must be noted that Equation 1-12 refers to a single

process in which an analyte transitions into the vapor phase. However, Equation 1-11 shows that

retention in GC is based on the partitioning of analytes which involves two processes. The first

process is a phase transition in which the analytes transition into the vapor phase. This process is

dependent on the respective volatility of the analytes established by Equation 1-12. The second

process occurs when the analytes are transferred from the solution or sorbent in which they are

contained onto the stationary phase. This process is dependent upon the Van der Waals

interactions between the stationary phase and the analytes. The strength of these Van der Waals

interactions is mainly dependent on the respective partition coefficients of the analytes[11, 19].

However, the discussion above also implies that partition coefficient is also affected by the vapor

pressure and boiling point of an analyte. This further indicates that the strength of the Van der

Waals interactions is also affected by the respective vapor pressures and boiling points of the

analytes. Thus, the discussion above ultimately establishes that retention in GC is dependent on

the partition coefficients, vapor pressures, and boiling points of the analytes. Polarity also

affects the strength of the Van der Waals interactions and will be discussed in a later section

since it is more critical for retention on the second column of GCxGC.

One of the most critical variables affecting retention is the temperature of the column. The

relationship between the column temperature and retention factor is expressed by Equation 1-13:

$$\ln K = -\frac{\Delta H}{RT} + \frac{\Delta S}{R} [27]$$ (Equation 1-13)

This equation is derived by combining Equations 1-5 and 1-6. The partition coefficient in

Equation 1-5 has been replaced with the retention factor by using the proportional relationship

between them established by Equation 1-11 which is known as the Vant Hoff equation. A plot of

ln K vs 1/T shows that the plot is linear where the slope is $\dfrac{-\Delta H}{R}$ and the y-intercept is $\dfrac{\Delta S}{R}$.

The fundamental relationship of Equation 1-13 is that retention varies inversely with

temperature. A closer look at the equation shows that ΔH decreases and ΔS increases with

temperature. Therefore, according to Equation 1-6, $\Delta G < 0$, indicating that the decrease of

analyte retention as column temperature increases is a favorable and spontaneous process.

In GC, the column temperature can either be held constant or changed at a constant rate. When

the temperature remains constant for the duration of an entire run, it is called an isothermal

separation[11, 19]. This type of separation is very useful for the analysis of samples containing

only a single component or a few components such as the certified reference standards used for

the quantitative analysis of the drugs discussed in this thesis. It is also used to determine critical

chromatographic parameters such as the void time of the column, t_o; the retention factor, k; the

selectivity, α; and the column efficiency, N. When the temperature is increased at a constant rate

throughout a single run, it is known as temperature programming[11, 19, 28]. It is very useful for

rapidly separating samples containing multiple analytes in single run such as the urine samples

spiked with full Yaba mixtures studied in this work. However, the major drawback for this

method is that the fundamental chromatographic parameters are more challenging to determine

often requiring more difficult calculations developed by Giddings[28].

The discussion above establishes the basic principles for how retention of analytes occurs in gas chromatography and the general retention mechanism that occurs in a typical GC system. Prior to discussing the two column separations and instrumentation used in this work, the methods of sample introduction as well as the inlet systems used in this work will be discussed.

1.2.3 Sample introduction in GC

1.2.3.1 Manual and Automated Injections

Sample introduction in GC is critical, especially when performing quantitative analysis, since the amount of sample loss during this process is dependent on the method of sample introduction. In this work, the sample was introduced by liquid injection using a gas tight microliter syringe or by thermal desorption from an SPME fiber. Both techniques can be performed by using either manual injection or an autosampler. While manual injection was the first method of sample introduction used in GC analysis, it primarily used today as training tool for new users of GC, due to the high availability of autosampler systems. Thus, the most common means of sample introduction today is by use of an autosampler which has proven to give better precision and accuracy in comparison to manual means of sample introduction. This primarily applies to liquid injection of the sample where accuracy and precision are often poor due human error in repeating the same volume of sample necessary for analysis when performing manual injections. Variation in the sample volume when it is transferred from its storage vial into the syringe results in a slight variation in the peak areas when the sample is vaporized in the inlet and then separated on the column resulting in poor repeatability of analyte retention times and distribution coefficients. It must be noted that some variation in the injection volume also occurs with the use of an autosampler. The variation comes from the inherent uncertainty of the syringe, but is often neglible since human error is eliminated by the use of an autosampler.

1.2.3.2 Liquid Injection and Thermal Desorption

For the purposes of this work, the method of sample introduction chosen was based on the

extraction technique performed and the concentration of the analyte introduced into the

instrument for analysis. As stated previously, SPME is a more sensitive technique than LLE

meaning that it is capable of extracting lower concentrations of analyte. The method used to

introduce the sample for SPME was thermal desorption which showed better repeatability than

liquid injection. Since no solvent focusing occurs in SPME, thermal desorption is limited to the

introduction of lower concentrations of analyte in order to avoid saturating the fiber and rampant

carryover. However, the introduction of an analyte concentration of only 1 μg/mL using SPME

can often yield large peaks and produce severe carryover. Thus, due to this limitation, LLE is

often better suited for the extraction of larger concentrations of analyte where the maximum

amount of analyte extracted in solely dependent on the amount of extraction solvent used. Since

it is possible to introduce much higher sample concentrations, liquid injection was used in

conjunction with LLE. As discussed above, one of the major drawbacks of liquid injection is due

to variability in the amount sample drawn up by the syringe, even when using automated

injection. Although this variation is often negligible when using an autosampler, it can cause a

slight variation in the injection volume in poor precision and accuracy. This was a recurring

trend observed through this work and will be discussed in later chapters as it pertains to each

experiment.

1.2.3.3 Split and Splitless Injection

After the sample has been extracted and all the necessary sample preparation steps have been

completed, it is injected into the instrument through a heated inlet at a temperature between

250°C and 280 °C and is held constant throughout a run of a single sample[11, 19]. At these

temperatures, most liquid samples are vaporized or in the case of SPME, these temperatures are

also high enough to desorb the analytes from the fiber into the inlet. For liquid injection, the

sample volume expands based upon the solvent present[29]. The most common type of inlet

system used in both GC and GCxGC is a split/splitless inlet. A schematic of the inlet illustrating

the configuration for both and split and splitless injections is shown in Figure 1-5. The main

difference between the two types of injections is determined by the status of the purge valve

attached to the inlet.

During a split injection, the purge valve remains open allowing only a fraction of the sample to

be injected onto the column and is used when injecting unknown samples and "dirty" samples.

These type of injections prevent nonvolatile components and/or other contaminants that could

potentially damage the capillary columns or glass inlet sleeves from entering the system. The

main advantages are that they are fast producing narrow and sharp peaks, they allow complex

and unknown samples to be injected, and can be used under isothermal or temperature

programming runs[11, 19, 29]. The main disadvantages are that they cannot be used for trace

analysis, cannot be used in conjunction with extraction techniques such as SPME, and not an

accurate as splitless for quantitation studies. The amount of sample that actually enters the

column during a split injection is determined by the split ratio which is set by the user and

defined by Equation 1-14:
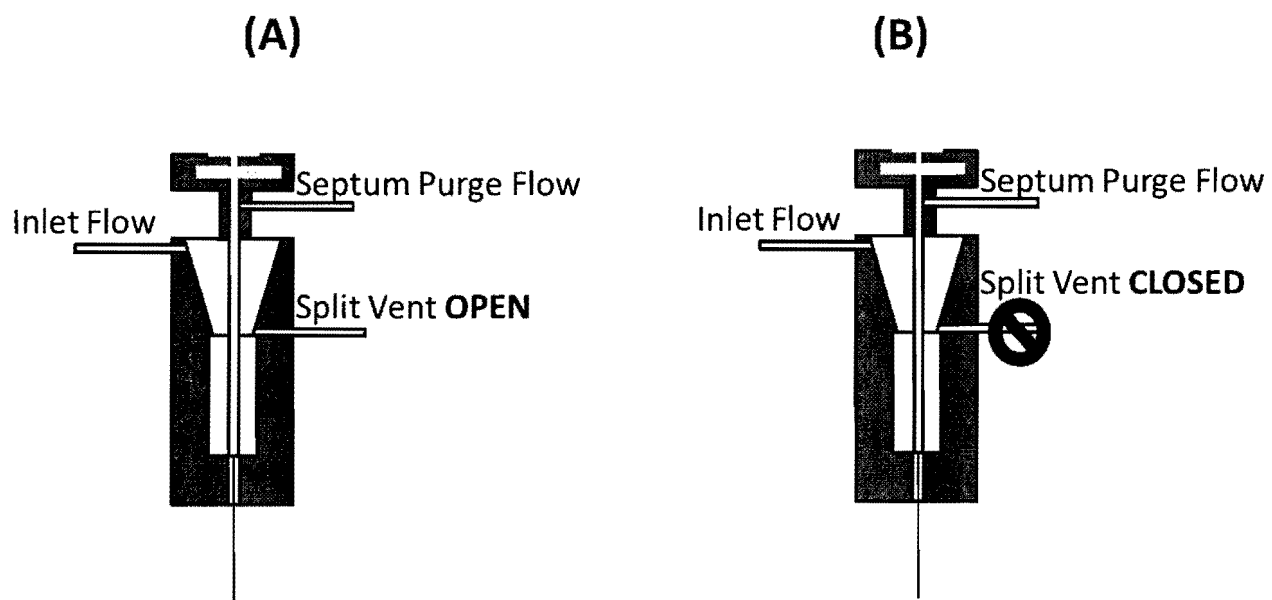
Figure 1-5 – GC inlet configuration for (A) Split Injection and (B) Splitless Injection.

$$\frac{split\_flow(mL/\min)}{column\_flow(mL/\min)} [19, 29] \hspace{4cm} \text{(Equation 1-14)}$$

This value may also serve as a dilution factor to estimate the sample concentration on column when the original concentration of the sample is known. Splitless injection was invented by K. Grob when the split vent was accidentally left closed after performing the injection resulting in the entire volume of sample being injected[29]. Grob had originally thought that performing such an injection would overload the volume capacity of the liner and damage the inlet, producing severely fronted peaks. However, the peaks Grob observed were nearly symmetrical, showing only a larger peak width. It was also noted that although the entire volume of sample was injected, the retention and selectivity of the analytes was not affected. Thus, in splitless injections, the wider peak widths produced result in lower efficiencies for each analyte.

When splitless injection is performed under temperature programming conditions, the sample is focused in a narrow band upon transfer from the heated inlet onto the cold column resulting in much sharper peaks and greater analyte efficiencies. This process is called "cold trapping" and occurs due to the large temperature difference between the inlet and the capillary column[11, 19, 29]. It should be noted that Grob also observed "cold trapping" under isothermal conditions, however, unless the column is at very low temperature, the effects on the peaks are minimal[29]. Therefore, it is for the reasons above that the preferred method used with splitless injections is temperature programming[11, 19, 29].

One of the main disadvantages of splitless injections is that they take much longer time to perform in comparison to split injections. The average time is approximately 45 seconds to 1 minute for each injection and is necessary in order for entire sample to be vaporized, focused,

and transferred to the column[11, 19, 29]. However, the longer time spent in the inlet often results in unwanted interactions between the sample and the glass sleeve thereby causing peak tailing if the inlet is not completely purged after the sample has been transferred to the column. This phenomenon can be corrected if the purge time is increased. The purge time refers to the time after the start of the run when the purge vent on the inlet, shown in Figure 1-5, is opened thereby evacuating any sample or carrier gas from the inlet. During method development, the purge time is optimized by injecting an analyte with the same concentration at several different purge times and then recording the analyte peak area. A plot of the analyte peak area vs. the purge time is constructed where the optimal purge time is point on the curve where the peak area reamins constant despite any further increase to the purge time. This process is similar to the optimization of extraction time performed during SPME method development. In this work, splitless injections were used during the analysis of the all the drugs studied.

The glass sleeves shown in Figures 1-6A and 1-6B show typical glass sleeves used for split injections and splitless injections, respectively. For split injections, a cup or piece of glass wool in the glass sleeve, shown in Figure 1-6A, traps the nonvolatile sample components thereby preventing them from entering the column in split injections[29, 30]. For splitless injections, the glass sleeve in Figure 1-6B does not contain any obstructions thereby allowing all sample components to enter the column. It is for this reason that only pure samples or "solventless" samples are injected into the inlet in order to prevent damage to the column[11, 19, 29]. The internal diameter of the glass sleeve in Figure 1-6A is much greater than the sleeve in Figure 1-6B[30]. Therefore, the maximum sample volume present after vaporization is about four times greater for split injections compared to splitless injections. Thus, Boyle's Law states that the head

Split Liner with cup   Splitless Liner

Figure 1-6 – Comparison of Typical Glass Sleeves for Split and Splitless Injections.

pressure of carrier gas in the inlet will be about four times lower during split injections compared to splitless injections. The head pressure of the carrier gas inside the inlet prevents the sample from exceeding the maximum volume of the glass sleeve by pushing the vaporized sample through the inlet into the column[19, 29]. In splitless injections, the head pressure is often higher due to the smaller volume inside the glass sleeve resulting increasing rate at which sample focusing occurs during "cold trapping" resulting a reduction of the overall injection time[19, 29].

1.2.3.4 The Solvent Effect

The "solvent effect" is a well-known phenomenon that occurs in GC and illustrates the influence of polarity on retention[19]. Figure 1-7 shows the process of how the "solvent effect" occurs. Figure 1-7A shows the sample as it is injected into the column. The flow of the carrier gas causes the sample to eventually spread into a thin film coating the inside of the column. The pressure of the carrier gas flowing through the column causes beads of solvent to form along the length of the column. This is shown in Figure 1-7B. The analytes inside the beads interact with the stationary phase via dispersive van Der Waals interactions and eventually a solvent plug formed as the size of the solvent bead shrinks due to the pressure of the carrier gas the sample through the column. This is shown in Figure 1-7C. As the temperature of the column increases, the analytes begin to elute from the column according to their respective vapor pressures. The end result of this "solvent effect" is that the analytes have lower distribution coefficients than reported in the literature and therefore lower retention times on the column[19]. As previously noted, the solvent effect does not occur in SPME and/or thermal desorption since it does not require the use of an extraction solvent. This results in less focusing of the sample prior to separation on the column often resulting in more band broadening and more fronting in the analyte peaks.
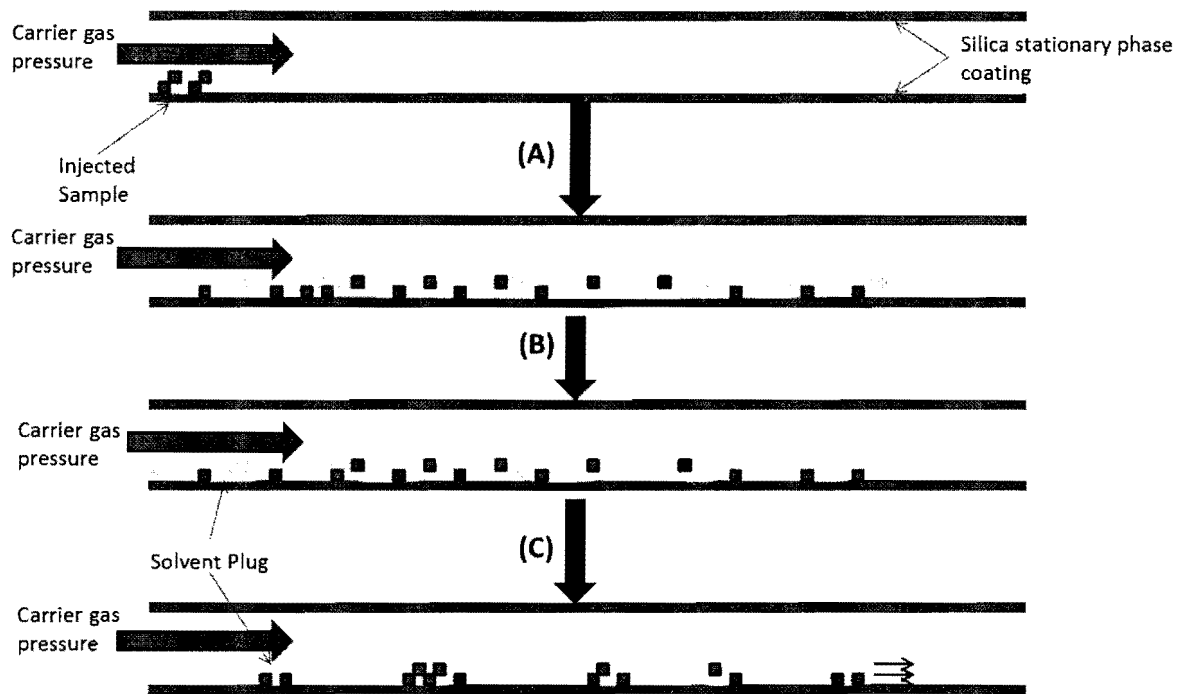
Figure 1-7 – Illustration of "solvent effect" (A) Injected sample spreads along column; (B) Solvent Plugs begin to form; (C) Solvent Plugs elute from column

1.3 Two Column Separations

Since the primary instrument used during this work employed two capillary columns in a tandem configuration for analysis of the drugs studied, the following section will discuss the mechanisms and critical instrumentation required to perform these complex types of separation. The most critical feature of performing two columns, or two dimensional, separations in GC is that the peak capacity is increased compared to any standard single column GC separation technique. Peak capacity is defined as the number of possible peaks that can be resolved after separation on a single column determined by Equation 1-15:

$$n = \frac{\sqrt{N}}{2R} \ln\left(\frac{t_2}{t_1}\right) + 1 \quad [19, 31, 32]$$ (Equation 1-15)

$$n_{GC \times GC} = n_{column1} \times n_{column2} \quad [19, 31, 32]$$ (Equation 1-16)

In Equation 1-15, n is the total number of peaks resolved, N is the column efficiency, R is the resolution between two adjacent peaks, t_2 and t_1, are the end time and start time of the run, respectively. It must be noted that the increased peak capacity only applies to comprehensive two dimensional gas chromatography since the entire sample is separated on both columns. Table 1-2 shows a comparison of peak capacities obtained from comprehensive two dimensional GC and conventional single column GC. The peak capacity for the comprehensive technique was calculated using Equation 1-16 and the peak capacity for the conventional technique is equal to the peak capacity calculated for column 1 in the table. The calculations performed are theoretical, however Table 1-2 shows that the increased peak capacity for the comprehensive two column separation is mainly due to the incorporation of the second column. This observation is also supported by the literature[31-37].

	N	R	t_2	t_1	n
Column 1 (30m x 0.250mm x 0.25 µm)	50000	1.5	20 min	3 min	142
Column 2 (1.5m x 0.100mm x 0.1 µm)	5600	1.5	5 sec	1 sec	41

	n
GC-MS	142
GCxGC-ToFMS	5822

Table 1-2 – Comparison of typical peak capacities for a conventional single column separation and comprehensive two column separation using a typical column set. Peak capacities for each column was calculated using Equation 1-15.

1.3.1 Heart Cutting Vs. Comprehensive Two Dimensional GC

The difference between "heart-cutting" and comprehensive two dimensional gas chromatography

is amount of sample that is separated on the second column. In "heart-cutting", only selected

portions of the sample are analyzed on the second column, thus the peak capacities for the first

and second columns are added together to obtain the total peak capacity for the technique[33].

However, in the comprehensive technique, the entire sample is separated on both columns, thus

the peak capacity of the first and second columns are multiplied, not added, to give the total peak

capacity for the system as shown in Table 1-2. Thus, in order to distinguish between the two

types of techniques, the notation for the comprehensive technique is denoted as "GCxGC"

whereas the notation for the "heart-cutting" technique is denoted as "GC-GC".

Figure 1-8 shows a schematic of GC system that has been set-up for "heart-cutting" using a

Deans switch. The figure shows a dual-detector setup in which a separate detector records the

data from each column. The most commonly used detectors are flame-ionization

detectors(FIDs), for more specialized analyses an electron capture or nitrogen-phosphorus

detector may be in used as the second detector[33]. This allows the instrument to detect specific

types of compounds after being separated on the second column. The figure also incorporates the

use of a Deans switch which is a device that serves to direct the flow of the sample to the second

column using solenoid valves[33]. It also prevents interference between separations occurring on

each column. The main advantage of this technique is that it allows rapid isolation and analysis

of critical individual compounds from a complex sample.
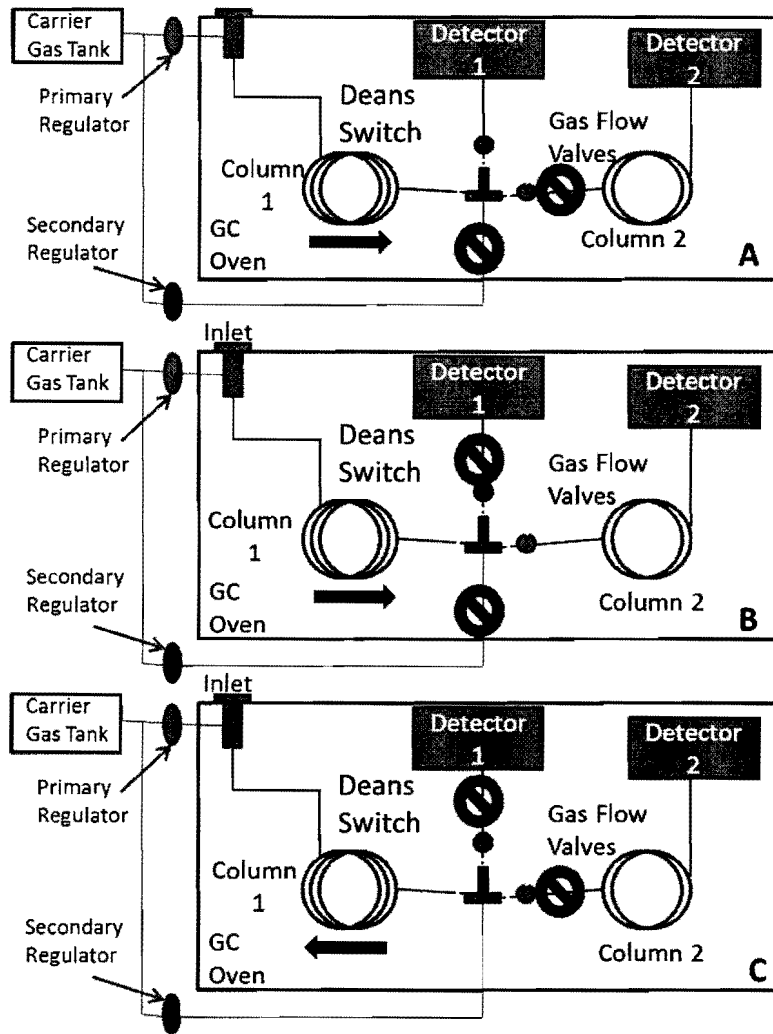
Figure 1-8 – Schematic of GC-GC
System confirmed for "Heart-Cutting"
Using Dean Switch
A- Prefractionation.(Dean Switch OFF)
Sample Flow through Column 1 ONLY
 Yellow Arrow is carrier gas
Flow through column 1

B- Sample Transfer(Dean Switch ON)
Sample flow through both columns
Yellow arrow is carrier gas
Flow through column 1

C- Backflushing(Dean Switch OFF)
No Sample flow through either column
Yellow arrow is carrier gas
Flow through column 1. Direction of
Carrier gas flow is opposite.

Figure adapted from A.C.Lewis in L. Mondello,
A.C. Lewis, K. Bartle. Multidimensional Chromatography.
John Wiley & Sons, Inc. New York. 2002. 54.

The Deans switch has three modes of action that are preformed sequentially when a "heart-cut" is made[33]. The three modes are (1)prefractionation, (2)sample transfer, and (3)backflushing. During prefractionation, the Deans switch is off and sample flow is directed through the first column to the first detector only. When the Deans switch is on during sample transfer, sample flow is redirected through both columns to the second detector. During backflushing, carrier gas is provided by the secondary regulator is flowing in the opposite direction of the normal carrier gas flow that occurs while a sample is being separated. The purpose of backflushing is to remove contaminants and/or fractions of the sample that did not elute during analysis. The direction of sample flow and function of the Deans switch during each mode are also shown in Figure 1-8.

Comprehensive two dimensional gas chromatography means that the entire sample is separated on both columns and was invented by Phillips and co-workers[32, 34-37]. The analysis time of each sample is reduced and interference with the separation on each column is minimized by using a modulator. The modulator is placed close to the beginning of the second column and regulates the amount of sample that flows into the second column for separation[32, 34-37]. There are several types of modulators have been used in comprehensive two dimensional gas chromatography. The most common type of modulator used today, and the one used in this work, is a cryotrap modulator. The function of the modulator will be discussed in detail in the following section. A second device that is critical to this technique is the secondary oven. For the instrumental set-up used in this research, the secondary oven is placed inside the main oven of the instrument and is located between the modulator and the transfer line[36]. In GCxGC, both the primary and secondary ovens each have separate temperature programs. The purpose of each temperature program is separate the sample on each column by increasing the temperature at a

constant rate enabling the complete separation of the volatile analytes contained in a given sample[32, 34-37]. The initial temperature of the secondary oven is generally kept at least 5 degrees higher than that of the primary oven which helps to ensure rapid, separation of the sample on the second column. Figure 1-9 shows a schematic of the instrument used in this work.

Another popular configuration for GCxGC is the Low Thermal Mass (LTM) Oven in which each column is housed in a separate LTM Oven. The flow and peak modulation in the second dimension are controlled by a flow modulation device. This configuration and some of its applications have been discussed in the literature[38]. The combination of the modulator, the secondary oven, and the difference in the stationary phases coating each column generates a phenomenon known as orthogonal separation. Orthogonal separation means that there are two independent separation mechanisms occurring simultaneously without interference between them.

It is important to stress that orthogonal separations occur with both heart-cutting and comprehensive two dimensional techniques[31-38]. In "heart-cutting", when a portion of the sample is analyzed on the second column, carrier gas flow to the first column is stopped and then diverted to the second column. Although only one separation mechanism occurs at a time in "heart-cutting", this process still involved two independent separation mechanisms, and can therefore be considered an orthogonal separation. In the comprehensive technique, the modulator regulates the flow of the sample by continuously transferring small fractions of it onto the second column making it critical for performing the orthogonal separation.
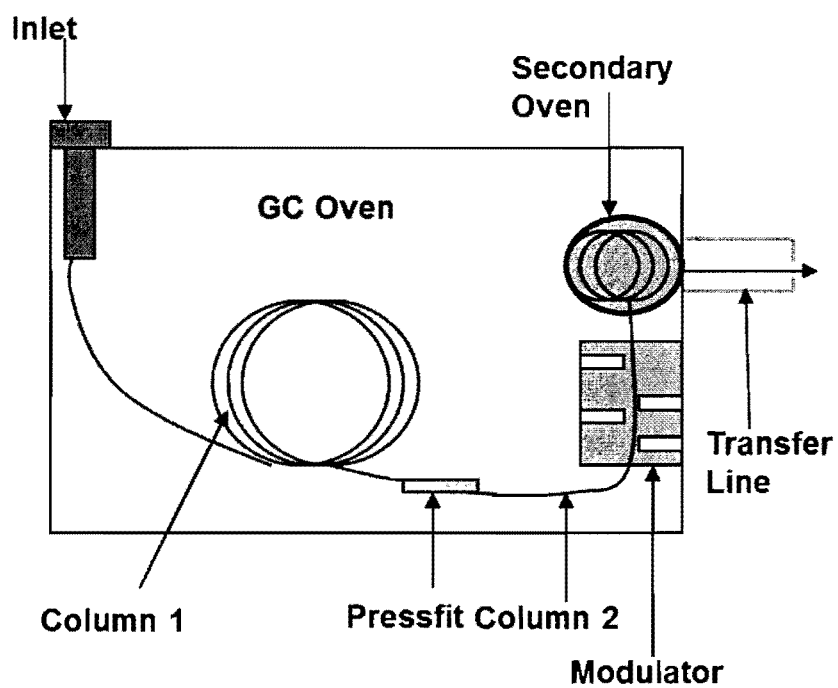
Figure 1-9 – Schematic for GCxGC system configured for Comprehensive Analysis. Image adapted from www.leco.com/pegasus4D

The following sections will discuss orthogonal separations in more detail, focusing on the

dimensions and stationary phase of each column, set-up inside the instrument, and retention

mechanism of the second column. This section will conclude with a discussion of the column

selection process and how the specifications of both columns are considered.

1.3.2 Column Dimensions and Stationary Phases

The columns used for a GCxGC technique generally differ in the lengths, internal diameters, and

film thickness of the stationary phase. The dimensions of the first column are typical of a column

that is normally used in a standard single column GC or GC-MS system. The dimensions of the

second column typically have lengths between 1 and 2 meters and internal diameters about half

the size of the first column diameter[32, 34-37]. These smaller dimensions result in much higher

linear velocities for analytes moving through the second column. The main purpose of the

second column is to perform rapid separation of the eluent from the 1st column using a more

polar stationary phase on the second column resulting a thorough separation of the volatile

analytes[32, 34-37].

The average linear velocity of the carrier gas is defined by Equation 1-17:

$$\bar{\mu} = \frac{L}{t_0}$$
(Equation 1-17)

where L is the length of the column in centimeters and t_0 is the hold-up time of the second

column in seconds[11, 19]. In physical terms, it is the linear velocity of the carrier gas traveling

through the column which increases along the length of the column. There is a large increase in

the linear velocity of the carrier gas as it is transferred from the first column into the second

column resulting due to the difference in the internal diameter of each column. This also results

in different flow rates for the sample traveling through each column. However, the flow rate is kept constant during a single analysis due to a pressure ramp within each column which is controlled by the system software and is dependent on the column dimensions[32, 36]. When the instrument is set for constant flow, these pressure ramps regulate the individual flow rates within each column in order to maintain a target flow rate through both columns that remains constant during an analysis.

The combination of the length of the second column and the internal diameter of the second column result in high linear velocity and a lack of retention for each analyte. Although the second column uses a temperature program, the linear velocities inside the second column are so high that the temperature program has little effect on analyte retention thereby resulting in rapid isothermal separation[37]. This is a major trade-off in GCxGC and GCxGC-ToFMS in which the chromatographic performance of the second column is sacrificed for speed. This phenomenom was studied in this work using the Grob mixture, which is a standard test mixture used in GC consisting of 12 compounds with various boiling points and polairities used to test the separation ability of GC capillary columns[39, 40]. The results of this study are discussed in Chapter 3.

The final parameter of the column to discuss is the film thickness of the stationary phase and the type of stationary phase. Like SPME, Choosing the film thickness is based on the volatility of the analytes[11, 19, 29]. As stated previously, analyte volatility is inversely proportional to analyte retention. Since retention is directly proportional to the partition coefficient of the analyte as expressed by Equation 1-11, it follows that analyte retention is also inversely proportional to analyte volatility. The equation for the phase ratio corresponding to capillary columns is also

shown in Equation 1-11 and establishes that the film thickness of the stationary phase is inversely proportional to the phase ratio. Thus, from the discussion above it follows that the volatility of the analyte varies inversely with the film thickness of the stationary phase.

Selection of the stationary phase composition itself is a more critical parameter in GCxGC analysis than the thickness of the phase coating. The typical column set-up is that the first column contains a non-polar stationary phase and the second column contains a more polar stationary phase than the first column[32-37]. One critical feature of the type of stationary phase reveals how strong the retention of the analyte is. This becomes critical when trying to eliminate carryover of analytes on the column which occurs when the interaction between an analyte and stationary phase is so strong resulting in the presence of the analyte on the column after multiple runs. One of the most common causes of carryover is that the concentration of the analyte injected into the instrument is too high. This is more of a problem with GCxGC-ToFMS due to their high sensitivity resulting in the detection of multiple peaks and tailing peaks for the same compound. This is avoided by injecting diluted concentrations of analytes or by flushing the column with a solvent bearing the same polarity as the analyte. Carryover on the second column is known as wraparound which will be discussed in conjunction with peak modulation and the role of the modulator.

Figure 1-10 shows a two dimensional chromatogram observed following the single analysis of a BP oil sample by GCxGC. The x-axis and y-axis corresponding to the retention time on the first and second column, respectively. Thus, the coordinates for each peak are read as the retention time on the first column followed by the retention time on the second column. The plot itself is

known as a contour plot and is similar to looking at a topographical map in which the observer is looking down on plots and the peaks are coming out of the x-y plane in the z-direction toward the observer. Thus, the chromatogram is a three dimensional representation of the data which is the typical form produced by the instrument. The colors on the plots indicate the abundance of the peaks shown on the plots where the red regions have the greatest abundance and the blue regions have the lowest abundance[36]. The black dots on the plot correspond to each peak identified by the ToFMS. Therefore, although the GCxGC contour plot is unique, it can provide more detailed information in terms of the separation of analyte peaks in comparison to a typical GC chromatogram.

1.3.3 Retention Mechanisms

The retention mechanism that occurs on the first column, if it is non-polar stationary phase, is based on the vapor pressure of the volatile analytes in a sample and their interaction with the stationary phase of the column due to Van der Waals forces. The main factors affecting the basic retention mechanism in capillary column GC are essentially the same regardless of the dimensions and type of capillary column used[11, 19, 29]. Therefore, it follows that the retention mechansims occurring in both columns in GCxGC essentially the same. The main difference is that the stationary phase of the second column is usually more polar than that of the first column and should result in stronger retention, due to greater Van der Waals forces between the analyte and statationary phases as the analyte polarity increases. However, retention in the second column is poor, due to the much higher linear velocity of the carrier gas as a result of the smaller dimensions typically employed[37].
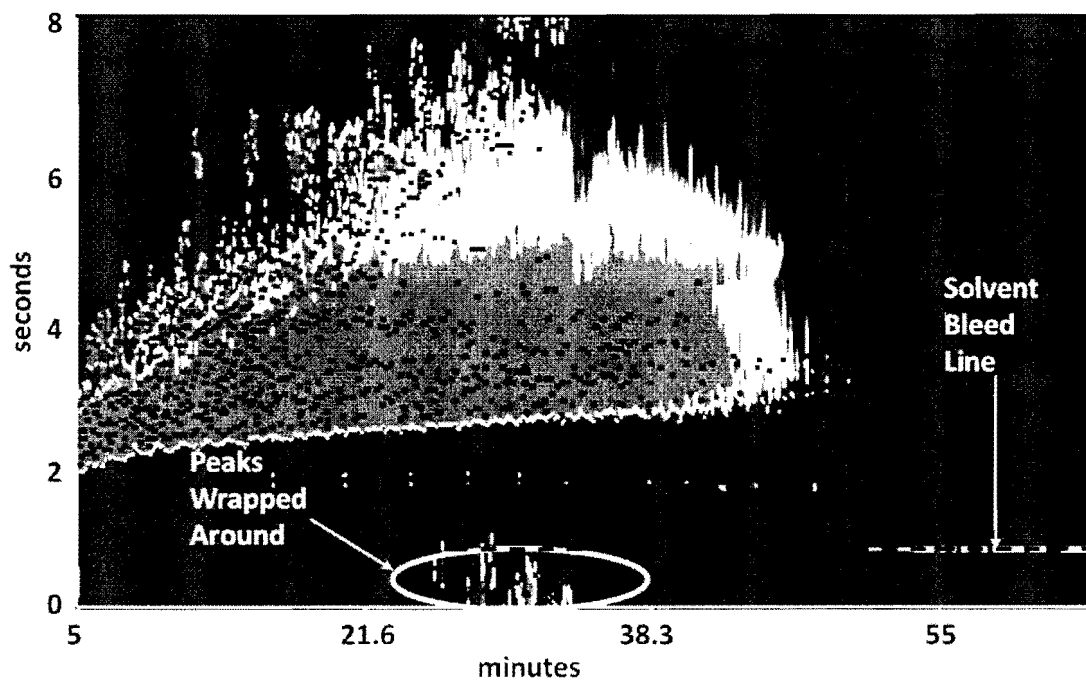
Figure 1-10 GCxGC contour plot of oil spill sample showing presence of wraparound

The internal diameter can be related to the partition coefficient for an analyte using Equation 1-11. As stated in the previous section, the partition coefficient is proportional to the phase ratio. For capillary columns, the phase ratio is proportional to the internal radius. Therefore, the narrow internal diameter typically used in the second column results in low partition coefficients implying from Equation 1-10 that there is a larger concentration of analyte in the mobile phase. Since the narrow internal diameter of the second column results in both a high linear velocity for the carrier gas and low partition coefficients for analytes in a sample, it follows that this internal diameter is a critical factor responsible for the poor retention of analytes in the second column.

It must be stressed that the separation mechanisms that occur in both the first and second column occur simultaneously during a single run, but function independently of each other and do not interfere with each other[32, 34-36]. Thus, the difference in stationary phase between the two columns is required for orthogonal separation to be achieved. The other requirement for orthogonal separation is the employment of the cryotrap modulator which will be discussed in the next section along with the other features of the GCxGC-ToFMS system.

1.4 Intsrumentation of the GCxGC-ToFMS

1.4.1 Role of the Pressfit

The two columns are connected by a pressfit connector made of a deactivated fused silica which provides an inert pathway as the sample passes between the two columns. During the course of the research, it was noted that the pressfit is *very* prone to leaks. In order to ensure a good seal at the pressfit, the columns were required to have flat cuts, a snug fit between each column and the pressfit, and an internal diameter in the second column that is equal to or less than that of the first column. This is shown in Figure 1-11. The end of the column and the pressfit were held in place
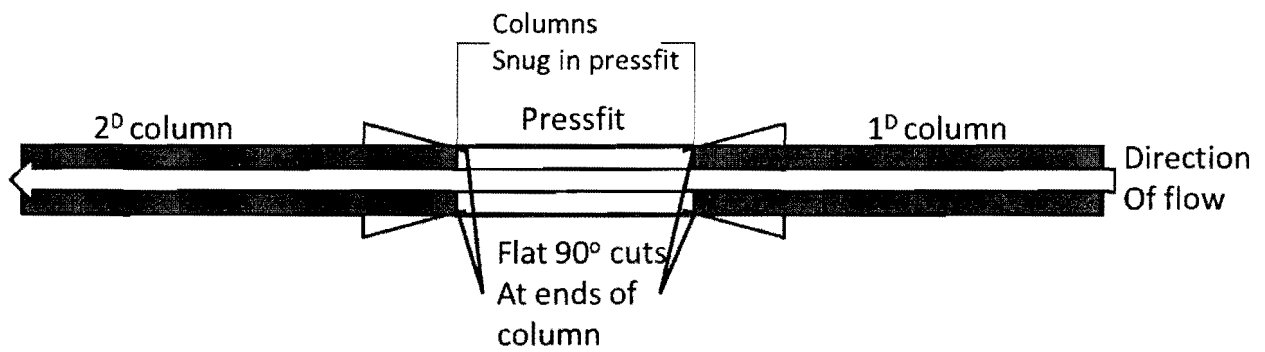
Figure 1-11 – Schematic of Proper installation of a pressfit in GCxGC

for approximately 45 seconds to 1 minute to allow the pressfit to seal around the column. If resistance was felt at the pressfit when the end of the column was gently pulled, then the seal was considered good. In GCxGC-ToFMS, the only way to test if the seal of the pressfit is by performing a leak check for air and water on the instrument[36]. If a leak is detected at the pressfit, polyimide resin can be applied to the ends of the pressfit to plug a leak or the pressfit itself must be replaced. The most common causes of a leak detected at the pressfit came from poor column cuts or the use of a capillary column with a larger internal diameter than the first column.

1.4.2 Peak Modulation and the function of the Modulator

Peak modulation is the defining characteristic of GCxGC analysis resulting in the focusing of the entire eluent from the first column in small fractions consisting of narrrow peaks each having a bandwidth of around 1 ms[32, 34-36]. These peaks are essentially "slices" of each fraction in the eluent where each "slice" corresponds to a different component in the sample resulting in a much higher peak capacity for a single separation performed with GCxGC[32, 34-36]. Ideally, the total peak profile of the "slices" for each fraction should correspond with the peak profile of the fraction seen on the first column. Figure 1-12 compares a modulated and unmodulated peak for phenanthrene injected at a split ratio of 100:1. It is important to note that both the total peak width and the total profile for phenanthrene have been preserved.
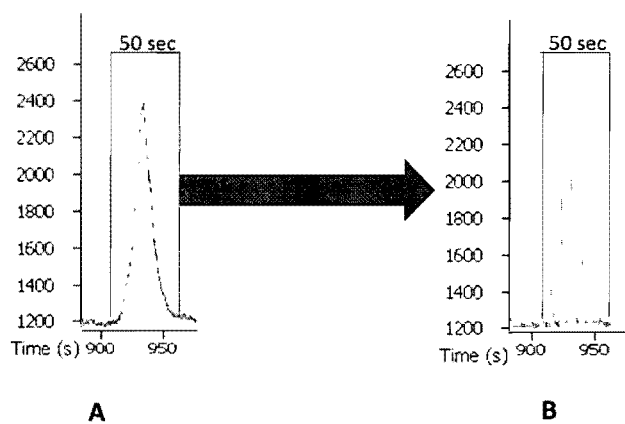
Figure 1-12 - 1 mg/mL phenanthrene at 100:1 S/R
(A) No peak Modulation, Modulator off
(B) Peak Modulated, Modulator on

This entire process is performed by a modulator located between the two columns. There are currently several modulators available for GCxGC systems. The most commonly used modulators are the thermal sweeper, Deans switch, and the cryotrap modulator. The Deans switch was discussed previously as the device responsible for controlling the flow of the sample into the second column in order to perform "heart-cuts" at certain points on the sample. This device has been used for comprehensive GCxGC, as discussed by Mondello, Lewis, and Bartle [33, 34]. In this research, a quad-jet cryotrap modulator was used. The modulator is often referred to as the "heart" of GCxGC, since it is primarily the device responsible for generating the orthogonal separation of the sample. A schematic of the modulator and the modulation process it undergoes is shown in Figure 1-13.

The cryotrap modulator uses alternating jets of cold and hot nitrogen gas to perform peak modulation in a two stage process[36]. The two cold jets focus the fraction of eluent to narrow the bandwidth and then ultimately split the narrow peak forming slices of eluent fraction. The two hot jets keep the fraction of eluent moving through the modulator thereby making the process continuous as well as preventing interference between the fractions. The nitrogen gas is cooled by liquid nitrogen which enters the instrument from a small dewar attached to the back of the GC oven. The dewar is directly attached to a tank of liquid nitrogen. The flow of the liquid nitrogen into the dewar is controlled by the data acquisition software or by the user[36].
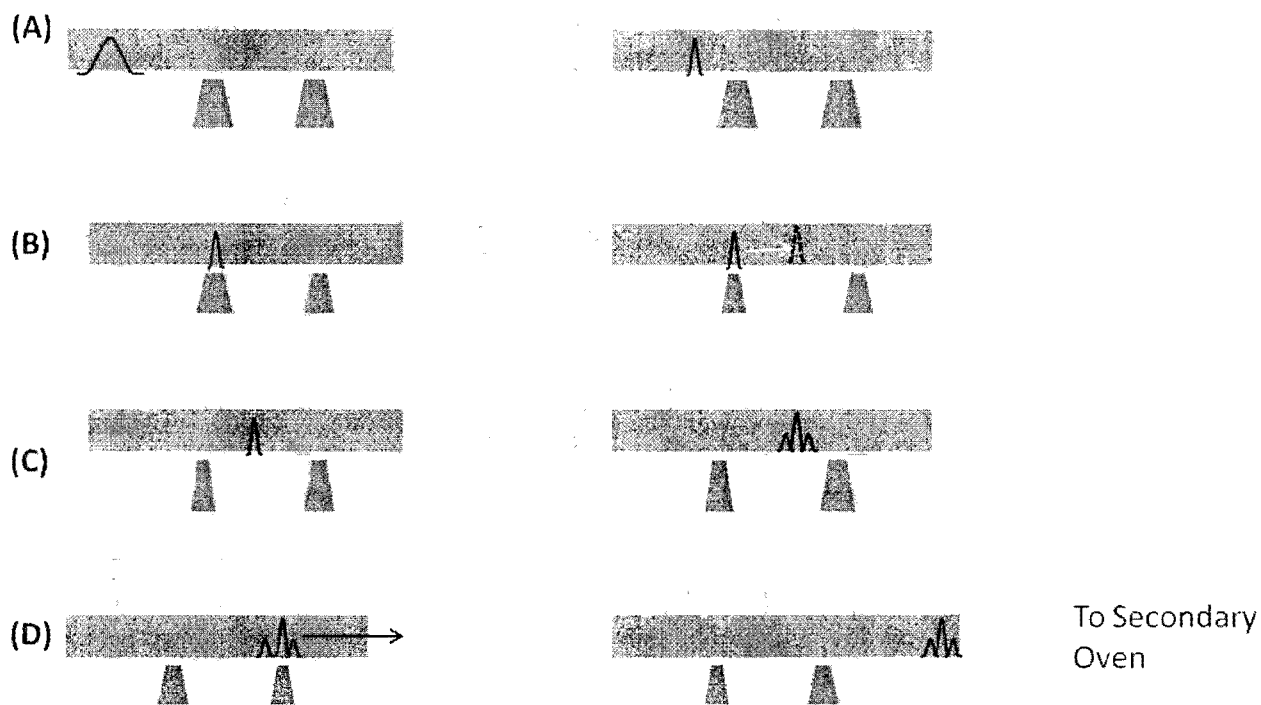
Figure 1-13 – Schematic of the cryotrap modulator and peak modulation process (A) 1st cold jet focuses peak of single component; (B) 1st hot jet moves peak to second cold jet ;(C) 2nd cold jet splits peak of component; (D) 2nd hot jet moves Peaks for component into secondary oven

One feature of the cryotrap modulator used is the length of time for the hot pulse is slightly shorter than that of the cold pulse. This is controlled by the system software as one of the fail-safes which prevent damage to the instrument or poor performance. This is critical is in order to preserve both the bandwidth of the sample fraction and the orthogonal separation. The time for the hot pulse and cold pulse times are determined based off total modulation period, or second dimension separation time. The software allows the user to change the modulation period, modulation temperature, and the hot pulse time for the hot jets, the instrument automatically calculates the necessary cold pulse time for the cold jets.

It is also important to note that the modulation process described above occurs continuously throughout an analysis of a sample. This enables the entire sample to pass through the modulator rapidly and also helps to prevent interference between the separations occurring on each column. However, sometimes part of eluent fraction will interact too strongly with the stationary phase in the second column preventing one or more of the second dimension peaks from eluting during the same modulation period. Instead, these peaks elute during a later modulation period and with a different fraction and literally become "wrapped around" the second column as seen in Figure 1-10.

Wraparound can be corrected by increasing the hot pulse time of the hot nitrogen jets of the modulator or by increasing the modulation, or second dimension separation, time. Since wraparound is due to the interaction of the sample with the stationary phase in the second column, increasing the hot pulse time of nitrogen jets or the modulation period mentioned above may have no effect as far as eliminating wraparound. Under these circumstance the only way to

eliminate wraparound is to replace the column with one that contains a stationary phase of a different polarity.

The modulator is also used to manipulate the retention of analytes on the second column during method development by changing the modulation period and the pulse time for the two hot nitrogen jets in the modulator[36]. Due to much smaller dimensions of the second column and in order to maintain fast separation in the second dimension, the length of time for the second dimension separation time is normally between 5 and 8 seconds and is dependent on the complexity of the sample matrix. For very complex matrices such as the BP oil samples, the time used was 8 seconds. The time used for simple matrix such as calibration standards was only 5 seconds. A longer modulation period was necessary for the oil samples in order to thoroughly separate the 100s of compounds and avoid wraparound in the second dimension. However, the shorter modulation period used for the calibration standards was enough to separate the single, desired analyte and minimize the amount of empty space on the contour plot. This point will be clearly illustrated in the next chapters upon discussion of the method development process used for GCxGC analysis of each sample.

The pulse time for the hot nitrogen jet can also be used to manipulate the retention time of analytes on the second column[36]. In order to prevent disrupting the peak focusing performed by the cold jets and to preserve the separation generated from the first column, the hot pulse time is normally between 0.60 sec and 1.2 sec. The hot pulse time it is limited by the modulation period and the interactions between the stationary phase of the second column and the analytes in

the sample. Thus, increasing the hot pulse time only slighty affects the second dimension retention time and is usually changed in to eliminate wraparound.

The final parameter of the modulator that can be changed is the temperature of the modulator. As a failsafe built-in to the software, the modulator temperature is held higher than the initial temperature of the secondary oven. However, the temperature of the modulator does not interfere with the peak modulation process nor does it affect the separation occuring on the second column. Thus, the main purpose of increasing the temperature of the modulator is to reduce overload of the sample on the second column.

1.5 Quadrupole and Time of Flight Mass Spectrometry

After the sample has been separated on both columns, it passes through a heated transfer line that serves to transfer the sample from the gas chromatograph to the mass spectrometer and also ensures that the sample remains in the gas phase upon entering the ion source of the mass spectrometer[41-43]. The temperature of the transfer line is dependent upon the type of analytes contained in the sample and must be high enough to keep the sample in the vapor state, but low enough that it does not degrade any of the analytes.

In the mass spectrometer, the volatile analytes are ionized, fragmented, analyzed, and then identified based on their fragmentation pattern. A typical mass spectrometer has three main parts: the ion source, the mass analyzer, and the detector in which the mass analyzer defines the sensitivity, resolution, and speed of the mass spectrometer. Common types of mass analyzers include magnetic sector, ion traps, quadrupoles, and time-of-flight analyzers. During this

research, quadrupole and time-of-flight mass analyzers were used. However, before discussing the theory and function of each these analyzers, the function of the ion source and detector will be discussed.

1.5.1 Role of the Ion Source

The main purpose of the ion source is to ionize and fragment the analytes in a given sample[42, 43]. There are two modes of ionization commonly used in gas chromatography- mass spectrometry: electron impact ionization(EI) and chemical ionization(CI). EI involves the removal of a valence electron from the atom with the lowest ionization energy in the structure of the analyte by bombarding it with high energy electrons resulting in the formation of an typically unstable radical-cation which then undergoes rearrangements and/or fragmentations depending on their structure[43, 44]. Thus, these fragments and rearrangements are unique are unique to each analyte, producing a "fingerprint" used to determine its structure.

CI differs from hard ionization in that it requires a separate reagent gas that collides with the analytes[42, 43, 45]. The energy required for this collision is much lower than EI resulting in less fragmentation of the analytes. Thus, this type of ionization is generally not used to determine the identity of a particular analyte, instead it is often used to determine the molecular weight of a particular analyte. CI mainly used with LC-MS for the analysis of non-volatile compounds, but it is also a common technique used in GC-MS for analytes that typically show a weak or non-existant signal for their molecular ions. Throughout the course of this research, EI was the only mode of ionization used and therefore will be the only mode that will be discussed. A schematic of the ion source is shown in Figure 1-14. The ion source has three main parts the heating block, the filament, and the repeller.
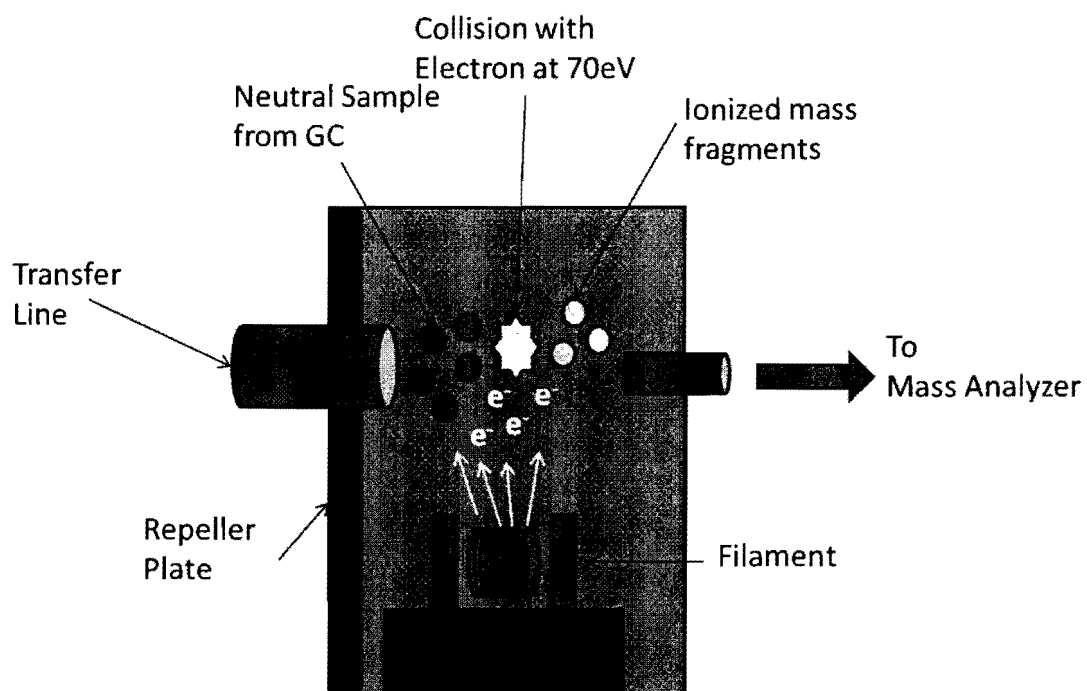
Figure 1-14 — Schematic of Electron Impact Ion Source.

The heating block is held at constant temperature and serves to keep the sample in the vapor phase as it comes out the transfer line, however like the transfer line, the temperature must be also be kept low enough to prevent the analytes from degrading and was kept between 200°C and 230°C for this work[41-43]. This was sufficient to prevent analyte degradation phase transition into the liquid phase.

The filament can be considered to be the heart of the ion source since it generates the high energy electrons necessary for removing the initial electron from the analyte. In EI mass spectrometry, the energy of the electrons from the filament is generally held at 70 eV. Further, the number of 70 eV is critical since the number of ions produced per the total numbers of molecules in a sample, or ion yield, is the highest at this level for most organic molecules[42-45]. Each analyte will fragment according to its structure and also according to the functional groups present by following three main unimolecular reactions: homolytic cleavage, heterolytic cleavage, and Hydrogen rearrangements[44]. Homolytic cleavage mechanisms involve the movement of one electron and often result in the formation of radicals. Heterolytic cleavage mechanisms involve the movement of an electron pair and often results in the neutralization of charged molecules or a transfer of charge from one atom to an adjacent one. Hydrogen rearrangements involves the overall rearrangement of the electrons in the molecule which may involve the formation of new bonds, breaking of bonds, and the shifting of hydrogen atoms in the fragment.

The mechanisms and rules that govern these three types of reactions, as well as the fragmentation of the major organic functional groups are described by McLafferty and will not be described in

detail here[44]. However, it is important to remember that all of the fragmentation reactions for EI are unimolecular. Collisions between the analytes result in secondary fragmentation known as collision induced dissociation(CID) and are considered a random phenomenon in EI. It results in the formation of small atypical fragments that can interfere with the signals of the expected fragments ultimately resulting in a noisy base line in the spectra.

CID is minimized in EI by the presence of the repeller within the ion source and the low vacuum of the MS system. The repeller pushes the fragments out of the ion source through a small opening leading to the mass analyzer. The pressure of the vacuum is kept at 10^{-5} torr or lower for a quadrupole mass analyzer by a diffusion pump and 10^{-7} torr for a time of flight mass analyzer by two turbomolecular pumps. The purpose is to remove a majority of the carrier gas from the system and also to slow the velocity of the ions during fragmentation in the ion source. Thus, although the type of vacuum pump used is dependent on the type of mass analyzer, their overall purpose is to create a "mean free path" for the ions as they travel through the mass analyzer[42, 43, 45]. The "mean free path" in the time-of-flight used in this work was two meters, which was approximately four times as long as the "mean free path" or the quadrupole. Certain features within each mass analyzer also help to maintain the "mean free path" and will be discussed in a later section. The important point to remember is that the ion source used with both types of mass analyzers is the same and therefore, performs the same functions.

1.5.2 Function of the Detector

Like the ion source, the same type of detector was also used for both techniques. The detector used is known as an electron multiplier tube(EMT) and is the standard type of detector for most MS systems regardless of the type of analyzer or mode of ionization used[41- 45]. Figure 1-15
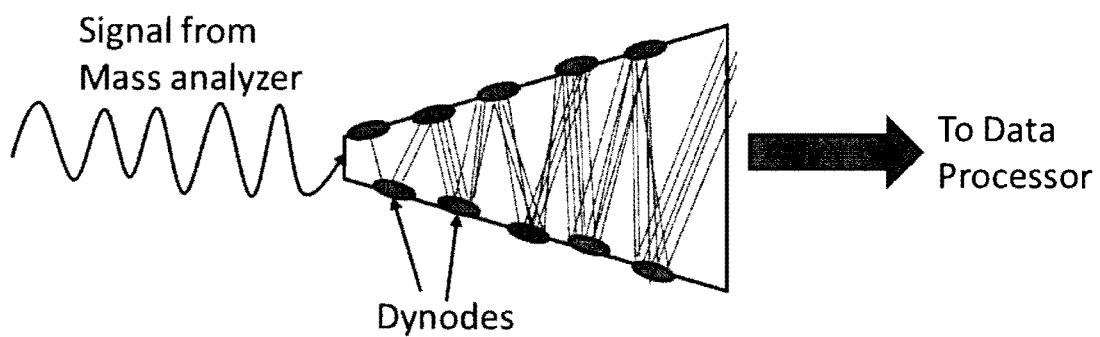
Figure 1-15 – Schematic of electron multiplier tube(EMT) detector

shows a schematic of a typical EMT detector. The purpose of the device is to count the number of each mass fragment and to amplify the signal produced by the ion after it reaches the detector. The shape of the detector suggests it functions similar to that of a reverse funnel. The ion enters at the narrow end and is converted into a current in the form an electron which travels through the detector in a zig-zag pattern by rebounding off the walls until the amplified current exits at the wider end. The walls of the detector are lined with a series of continuous diodes that doubles the number of electrons each time they strike the wall thereby ultimately amplifying the current by about one million times[42, 43]. The amplified current for each analyte is converted into a mass spectrum by a computer. This process is the same for both quadrupole and time-of-flight mass spectrometry.

It is also important to note that the sensitivity of the technique, detection limit, and quantitation limit are established by the detector, however, they are controlled by the type of mass analyzer used. For example, a quadrupole mass analyzer having an EMT detector can produce the detection limits in the range of low nanograms whereas a time-of-flight mass analyzer also having an EMT produces detection limits at least two orders of magnitude lower[42, 43]. The ion source can produce a higher background noise and greater interferences observed in the mass spectra if oxidation inside the source is allowed to build-up due to not cleaning the ion source or a leak in the system resulting a in high pressure vacuum. Thus, although the same type of detector and ion source is used in instruments, it is the mass analyzer that determines the thresholds for between the sensitivity and limit of detection.

1.5.3 Mass Analyzers

1.5.3.1 Quadrupole: Theory of Operation

A typical quadrupole mass analyzer consists of four parallel steel or quartz rods arranged at right angles to each other where each has an electrostatic charge, two of the poles have a positive charge and two of the poles have a negative charge. There is also a radio frequency around all four poles that induces a magnetic field. Figure 1-16 shows a schematic of a typical quadrupole mass analyzer, indicating the charge of each pole.

The ions move through the center of the quadrupole in a spiral pattern created by the combination of the electrostatic charges on each of the poles and the magnetic field[42, 43, 45]. The strength of the electrostatic and magnetic fields in the poles is dictated by the mass range entered by the user thereby allowing only ions falling within the mass range to reach the detector. Ions with masses that do not fall within the scan range collide with one of the poles and are not detected. Further, the quadrupole has two modes of operation: scanning and selected ion monitoring(SIM). When the quadrupole is in scan mode, the electrostatic potential of the four poles is held constant to ensure that the ions move along a straight path through the center of the four poles. The radio frequency oscillates when the quadrupole is in scan mode causing the ions to move in a spiral fashion through the center of the quadrupole along a "mean free path". The trajectory of the ions is given by Equation 1-18[42, 43]:

$$\phi = 2(U + V \cos at) \qquad\qquad\qquad \text{(Equation 1-18)}$$
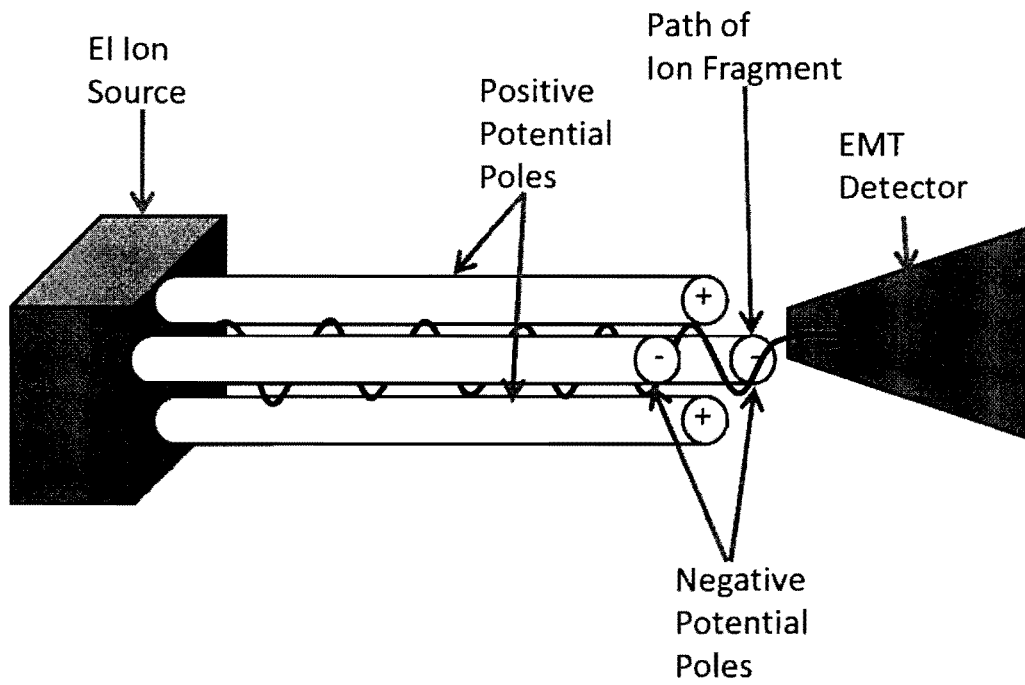
Figure 1-16 – Schematic of Quadrupole Mass Analyzer

In the equation above, U is the electrostatic potential for the 4 poles, V is the potential of the radio frequency, a is a constant based on the scan range of mass-to-charge ratios(m/z) selected by the user, and t is the total time for the scan. It is important to note that the signs for U and V can also be negative to account for the negative electrostatic potential produced by negative charge on two of the poles. When the quadrupole is operating in SIM mode, only specific m/z ratios, set by the user, are allowed to reach the detector. In this case, both the electrostatic and the radio frequency are held constant thereby increasing the selectivity of the quadrupole by eliminating the signals from the additional analytes present in the sample. This increases the selectivity of the quadrupole and results in higher abundance and S/N ratio for the m/z ratios selected.

Although a quadrupole is the one of the most popular types of mass analyzers and is considered to have good sensitivity, reaching detection limits on the order of low nanograms, the speed of analysis for a single sample is limited. The reason is due to the limited scan rates that are typical of the quadrupole. The scan rate refers to the number of full acquisition scans of the mass spectra produced across one peak on the chromatogram. Thus, the low scan rates of a typical quadrupole result in jagged, misshapen peaks in the reconstructed total ion chromatogram (RTIC) and higher noise levels in the chromatogram and mass spectra[42, 43]. This results in lower overall sensitivity since the higher noise levels produce greater interference with the analyte signals thereby lowering the S/N ratio. A higher scan rate decreases the baseline noise in the mass spectra of the analytes and generates a smoother reconstructed total ion chromatogram (RTIC) thereby generating a higher S/N for each analyte detected.

As discussed above, using SIM mode increases the selectivity of the quadrupole, it does not affect the sensitivity, since the electrostatic charge and magnetic field are kept constant resulting in a scan rate of zero. Thus, SIM is often used to confirm or deny the presence of a particular analyte in a sample[42, 43]. However, since the enhanced selectivity of SIM mode often results in a reduction of background noise and higher S/N for the analytes, it can be argued the SIM does increase the sensitivity of the quadrupole. The discussion above demonstrates that quadrupole mass analyzers are that is suitable for identifying and quantifying the components present in simple and clean samples such as standards and purified extracts. However, in order to identify all of the analytes separated as result of GCxGC analysis, a faster and more sensitive mass analyzer, such as time-of-flight, is required. The theory of operation and comparison to the performance of quadrupole are discussed below.

1.5.3.2 Time-of-Flight: Theory and Operation

Time-of-flight mass analyzers sort the ions of a sample based on their respective kinetic energies. The equations for kinetic and potential energy are in Equation 1-19 and Equation 1-20, respectively.

$$kE = \frac{1}{2}mv^2$$
(Equation 1-19)

$$pE = qV$$
(Equation 1-20)

In Equation 1-19, m and v are the mass and velocity of the ion, respectively. In Equation 1-20, q is the charge of the ion and V is the accelerating potential of the repeller. Time of flight systems operate on the assumption that the potential energy and the kinetic energy for each ion are equal

to each other. Therefore, combining the equations for the potential and kinetic energy yields

Equation 1-21:

$$qV = \frac{1}{2}mv^2$$

(Equation 1-21)

Rearranging this equation yields the expression for the velocity shown by Equation 1-22:

$$\sqrt{\frac{2Vq}{m}} = v$$

(Equation 1-22)

The relationship states that the velocity of the ion is inversely proportional to the m/z ratio of the

ion meaning that smaller ions will travel faster than larger ions[46]. Since velocity is defined as

distance travelled over time, the equation above can be further manipulated into the expression

for the time it takes an ion to travel through the mass analyzer Equation 1-23:

$$t = L\sqrt{\frac{m}{2Vq}}$$

(Equation 1-23)

In the equation above, t is the time an ion spends in the flight tube, L is the length of the tube, m

is the mass of the ion, V is the accelerating potential of the repeller, and q is the charge of the

ion[46]. It must be stressed that the time, t, only refers to the time the ion spends in the flight

tube, this does not include the time spent in the ion source or in the reflectron. Calculations of

these quantities are beyond the scope of this thesis and will not be discussed here.

A schematic for the time of flight mass analyzer used in this work is shown in Figure 1-17. The

first part of the flight tube, known as the time lag focusing region, consists of a series of

electrostatic steering plates that serve to decelerate the ions until they have a velocity of zero

thereby giving the ions a constant kinetic energy prior to travelling down the flight tube[42, 43,

46]. This region also regulates the flow of ions using short pulses of energy from the electrostatic
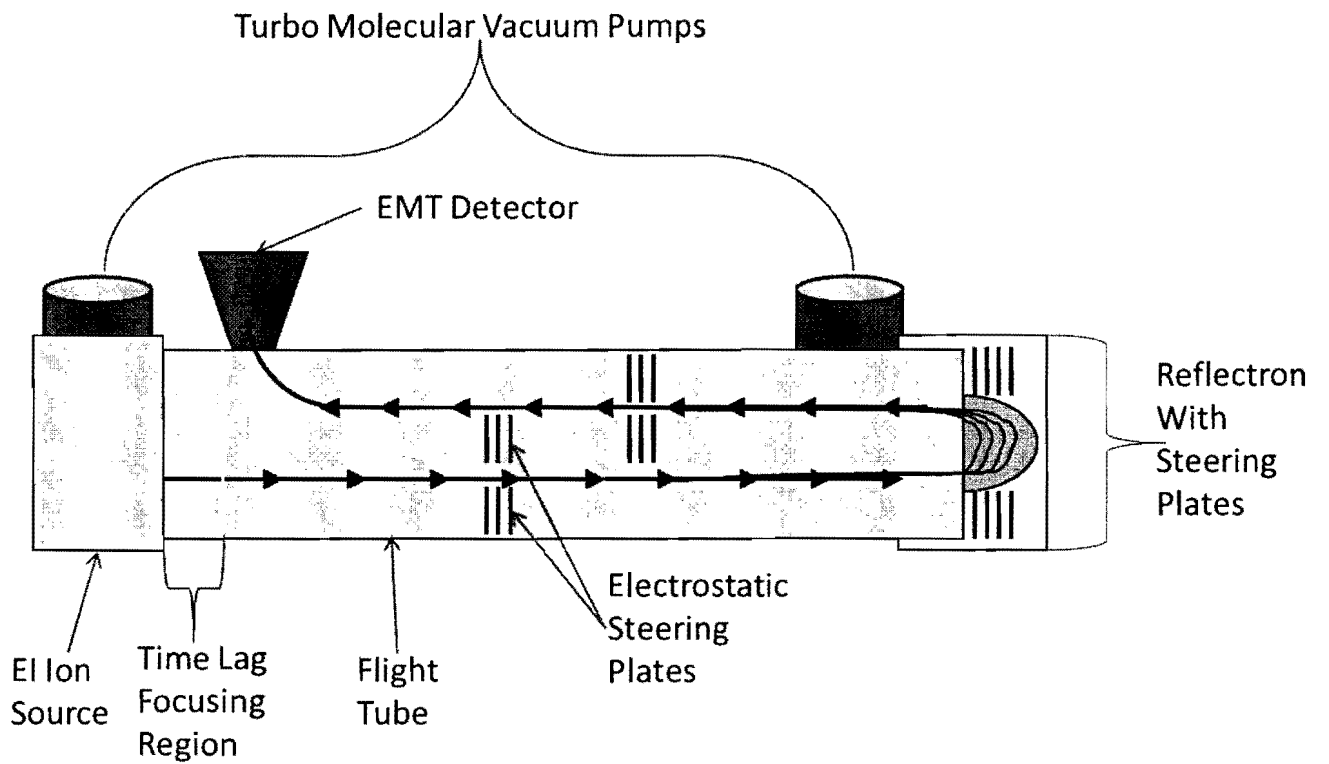
Figure 1-17 – Schematic of Time-of-Flight Mass Analyzer

plates so that the ions travel down the flight tube in small packets. This prevents interference between other ions and secondary collisions from occurring within the flight tube. Thus, time-lag focusing ultimately serves to preserve the spatial arrangement of the ions, the distance between the individual ions, and the distance between the ion packets resulting in an increase in the overall resolution of the technique. The speed at which the ions travel down the 1 meter flight tube is dependent upon their m/z ratios as described from Equation 1-23 above. The flight tube contains a series of electrostatic steering plates that ensure the ions travel the length of the flight tube in a linear fashion along a "mean free path".

At the opposite end of the flight tube is a mirror surrounded by another series of electrostatic plates called a reflectron. The purpose of the reflectron serves to turn the ions packets around allowing the ions in each packet to travel 1 meter up the flight tube in the reverse direction reaching the EMT detector at the same time. The ions penetrate the reflectron based on their m/z to charge ratio and their velocity. Larger ions with slower velocities penetrate the reflectron less than the smaller ions with higher velocities. Thus, the ion packets traveling along the reverse path up the flight tube to the detector maintain a constant velocity and preserve resolution regardless of the m/z ratios of the individual ions. This process is accomplished by the electrostatic plates surrounding the reflectron that decelerate and accelerate the ions as they pass through the reflectron.

Time of flight systems are known for their high sensitivity, high resolution, and faster scan rates in comparison to quadrupole MS systems. However, they cannot perform as a high resolution technique and a rapid scanning technique simultaneously. High resolution ToFMS produces

exact mass determination of analytes, but requires lower scan rates, thereby resulting in overall

slower analyses. ToFMS using rapid scan rates produces full scan mass spectra for all analytes,

but requires lower resolution, resulting in less accurate analyte masses detected. Therefore,

speed must be sacrificed to achieve high resolution and vice versa. However, the speed capable

with ToFMS make it the preferred technique to use in conjunction with GCxGC.

A final point to discuss in regards to MS systems is peak deconvolution which allows the data

processing system to pinpoint the location of a specific m/z ratio in the total ion

chromatogram(TIC). This allows the user to isolate the mass corresponding to a specific

compound in a complex sample, such as the presence of methamphetamine in a urine sample.

The isolated mass is known as an extracted ion chromatogram(EIC) which shows only peaks for

ions only corresponding to the isolated mass. ChromaTOF and Chemstation both have a peak

deconvolution algorithms built into the data processing software allowing the user to input

multiple masses producing multiple EICs on a single chromatogram. Due to the higher

sensitivity of the ToFMS system, the EICs produced by the software have a more stable baseline

in the spectra and higher S/N ratios for the masses identified. ToFMS also has a virtually

unlimited mass range allowing the system to isolate ions corresponding to an m/z ratio of any

size. Quadrupoles can only detect masses as high as approximately 1000 amu and also has a

lower sensitivity limiting them to analyzing and detecting only small molecules from less

complex samples.

In this chapter, the basic functions and advantages of using SPME-GCxGC-ToFMS have been

discussed. Previous studies have shown how effective SPME or GCxGC-ToFMS have been

when used individually for the analysis of street drugs[47-54]. The remainder of the thesis will discuss the application of SPME-GCxGC-ToFMS as one of the most effective tools for the analysis of the various street and designer drugs extracted from urine and well as an environmental application of the technique for the analysis of oil samples. The results will show that not only is SPME-GCxGC-ToFMS capable of achieving much lower LODs and LOQs for each drug that are well below the accepted toxicological limits, but it will also show that the technique is effective for identifying various impurities and drug metabolites present in complex samples. It is expected that the work from this thesis will provide the groundwork for obtaining impurity profiles for each of the drugs analysis which can be beneficial to law enforcement and forensic scientists in targeting known drug traffickers and drug dealers.

CHAPTER 2 - MATERIALS AND METHODS

2.1. Materials

2.1.1 Drug Standards

Cocaine, methamphetamine, and 3,4-methylenedioxymethamphetamine(MDMA) drug standards

at concentrations of 1 mg of each drug dissolved in 1 ml of methanol were purchased(Restek,

Inc. Bellefonte, PA). Ketamine drug standards at a concentration of 1 mg of the drug dissolved

in 1 ml of methanol were purchased (Alltech Associates, Inc. Deerfield, IL). 10 mg solid

standards and 10 mg 'Dilute N' Shoot' standards of salvinorin A were also purchased. (Alltech

Associates, Inc. Deerfield, IL). In addition, solid 1-dehydro-17α-methyl-testosterone and

caffeine were purchased (Sigma-Aldrich, Inc. St. Louis, MO).

2.1.2 Oil Samples and Standards

Two samples of BP crude oil were collected from the surface of the Gulf of Mexico. One sample

was taken from one of the mousse patties and one sample was taken from one of the oil slicks

closer to the shoreline near Venice, LA. Two samples of BP oil were at different depths in the

Gulf of Mexico. One sample was taken from the well-head below the ocean floor and the other

sample was taken from the oil rising from the fractured pipe approximately 1 mile below the

surface. All BP oil spill samples were provided by Dr. John R. Sowa. Alkane standards and EPA

Method 8270 MegaMix standards were purchased (Restek, Inc. Bellefonte, PA). EPA Method

610 standard of polyaromatic hydrocarbons(PAH) was also purchased (Supelco Bellefonte, PA).

2.1.3 Biological Samples

Urine was provided by human volunteers and pooled before use. *Salvia divinorum* plants were

provided by Mr. Eric Stroud. *Salvia apiana* and *Salvia dorii* incense sticks were purchased (East

Meets West Toms River, NJ). *Salvia officinalis* was provided by the author of this thesis.

2.1.4 US Currency samples

One dollar banknotes of US currency were provided by the author of this thesis.

2.2. Methods

2.2.1 Preparation of Calibration Standards

2.2.1.1 Cocaine

Duplicate sets of standards with a concentration range of 2 ppm to 500 ppm were prepared by

serial dilution using an adjustable pipette. A summary of all calibration standards prepared for

cocaine is shown in Table 2-1. An aliquot of 5 μL of the 1mg/mL drug standard was transferred

to a fresh 2 mL autosampler and diluted to 2 mL with methanol yielding a working standard with

a concentration of 10 ppm. The working standard was used to prepare calibration standards

below 10 ppm which are also included in Table 2-1.

Two additional sets of calibration standards for cocaine were prepared for the extraction of

cocaine from deionized water and urine using SPME. The standards were prepared by serial

dilution with a concentration range of 31 ppb to 500 ppb using a adjustable pipette. The pH of

the deionized water was kept at its ambient pH of 6.5 and not adjusted for this experiment. Urine

was adjusted to a pH of 14 using 1.0 M NaOH. An aliquot of 10 μL of the 1 mg/mL drug

standard was spiked into a 20 mL urine sample yielding a working standard with a concentration of 1 ppm. The calibration standards prepared for SPME are also summarized in Table 2-1.

2.2.1.3 Salvinorin A

A 10 mg salvinorin A 'Dilute N' Shoot' standard was dissolved in 10 mL of deionized water yielding a concentration of 1 mg/mL salvinorin A served as the stock solution used to prepare calibration standards for LLE. Two working standards, each with a concentration of 5 ppm salvinorin A, were prepared using an aliquot of 100 µL of the 1mg/mL stock solution was spiked into separate samples of 20 mL deionized water. Duplicate sets of calibration standards were prepared from the working standard by serial dilution using an adjustable pipette with a concentration range of 310 ppb to 5 ppm. Preparation of the calibration standards is summarized in Table 2-2. A 10 ppm solution of 1-dehydro-17α-methyltestosterone was prepared and used as the internal standard. Aliquots of 10 µL were added to the spiked water samples.

A second stock solution prepared in the same manner as described above served as the stock solution used to prepare calibration standards for SPME. Two working standards, each with a concentration of 1ppm salvinorin A, were prepared using an aliquot of 20 µL of the 1mg/mL stock solution spiked into separate samples of 20 mL deionized water. Duplicate sets of calibration standards were prepared by serial dilution using an adjustable pipette with a concentration range of 8 ppb to 500 ppb. Preparation of these calibration standards are also summarized in Table 2-2. The same volume of the internal standard described above was added to each sample.

Cocaine calibration standards prepared				
Standard	Initial conc.(µg/mL)	Aliquot(µL)	Final Conc.(µg/mL)	Final Volume(mL)
1	1000	15	15	1
2	1000	31	31	1
3	1000	62	62	1
4	1000	125	125	1
5	1000	250	250	1
6	1000	500	500	1
Cocaine calibration standards prepared from working standard				
Standard	Initial conc.(µg/mL)	Aliquot(µL)	Final Conc.(µg/mL)	Final Volume(mL)
1	10	200	2	1
2	10	400	4	1
3	10	800	8	1
Cocaine calibration standards prepared for analysis using SPME				
Standard	Initial conc.(µg/mL)	Aliquot(mL)	Final Conc.(ng/mL)	Final Volume(mL)
1	1	0.31	15	20
2	1	0.62	31	20
3	1	1.25	62	20
4	1	2.5	125	20
5	1	5	250	20
6	1	10	500	20

Table 2-1 – Calibration standards prepared for cocaine.
All standards were diluted to their final volume using methanol.

Preparation of Salvinorin A calibration standards used for LLE

Standard	Initial Conc.(µg/mL)	Aliquot(mL)	Final Conc.(µg/mL)	Final Volume(mL)
1	5	1.25	0.31	20
2	5	2.5	0.62	20
3	5	5	1.25	20
4	5	10	2.5	20
5	5	20	5	20

Preparation of Salvinorin A calibration standards used for SPME

Standard	Initial Conc.(µg/mL)	Aliquot(mL)	Final Conc.(µg/mL)	Final Volume(mL)
1	1	0.16	0.008	20
2	1	0.32	0.015	20
3	1	0.64	0.031	20
4	1	1.25	0.062	20
5	1	2.5	0.125	20
6	1	5	0.25	20
7	1	10	0.5	20

Table 2-2 – Calibration Standards prepared for salvinorin A. Duplicate sets of standards were prepared. One set was diluted to final volume using Deionized water. The other set was diluted using urine.

2.2.1.4 Individual drugs in Yaba

Duplicate sets of calibration standards were prepared using an adjustable piptte for

methamphetamine, caffeine, ketamine, and MDMA for the extraction from water and urine using

SPME. The concentration range was 31 ppb to 500 ppb for all four drugs. Preparation of

calibration standards for each drug is summarized in Table 2-3. The urine was adjusted to a pH

range of 8 to 8.5 using 1M NaHCO₃. Working standards of 1 ppm were prepared for each of the

four drugs by spiking a 10 µL aliquot of each of the 1 mg/mL stock solutions into 20 mL

samples of deionized water.

2.2.2 Yaba Design of Experiments(DOE)

Yaba mixtures containing various concentrations of methamphetamine, MDMA, ketamine, and

caffeine were prepared using a full factorial DOE in order to determine the number of necessary

samples to prepare and analyze. The number of necessary experiments using a full factorial DOE

is determined by the number of critical variables to be analyzed in each experiment. A high and a

low level to conduct the analysis of each variable are selected and remains constant throughout

the DOE. The number of necessary experiments to perform is determined by Equation 2.1.

$$\# \text{ of levels}^{\# \text{ of variables}}$$ (Equation 2.1)

The number is the total number of experiments required to analyze each critical variable at each

of the levels. Yaba consists of four active drugs, however methamphetamine is known to be the

primary active drug in Yaba and was not considered as a critical variables. Therefore, the three

other drugs in Yaba were identified as the critical variables used to prepare the DOE.

Concentrations of 500 ppb and 31 ppb were selected as the high and low levels, respectively.

Equation 2.1 was used to determine that the number of yaba mixtures to prepare was equal to

eight. Table 2-4 shows the full factorial DOE matrix used to prepare each of the eight mixtures.

Preparation of Caffeine calibration standards			
Standard	Initial Conc.(µg/mL)	Aliquot(mL)	Final Conc.(ng/mL)	Final Volume(mL)
1	1	0.62	31	20
2	1	1.25	62	20
3	1	2.5	125	20
4	1	5	250	20
5	1	10	500	20

Preparation of Methamphetamine calibration standards			
Standard	Initial Conc.(µg/mL)	Aliquot(mL)	Final Conc.(ng/mL)	Final Volume(mL)
1	1	0.62	31	20
2	1	1.25	62	20
3	1	2.5	125	20
4	1	5	250	20
5	1	10	500	20

Preparation of MDMA calibration standards			
Standard	Initial Conc.(µg/mL)	Aliquot(mL)	Final Conc.(ng/mL)	Final Volume(mL)
1	1	0.62	31	20
2	1	1.25	62	20
3	1	2.5	125	20
4	1	5	250	20
5	1	10	500	20

Preparation of Ketamine calibration standards			
Standard	Initial Conc.(µg/mL)	Aliquot(mL)	Final Conc.(ng/mL)	Final Volume(mL)
1	1	0.16	8	20
2	1	0.32	15	20
3	1	0.62	31	20
4	1	1.25	62	20
5	1	2.5	125	20
6	1	5	250	

Figure 2-3 – Preparation of Calibration Standards for four drugs
in Yaba. Duplicate sets of each were prepared. One set was diluted
To final volume using deionized water. The other was diluted to final
Volume using human urine at pH 8.0.

	Methamphetamine(ppb)	MDMA(ppb)	Ketamine(ppb)	Caffeine(ppb)
1	750	500	500	500
2	750	500	500	31
3	750	500	31	500
4	750	500	31	31
5	750	31	500	500
6	750	31	500	31
7	750	31	31	500
8	750	31	31	31

Table 2-4 – Full Factorial Design of Experiments used for the analyses
Of the complete Yaba mixture

The concentration of methamphetamine was held constant at a concentration of 0.75 ppm for each of the eight samples. An aliquot of 15 µL of the 1 mg/ml methamphetamine drug standard was spiked into eight 20 mL samples of deionized water. The high concentrations were prepared by spiking an aliquot of 10 µL of the 1 mg/mL stock solution into 20 mL samples of deionized water yielding a final concentration of 500 ppb. Working standard at concentrations of 1 ppm were prepared for ketamine, caffeine, and MDMA by spiking an aliquot of 20 µL of the 1 mg/mL stock solution into 20 mL of deionized water. The low concentrations were prepared by spiking an aliquot of 620 µL of the working standard at 1 ppm into 20 mL samples of deionized water yielding a final concentration of 31 ppb.

2.2.3 Degradation Studies

2.2.3.1 Cocaine

A 1mg/mL cocaine standard was used for the degradation study. The standard was exposed to the laboratory conditions and injected in triplicate once a day for two weeks. The peak area and peak height of cocaine for any of the major metabolites that appeared in the chromatogram were monitored over the two week period. The structures of these major metabolites are shown in Figure 4-1.

2.2.3.2 Salvinorin A

Approximately 200 mg of *S.divinorum* leaves were soaked for 48 hours in methanol. The sample was held at 60°C and agitated with a magnetic stir bar at a speed of 100 rpm. Salvinorin A was extracted using the procedure described below. The extracts were injected twice noting the peak areas and peak heights of salvinorin A and any of its related analogues. Salvinorin A and its analogues are shown in Figure 5-1.

2.2.4 Extraction Methods

2.2.4.1 Solid-Liquid Extraction of Cocaine from US banknotes

Each banknote was soaked in approximately 15 mL of methanol for 3 hours followed by water

bath sonication for 15 minutes at room temperature. The banknotes were removed from the

liquid extract and rinsed with methanol to remove any loose cocaine from the surface. Methanol

was evaporated to dryness under N_2 gas at $40^{\circ}C$. The extracts were reconstituted with 0.5 mL of

methanol.

2.2.4.2 Liquid-Liquid Extraction of Salvinorin A from Salvia divinorum

Approximately 200 mg of leaves, stems, and roots were separated and ground using mortar and

pestle to extract plant chemicals and Salvinorin A hallucinogenic drug. Approximately 15 ml of

water was added to both the leaf and stem samples. Samples were vortexed for 1 min

immediately followed by water bath sonication at room temperature for 30 min. Samples were

vacuum filtered using a Buchner funnel and Whatman No.1 filter paper. The samples were

washed with three 5 ml aliquots of water. The filtrate was collected and the plant material was

discarded from each sample. Filtrates were placed into a 125 ml separatory funnel and

approximately 20 ml of chloroform was added to the funnel. Samples were vigorously shaken

and the funnel was vented three times. The layers were allowed to separate for approximately 15

minutes. The organic layer(bottom layer) was collected and dried down under N_2 gas at $40^{\circ}C$.

The extracts were reconstituted with 0.50 ml of chloroform.

2.2.4.3 Liquid-Liquid Extraction of Salvinorin A from spiked water and urine samples

One set of the water samples spiked with salvinorin A concentrations between 310 ppb and 5 ppm were added to separate 125 mL separatory funnels. A volume of 15 mL of chloroform was added to each funnel. Each funnel was shaken for one minute and vented three times. The layers were then allowed to separate for five minutes. The aqueous layer was removed and discarded. A 10 mL aliquot of the organic layer was collected and dried under N_2 gas at a constant temperature of 40°C. The residue was reconstituted with 0.5 ml of chloroform.

One set of the urine samples also spiked with salvinorin A concentrations between 310 ppb and 5 ppm were placed in separate 50 ml Erlenmyer flasks, vortexed for 1 min immediately followed by water bath sonication for 30 min. Each urine sample was vacuum filtered using a Buchner funnel and No.1 Whatman filter paper to remove salts, proteins, fats, etc. that may have been present in the urine. Each sample was washed with three 5 ml aliquots of chloroform. The filtrates were collected and added to separate 125 ml separatory funnel. A volume of 15 mL of chloroform was added each funnel and they were shaken vigorously for one minute and vented three times. The layers were allowed to separate for 2 hours. The aqueous layer was removed and discarded. A 10 mL aliquot of the organic layer was collected and dried under N_2 gas at 40°C. The extract was reconstituted with 0.50 ml of chloroform.

2.2.4.4 SPME of cocaine from water and urine

The water and urine samples spiked with cocaine were incubated at 30°C for 10 min at 250 rpm. Cocaine was extracted using a polydimethylsiloxane (PDMS) with a thickness of 100 μm. The extraction time was 30 minutes at an agitation speed of 250 rpm and a temperature of 30°C. The fiber was desorbed in the GC inlet at a constant temperature 250°C for 1 minute. The fiber was

kept in the inlet to bakeout for 11 minutes. The fiber was also baked out for an additional 20 min

between extractions in order to eliminate carryover. All of the SPME extractions were fully

automated using a GERSTEL MPS-2 Autosampler.

2.2.4.5 SPME of Salvinorin A from water and urine

The duplicate sets of urine and water samples spiked with concentrations of salvinorin A

between 8 ppb and 500 ppb were incubated at 30°C for 10 minutes. Salvinorin A was extracted

from the water and urine using a polyacrylate fiber with 85 μm film thickness from

Supelco(Bellefonte, PA). The extraction time was 30 minutes at an agitation speed of 250 rpm

and a temperature of at 30°C. Desorption of the Salvinorin A from the fiber was conducted in the

GC inlet and held at a constant temperature of 280°C with a desorption time of 1 minute. The

fiber was kept in the inlet and allowed to bake out for 13 minutes. The fiber was also baked out

for an additional 20 minutes between extractions in order to eliminate carryover.

2.2.4.6 SPME of Methamphetamine, MDMA, Ketamine, and Caffeine from water and urine

Samples spiked with methamphetamine were incubated for 10 minutes at 30°C and 250 rpm.

Methamphetamine was extracted using a polydimethylsiloxane-divinylbenzene(PDMS-DVB)

fiber with a thickness of 65μm. The extraction time was 30 minutes at an agitation speed of 250

rpm and a temperature of at 30°C. Desorption of the methamphetamine from the fiber was

conducted in the GC inlet and held at a constant temperature of 250 °C with a desorption time of

1 minute. The fiber was kept in the inlet and allowed to bakeout for 11 minutes. The fiber was

also baked out for an additional 20 minutes between extractions to eliminate carryover. Samples

spiked with MDMA and ketamine were extracted under the same conditions. The fiber was

baked out for 30 minutes between ketamine extractions due to carryover of the drug observed

with shorter bakeout times. Samples spiked with caffeine were incubated for 10 minutes at 40°C and 250 rpm. The remainder of the extraction conditions were the ones used for methamphetamine and MDMA.

2.2.4.7 SPME of Yaba from water and urine

Samples spiked with the full Yaba mixture were incubated for 10 min at 37°C and 250 rpm. The four drugs in the mixture were extracted using a PDMS-DVB fiber with a thickness of 65 μm. The extraction time was 40 minutes at 37°C and 250 rpm. Desorption of the drug mixture was conducted in the GC inlet constant temperature of 250°C for 1 minute. The fiber kept in the inlet and allowed to bake out for 11 minutes. The fiber was also baked out for an additional 30 minutes between extractions to eliminate carryover.

2.2.4.8 Extraction of the BP oil samples

Each of the oil samples were extracted using liquid-liquid extraction with dichloromethane. Aliquots of 3-5 mLs of each oil sample was added to a 20 mL headspace vial. A volume of 5 mL of dichloromethane was added each of the vials. The samples were shaken for 1 minute and the layers were allowed to separate for 5 minutes. Aliquots of 1 mL were transferred to 2 mL autosampler vials for instrumental analysis.

2.2.5 Instrumental Conditions

2.2.5.1 Cocaine

2.2.5.1.1 GC-MS

An Agilent GC Model 6890 and Agilent MSD Model 5973N equipped with a single rail ATAS autosampler was used for the analysis with GC-MS. A 15m column with a 0.25mm internal

diameter(I.D.) and 0.35μm DB-5 stationary phase film thickness(F.T.) was used for the analysis. The flow rate was 1.0 mL/min at constant flow. injections Samples were injected with a volume of 1.0 μL ±0.1 μL in splitless mode at purge times of 0.25 min, 0.50 min, and 0.75 min with the inlet at 250°C. The temperature ramp was 150 °C to 290 °C at a rate of 10 °C/min. The initial and final temperature hold times were each 1.00 min. The MSD temperature was 280 °C and the solvent delay time was set to 4.00 min. The scan range was 40 amu to 350 amu and the ions used for SIM mode were m/z:81-83, m/z: 94, m/z: 96, m/z: 105, m/z: 182, and m/z: 303.

2.2.5.1.2 GCxGC-ToFMS

A Leco® Pegasus 4D GCxGC-ToFMS system equipped with an Agilent GC Model 6890 and a GERSTEL MPS-2 autosampler was used for all analyses discussed in this thesis. A 30m x 0.25mm x 1.0 μm with an RTX-5MS stationary phase and a 1.5m x 0.10mm I.D. x 0.10 μm F.T. with an RTX-200 stationary phase were used as the column set. The flow rate was 1.0 mL/min at constant flow corrected via pressure ramps for both columns. Samples were injected with a volume of 1.0 μL ±0.1 μL in splitless mode at a purge time of 1.00 min with the inlet temperature at 250°C. For liquid injection samples were also analyzed in split mode with split ratios of 2:1, 4:1, 10:1, 20:1, 40:1, 50:1, and 100:10. SPME samples of cocaine were analyzed under splitless conditions only. The temperature ramp for the first column was 100°C to 290°C at 20°C/min with a hold time at the initial temperatures of 2.00 min and a hold time at the final temperature of 8.00 min. The temperature ramp for the second column was110°C to 300°C at 20°C/min with a hold time at the initial temperatures of 2.00 min and a hold time at the final temperature of 8.00 min. The temperature offset between ovens was 10°C. The modulator temperature was set at an initial temperature of 135°C. The modulation period was 5 seconds with a hot pulse time of 0.90 seconds and a cold pulse of 1.60 seconds. The transfer line and ion

source temperatures were 235°C and 200°C, respectively. The scan range was 45 amu to 550 amu at a scan rate of 100 spectra/second and a solvent delay time of 500 seconds.

2.2.5.2 Salvinorin A

The column set used for the qualitative study was a 15m x 0.250mm x 0.250μm of ZB-5 from Phenomenex(Tarrance, LA) and a 1.5m x 0.100mm x 0.100μm of RTX-200 from Restek(Bellefonte, PA). The column set used for the quantitative study was 15m x 0.250mm x 0.25μm of ZB-5 and 1.5m x 0.250mm x 0.25μm of DB-17 from Agilent(Wilmington, DE) as the first and second columns, respectively. The inlet was ran under splitless conditions with a 60 second purge time. The inlet temperature was held constant at 280°C. The flow rate through both columns was held constant at 1.0 ml/min. The temperature ramps for the 1st and 2nd columns in the qualitative study were 60°C to 300°C at 30°C/min and 65°C to 305 °C at 30°C/min, respectively, with a 5 °C offset between the primary and secondary ovens. The temperature ramps for the 1st and 2nd columns for the quantitative study were 60°C to 300 °C at 30°C/min and 75 °C to 315 °C at 30 °C/min, respectively. The hold times at the initial and final temperatures were 2 minutes and 10 minutes, respectively. The initial temperature of the modulator was 80°C with a second dimensional separation time of 6 seconds for the qualitative part. The initial temperature of the modulator was 85 °C with second dimension separation time of 8 sec for the quantitative part. The temperature of the modulator increased at a rate of 30 °C/min to a final temperature of 340 °C. This is the maximum temperature for the first column as recommended by the vendor. The hot pulse and cold pulse times were 0.90 sec and 2.10 sec for each jet, respectively. The transfer line and ion source temperatures were 280 °C and 230 °C,

respectively. The scan range for the mass spectra was m/z: 45 amu to m/z: 450 amu at a scan rate of 100 spectra/second. The detector voltage was set at 1450V.

2.2.5.3 Yaba

2.2.5.3.1 Methamphetamine

The column set used was a 15 m x 0.250 mm x 0.250 μm of DB-5 from Phenomenex(Terrance, LA) and a 1.5 m x 0.100 mm x 0.100 μm of RTX-200 from Restek(Bellefonte, PA) for the first and second column, respectively. The inlet was ran under splitless conditions with a purge time of 2 minutes and held at a temperature of 250°C. The temperature of the first column was 70 °C to 190 °C at 6 °C/min and hold times at the initial and final temperatures were 1 minute and 2 minutes, respectively. The temperature of the second column was 80 °C to 200 °C at 6 °C/min and hold times at the initial and final temperatures of 1 minute and 2 minutes, respectively. The temperature offset between the columns was 10°C. The initial temperature of the modulator was 105 °C. The second dimension separation time was 5 seconds with a hot pulse time of 0.90 sec and cold pulse time of 1.60 sec. The temperature of the transfer line and ion source were 270 °C and 230 °C, respectively. The solvent delay time was 2 minutes. The mass range for MS was between 45 amu and 250 amu with a scan rate of 100 spectra/second and a detector voltage of 1450V.

2.2.5.3.2 MDMA

The column set, flow rate, and inlet conditions used to analyze MDMA were the same as those used to analyze methamphetamine. The temperature ramp used for the first column was 60 °C to

210 °C at 10 °C/min with hold times at the initial and final temperatures of 1 minute and 5 minutes. The temperature ramp for the second column was 70 °C to 220 °C at 10 °C/min with hold times at the initial and final temperatures of 1 minute and 5 minutes. The temperature offset between the colummns was 10 °C. The initial modualtor temperature was 100 °C. The remaining modulator conditions were the same as they were for the analysis of methamphetamine. The solvent delay time for the MS was 200 seconds. The MS mass range was between 45 amu and 300 amu with a scan rate of 100 spectra/second and detector voltage of 1500 V. The transfer line and ion source temperatures were the same as those used for the analysis of methamphetamine.

2.2.5.3.3 Ketamine

The column set, flow rate, and inlet conditions used to analyze ketamine were the same as those used to analyze the MDMA and methamphetamine. The temperature ramp used for the first column was 60 °C to 300 °C at 10 °C/min with hold times at the initial and final temperatures of 1 minute and 5 minutes, respectively. The temperature ramp used for the second column was 75 °C to 315 °C at 10 °C/min with hold times at the initial and final temperatures of 1 minute and 5 minutes. The temperature offset between the column was 15 °C. The initial modulator temperature was 110 °C. The second dimension separation time was 5 sec with a hot pulse time of 1.20 sec and cold pulse time of 1.30 sec. The transfer line temperature and ion source temperature were 270 °C and 200 °C, respectively. The solvent delay time for the MS was 200 seconds. The MS mass range was between 45 amu and 350 amu with a scan rate of 100 spectra/second and detector voltage of 1500 V.

2.2.5.3.4 Caffeine

The column set, flow rate, and inlet conditions used to analyze the three other drugs of Yaba was also used for the analysis of caffeine. The temperature ramp used for the first column was 40 °C to 200 °C at 10 °C/min with hold times at the initial and final temperatures of 2 minutes. The temperature ramp used for the second column was 55 °C to 215 °C at 10 °C/min with hold times at the initial and final temperatures of 2 minutes. The temperature offset between the columns was 15°C. The initial modulator temperature was 85 °C. The second dimension separation time was 8 seconds with a hot pulse time of 0.60 seconds and a cold pulse of 3.40 seconds. The solvent delay time was 200 seconds. The temperatures of the transfer line and ion source were both 200 °C. The MS mass range was 45 amu to 350 amu with a scan rate of 100 spectra/second and a detector voltage of 1475 V.

2.2.5.3.5 Full Yaba Mixture

The column set used was a 15 m x 0.250 mm x 0.250 μm of DB-5 from Phenomenex(Terrance, LA) and 1.5 m x 0.100 mm x 0.100 μm of RTX-200 from Restek(Bellefonte, PA). The column flow rate was 1.0 mL/min for both columns at constant flow corrected via pressure ramps. The inlet was run under splitless conditions with a purge time of 2 minutes and held at a temperature of 250 °C. The temperature ramps for the first and second columns were 50 °C to 300 °C and 65 °C to 315 °C , respectively. The ramp rate for both columns was 10 °C/min and the hold times at the initial and final temperatures for both columns were 1 minute and 5 minutes, respectively. The initial modulator temperature was 95 °C. The second dimension separation time was 5 seconds with a hot pulse time of 0.90 seconds and a cold pulse time of 1.60 seconds. The temperatures for the transfer line and ion source were 270 °C and 230 °C, respectively. The MS

solvent delay time was 200 seconds. The MS mass range was 45 amu to 400 amu at a scan rate of 100 spectra/second and a detector voltage of 1500 V.

2.2.5.4 BP Oil Samples

The column set used was a 15 m x 0.25 mm x 0.25 μm of ZB-5 and a 1.5 m x 0.25 mm x 0.25 μm of DB-17. One μL of each of the deepwater samples and the surface samples were injected under splitless conditions with a purge time of 15 sec at a constant inlet temperature of 250°C. The columns were held at a constant flow rate of 1.0 ml/min which was corrected via pressure ramps. The temperature programs for the first and second columns were 40°C to 300 °C and 55 °C to 315 °C, respectively. The temperature offset between columns was 15 °C. The temperature ramp rate was 5 °C/min for both columns. The hold times at the initial and final temperatures was 2 minutes and 10 minutes, respectively. The initial temperature of the modulator was 85 °C. The second dimension separation time was 8 sec with a hot pulse time of 1.5 sec and a cold pulse time of 2.5 sec. The transfer line and the ion source were held constant at 280 °C and 230 °C, respectively. The MS solvent delay time was 300 seconds. The MS mass range was 45 amu to 600 amu at a scan rate of 20 spectra/second and detector voltage of 1500 V.

2.3 Calculations Performed

2.3.1 Linear Range

Linear range was determined based on the appearance of the trendline line plotted for the calibration standards analyzed and the R^2 of each line. The trendline and R^2 were determined using the linear regression algorithm in Microsoft Excel. Linearity was also confirmed based on the precision and accuracy of the slopes calculated for each segment on the calibration curve. The %RSD was calculated to determine precision. The %error was determined by comparing the

average of the calculated slopes for each segment and the slope determined by the linear regression.

2.3.2 Limit of Detection and Limit of Quantitation(LOD/LOQ)

LOD was determined using the IUPAC method. The equation used to calculate the LOD is shown in Equation 2.2

$$LOD = ks_B / m$$ (Equation 2.2)

where k the S/N threshold which is equal to 3 for the LOD and equal to 10 for the LOQ[55]. s_B is the standard deviation of the blank which was determined taking the standard deviation of the noise readings from 10 data points adjacent to the peak at S/N between 2 and 3. The noise of each point was determined by the ChromaTOF software. m is the slope of the calibration curve determined using the linear regression algorithm in Microsoft Excel.

2.3.3 %Recovery Determination

Three samples each of water and urine were spiked with three different concentrations of each drug. The drugs were extracted using the procedures described above. %Recovery from each sample was calculated using Equation 2.3:

$$\frac{conc.extracted\ (ppm)}{conc.spiked(ppm)} \times 100$$ (Equation 2.3)

The extracted concentration was calculated using the equation for the calibration curves determined using the linear regression algorithm in Microsoft Excel. The spiked concentration was the drug concentration added to the samples prior to extraction.

2.3.4 Accuracy and Precision

Accuracy was determined by calculating the %error between the spiked drug concentration in water or urine sample and the drug concentration extracted from the sample. Precision of the %recovery of each drug was determined using %RSD of the peak area calculated after triplicate runs of the samples. A blank was run between each sample in order to prevent carryover of salvinorin A between samples.

2.4. Validation Experiments

One liter of a 500 ppb stock solution was prepared from a fresh 1 mg/ml drug standards for cocaine, salvinorin A, methamphetamine, MDMA, ketamine, and caffeine. A volume 500 µL of the drug standard was added to a 1 L volumetric flask using a 0.5 mL volumetric pipette and then diluted to the mark with deionized water. A volume of 100 mL of same internal standard used for the analysis of salvinorin A was prepared at concentration of 100 ppb. A mass of 10 mg was added to a 100 mL volumetric flask and then diluted to the mark with acetonitrile to prepare the internal standard for the analysis of salvinorin A. A volume of 20 µL of the internal standard was added to all salvinorin A dilutions. All further dilutions of each drug prepared for the validation experiments were prepared from the respective stock solution.

2.4.1 Linearity

A set of calibration standards for GBL, cocaine, Salvinorin A, methamphetamine, MDMA, ketamine, and caffeine were prepared using calibrated volumetric pipettes. The concentration range prepared for each drug was the same concentration range used to produce the calibration curves using SPME. Refer to Tables 2-1 thru 2-4 above for calibrations standards prepared for

each drug. The standards were run in sequence from lowest to highest using the optimized SPME-GCxGC-ToFMS conditions described above of each drug. The peak area was calculated using the m/z ratio of the base peak corresponding to each drug. Calibrations curves were prepared for each drug using the linear regression algorithm in Microsoft Excel. Linearity was confirmed based on the precision and accuracy of the slope calculated for each segment on the calibration curve. Precision was determined by calculating the %RSD. The average slope of the segments was compared with the slope determined by linear regression and the %error was calculated to determine accuracy.

2.4.2 Precision

Volumes 2.5 mL, 4 mL, 10 mL of the stock solution of each drug were spiked into three separate 20 mL samples of deionized water for each volume yielding a set of 3 dilutions at concentrations of 62 ppb, 100 ppb, and 250 ppb. All 9 dilutions were run in sequence from lowest to highest concentration under the optimized SPME-GCxGC-ToFMS conditions described above for each drug. The peak area was calculated using the TIC and the m/z ratio of base peak corresponding to each drug. Precision for the analysis was determined from the %RSD calculated for each set of dilutions at each of the three concentrations.

2.4.3 Accuracy

Two sets of five dilutions of each drug were prepared at 250 ppb. A volume of 10 mL taken from the stock solution was spiked into five 20 mL samples of deionized and five 20 mL samples of urine. pH of the urine was adjusted as necessary based on the pKa for each drug. Each set of dilutions was run under the optimized SPME-GCxGC-ToFMS conditions described above for each drug. The peak area was calculated using the TIC and the m/z ratio of base peak

corresponding to each drug. The extracted concentration of each drug was determined using the

equation corresponding to the respective validated calibration curve. The spiked concentration of

each drug was 250 ppb. Accuracy was determined by calculating the %error between the

extracted and spiked concentrations for each drug.

CHAPTER 3 - RESULTS AND DISCUSSION OF ANALYSIS OF THE CHROMATOGRAPHIC PERFORMANCE OF THE SECOND COLUMN FOR GCXGC-TOFMS USING THE GROB TEST MIXTURE

3.1 Purpose of the Experiment

The Grob test mixture is a standard test mixture used to evaluate performance of GC capillary columns[39, 40]. GCxGC uses two columns to perform comprehensive orthogonal separations of complex samples[32, 34-37]. One of the drawbacks of GCxGC is that although it performs fast separations on the second column, the chromatographic performance of this column is often poor. The Grob test mixture was used in order to evaluate the performance of this column using a semipolar silica-based polymer stationary phase and an ionic liquid stationary phase. Values for the retention factor, selectivity, and efficiency were calculated and compared for each of the 12 components in the Grob mixture using each stationary phase.

3.2 Optimization of the Instrumental Method

The initial instrumental method was developed by this laboratory upon initial installation of the instrument as a generic method for testing the performance of both columns used in a GCxGC system. The initial contour plot from using this method is shown in Figure 3-1 and shows the elution 7 of the 12 compounds in the Grob mixture. It was observed that the larger more polar compounds did not elute indicating little retention on the second column. The modulation period and the hot pulse time of the modulator were changed in order to increase retention in the second column. The temperature offset between the two ovens was also changed improve the orthogonality of the separations of the two columns. The column mode, purge time, and temperature programming rate were also changed in order to increase the number of Grob mixture components eluted. These variables were changed using the "one variable at a time" method in order to determine the effect of changing a single parameter without interference due

to changing other parameters. Table 3-1 outlines the experiments performed, the parameters changed, and the number of Grob mix components eluted and identified by the ToFMS.

The initial time for the modulation period was only 2 seconds resulting in the elution of only the non-polar components of the Grob mixture. Since the modulation period directly affects the retention in the second dimension, it was increased from 2 seconds to 4 seconds resulting in the elution of the high polarity components in the Grob mixture. However, changing the modulation period alone did not elute all 12 components, nor did it generate an orthogonal separation indicating that retention in the second dimension was dependent on more than one variable. The hot pulse time of the modulator was decreased from 0.60 sec to 0.40 sec resulting in a slight increase in retention time for the components of the mixture that were eluted. Although the number of components that eluted from the mixture increased from 8 to 9, the amount of wraparound of the higher polarity components also increased on the second column, and the hot pulse time was therefore returned to 0.60 sec.

The temperature offset between oven was increased from 5°C to 10°C which resulted in a more orthogonal separation and also eliminated wraparound of the highly polar compounds previously observed. The temperature ramp rate for both columns was then decreased from 10 °C/min to 5 °C/min, this only resulted in increasing the overall run time. It did not increase the number of mixture components that eluted nor did it increase retention of the components on the second column. Therefore, the ramp rate was returned to 10°C/min. The inlet purge time was also increased from 15 sec to 60 sec in order to increase the number of components that eluted during the run from 9 to 12. The longer purge time allowed the entire sample to be transferred onto the

Experiment number	Instrumental Parameters changed	Number of Grob Test Mix components identified
1	No changes initial run	7
2	solvent delay time to 3 min, 2D sep. time to 4 sec	8
3	Column mode change to constant pressure	7
4	Modulator Hot Pulse time to 0.60 sec, column mode to constant flow with pressure ramp correction	8
5	Oven offset to 10 deg C	8
6	Column mode to constant pressure	7
7	Column to ramped flow	9
8	Modulator Hot Pulse time to 0.40 sec	9
9	ramp rate lowered to 5 deg C/min	9
10	Column mode to const.pressure	8
11	Column to ramped flow	9
12	Modulator Hot Pulse time to 0.60 sec	8
13	Purge time to 15 sec	8
14	Purge time to 30 sec	12
15	Purge time to 60 sec	12
16	Purge time to 60 sec	12
17	Purge time to 60 sec	12
18	Purge time to 60 sec	12
19	Purge time to 60 sec	12
20	Purge time to 60 sec	12

Table 3-1 – GCxGC-ToFMS experiments and parameters changed for analysis of Grob Mixture

first column without the sample loss which had been observed using shorter purge times. A second observation due to increase in purge time was that the peak width at half height, $w_{1/2}$ for the second dimension peaks decreased for all 12 components. This decrease became less pronounced as the mixture components increased in polarity and in retention on the second column.

The final parameter that was changed during optimization was the column mode which controls the column flow rate and pressure of the carrier gas within the column required to push the sample through the column. Normally, the pressure is corrected in order to maintain a constant flow rate through both columns. The instrument uses pressure ramps in each column in order to regulate pressure of the instrument as the sample passes from the first column into the second column. It was observed that when the pressure was not corrected, the column flow rate was not held constant; this resulted in significant changes in the retention time and the peak width in the second dimension from run to run regardless of the column mode selected. Therefore, in order to maintain constant retention times and peak widths between runs, the column was run at constant flow where the flow was corrected using pressure ramps. However, the retention of all components on the second column was still poor despite the flow correction. One reason for this behavior is that the average linear velocity for the second column is normally much higher than the target flow rate. The average linear velocity was calculated to be approximately 128 cm/sec using Equation 1-17 where the length of the column, L, was 150 cm and the hold-up time of the column, t_m, was calculated to be 1.17 seconds using the LECO Column Calculator software based off the dimensions of the second column and the modulation period. The hold-up time is

defined as the time it takes for the carrier gas to pass through the second column. The flow rate in the second column was determined to be 0.60 ml/min using Equation 3-1:

$$F_C = \frac{\pi r^2 L}{t_m} \text{ [11, 19]}$$ (Equation 3-1)

In Equation 3-1, L is the length of the second column, r is the internal radius of the column, and t_m is the hold-up time for the column. Although the target flow rate for the method was only 1.0 mL/min and the instrument uses pressure ramps in order to maintain the target flow rate through both columns, the linear velocity in second column is still the dominant factor for retention on the second column. This is one common observation that occurs in GCxGC and demonstrates how chromatographic performance of the second column is sacrificed to achieve fast separation. Figure 3-2 shows a GCxGC contour plot of the Grob test mixture ran under the optimized method.

3.3 Determination of the chromatographic parameters

Table 3-2 shows the average and standard deviation for each of the chromatographic parameters determined for each of the 12 compounds in the mixture. The data in Tables 3-2 represent the best chromatographic performance that was achieved for the Grob mixture without sacrificing speed or the orthogonality of the separation.

3.3.1 Retention factor

Retention factor, k, was determined for each of the 12 Grob mixture components using Equation 3-2:

$$k = (t_R - t_o)/t_m$$ (Equation 3-2)

Legend
1) 2,3-Butanediol
2) Decane
3) 1-Octanol
4) 2,6-Dimethylphenol
5) Nonanal
6) Undecane
7) 2,6-Dimethylaniline
8) 2-ethylhexanoic acid
9) Decanoic Acid methyl ester
10) Dodecanoic Acid methyl ester
11) Undecanoic acid methyl ester
12) Dicylcohexylamine
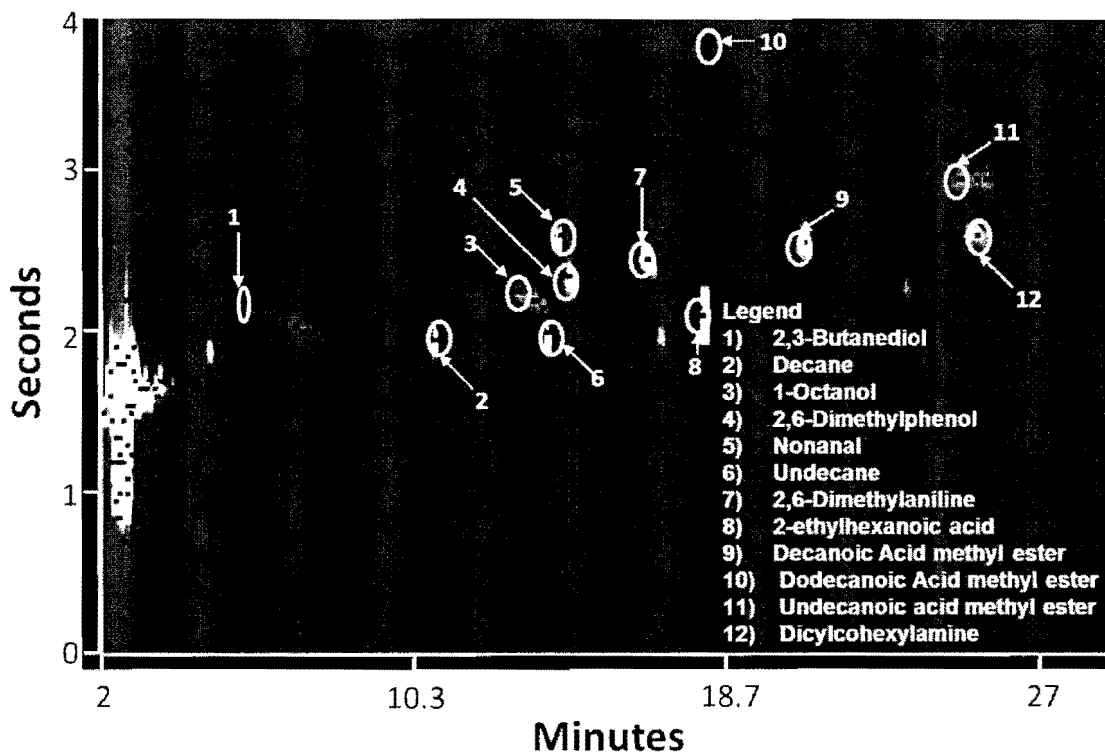
Figure 3-1 – GCxGC Contour Plot of Grob Mixture

t_R is the second dimension retention time for a single component and t_m is the hold-up time,. The retention factors for the Grob mixture components in the second column increased with increasing in polarity which is not surprising since the separation mechanism in the second

column is based on the respective polarity of the sample components. The typical values for the retention factor calculated after separation on a GC capillary column normally range between 2 and 10 indicating good retention for components that fall within this range[19]. The calculated values for the retention factor are reported in Table 3-2 and were all lower than 2 indicating poor retention on the second column. This observation was due to the smaller dimensions of the second column and the very low vacuum of the MS system attached to one end of the column resulting in a much higher linear velocity for the carrier gas in the column.

.

3.3.2 Selectivity

Selectivity,α, is the ratio of the retention factors between adjacent two peaks and expresses the separation of these two peaks, calculated using Equation 3-3:

$$\alpha = k_2/k_1 \qquad\qquad\qquad \text{(Equation 3-3)}$$

k_2 and k_1 are the retention factors corresponding to two adjacent peaks on the chomatogram. The value for selectivity should be greater than 1.0 between any two adjacent peaks in order to esnure that they do not overlap upon separation using a typical GC capillary column[19]. The values for α were calculated based on their elution order determined by the retention factor on the second column for each component reported in Table 3-2. Each of the values for α were generally greater than 1.0 and showed that the column used in this work shows good separation and selectivity despite the poor retention and high linear velocity. However, the overall trend in values for k and α for the RTX-200 phase showed that as the polarity of the compounds increase,

	Average 2D $t_R(s)$	Average 1st Column Elution Temperature(°C)	k	N
Decane	1.967	110	0.681 ± 0.022	1.80 x 10^3 ± 240
Undecane	1.992	127	0.702 ± 0.017	2.27 x 10^3 ± 250
2,3-butanediol	2.025	86	0.731 ± 0.080	2.97 x 10^3 ± 1000
2-ethylhexanoic acid	2.100	145	0.795 ± 0.038	3.41 x 10^3 ± 180
1-octanol	2.217	120	0.895 ± 0.022	3.99 x 10^3 ± 725
2,6-dimethylphenol	2.342	130	1.00 ± 0.032	3.27 x 10^3 ± 480
2,6-dimethylaniline	2.433	140	1.08 ± 0.022	4.31 x 10^3 ± 290
C10 FAME	2.550	155	1.18 ± 0.000	3.85 x 10^3 ± 420
Nonanal	2.583	130	1.21 ± 0.022	3.50 x 10^3 ± 400
Dicyclohexylamine	2.600	160	1.22 ± 0.000	4.60 x 10^3 ± 480
C11 FAME	2.950	160	1.52 ± 0.000	4.90 x 10^3 ± 680
C12 FAME	3.425	150	1.93 ± 0.20	2.57 x 10^3 ± 1200

Table 3-2 – Statistical Values for Chromatographic Parameters determined for each of the Grob Mixture Components

the selectivity decreases, and the retention factor increases, indicating that the interaction between the stationary phase of the second column and the components become stronger. Since retention and overall separation increases with column length, this behavior suggests that a longer column with a more polar stationary phase in the second dimension would not only result in an increase of retention for each component in the Grob mixture, but also increase the selectivity between adjacent components[19]. Further, an evaluation of the selectivity and the retention factor have not supported the original statement that the performance of the second column in poor due to its high linear velocity.

3.3.3 Efficiency

The efficiency, N, was determined using Equation 3-4:

$$N = 16\left(\frac{t_R}{w_b}\right)^2 = 5.54\left(\frac{t_R}{w_{1/2}}\right)^2 \tag{Equation 3-4}$$

t_R is the retention time for the component and w_b or $w_{1/2}$ are the peak widths at the base or at half height, respectively. Thus, efficiency depends on both retention and the band width of a component. Typical values for N per meter of column using a standard capillary GC column with lengths between 15 meters and 60 meters are about 2,900 plates/meter[11]. Since the length of the second column is so much shorter, the number of plates/meter should be much lower. The values calculated for N for each of the 12 components are shown in Table 3-2 and were lower than the typical values by at least a factor of 10. However, due to peak modulation and more the narrow internal diameter, the peak widths in the second dimension are more narrow resulting in an average plates/meter value similar to that of capillary columns with typical lengths. It was observed that the loss of column efficiency was greatest when the pressure correction was turned off resulting in wider peaks and lower retention. These observations indicate that efficiency is

also dependent on the flow rate and pressure of carrier gas inside the column. Therefore, efficiency one of the most important parameters used in to determine column performance since it is affected by a variety of variables where the previous two parameters discussed depend mainly on the interaction between the stationary phase and the sample component. Another observation was that the trend mentioned above only occurred with the non-polar components. The trend for the more polar components was the opposite than for the non-polar compounds. These trends further indicate that the separation mechanism present in the second column is still a significant factor despite the high velocity of the second column.

Further, the standard deviation calculated for the efficiency of each component after three runs indicate poor precision for these values. This can be related to the high linear velocity in the second column which results in narrow peaks widths, but poor retention. The data shows that the retention factors for each component are below the range for good chromatography, but the standard deviation shows that they are precise. However, efficiency is dependent on both retention and the peak width of the component, therefore, the variation in N for each component must be due primarily to a variation in the peak width for each component from run to run. This variation in peak width is due to the combination of the interaction between the stationary phase and the component in the second column as well as the high linear velocity in the second column.

3.4 Application of the Golay Equation

In order completely understand the relationship between the retention behavior observed and the high linear velocity of the second column, a discussion of the Golay equation is warranted. As stated previously, the average linear velocity for the second column was calculated to be 128

117

cm/sec. On a typical van Deemter plot, shown in Figure 1-3, the location of this linear velocity would lay far in the mass transfer region indicating it has a much greater effect on the plate height in the second column than the longitudinal diffusion. In Figure 1-3, the plate height corresponding to mass transfer region and high linear velocity is located above the lowest point on the curve. As discussed in Chapter 1, resistance to mass transfer is dependent on the resistance in both the stationary and mobile phase. The values for the partition coefficient for each Grob mixture component were determined and found to be much greater than one indicating that the analyte concentration was higher in the stationary phase than the mobile phase. Therefore, in the second column, resistance to mass transfer occurs mainly in the mobile phase. Plate height is also proportional to column length, L, and inversely proportional to column efficiency, N, also defined by Equation 3-5:

$$H = L/N \hspace{6cm} \text{(Equation 3-5)}$$

Therefore, the high plate height in second column resulting from the high linear velocity produces the low efficiencies in Table 3-2 as the result of three factors: a very short column, a high plate height, and band broadening caused by a high resistance to mass transfer in the stationary phase.

3.5 Comparison of the performance of the two stationary phases

Figure 3-2 shows the contour plot for the Grob mixture separated using an ionic liquid stationary phase called IL-69. A comparison of Figures 3-1 and 3-2 shows that worse retention for each of the Grob components on the ionic liquid column. Table 3-3 shows a comparison of the values of k and N for each of the 12 Grob mixture components between the silica-based polymer and the ionic liquid stationary phases. Many of the values of k for the ionic liquid were much less than one, indicating poor retention of each component regardless of the functional group present.
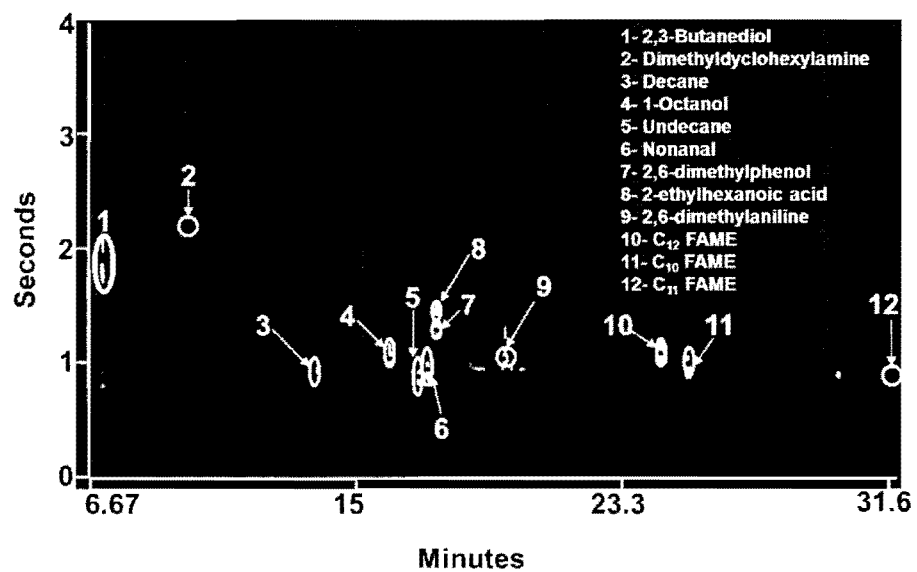
Figure 3-2 – GCxGC contour plot of Grob mixture using ionic liquid stationary phase in second column.

RTX-200		
Compound	k	N
Decane	0.681	$1.80 \times 10^3 \pm 240$
Undecane	0.702	$2.27 \times 10^3 \pm 250$
2,3-butanediol	0.731	$2.97 \times 10^3 \pm 1000$
2-ethylhexanoic acid	0.795	$3.41 \times 10^3 \pm 180$
1-octanol	0.895	$3.99 \times 10^3 \pm 725$
2,6-dimethylphenol	1.00	$3.27 \times 10^3 \pm 480$
2,6-dimethylaniline	1.08	$4.31 \times 10^3 \pm 290$
C10 FAME	1.18	$3.85 \times 10^3 \pm 420$
Nonanal	1.21	$3.50 \times 10^3 \pm 400$
Dicyclohexylamine	1.22	$4.60 \times 10^3 \pm 480$
C11 FAME	1.52	$4.90 \times 10^3 \pm 680$
C12 FAME	1.930	$2.57 \times 10^3 \pm 1200$

SLB IL-69		
Compound	k	N
Decane	0	326
Undecane	0	409
2,3-butanediol	1.06	197
2-ethylhexanoic acid	0.556	377
1-octanol	0.167	260
2,6-dimethylphenol	0.444	243
2,6-dimethylaniline	0.222	359
C10 FAME	0.111	307
Nonanal	0.0370	524
Dicyclohexylamine	0.148	22.7
C11 FAME	0.148	622
C12 FAME	0.167	522

Table 3-3 – Comparison of chromatographic parameters for each of the 12 Grob components using ionic liquid(IL-69) and RTX-200 stationary phases used in second dimension

Further, the values for k do not show the increasing trend with polarity that was observed on the RTX-200 column. This suggests that other types of interactions are occurring between the ionic liquid and the Grob components. The exact structure of the ionic liquid used for this experiment is unknown, however the general structure consists of a large cation and a much smaller anion held together by ionic bonds. This gives ionic liquids similar properties to that of a salt, instead of a polymer like RTX-200. This allows ionic liquids to interact with the Grob mixture components with additional types of intermolecular forces that were not possible with polymeric stationary phases. These forces include dipole-dipole interactions and induced dipole interactions and should result in better retention for more polar compounds. However, the major drawback of ionic bonding holding the ionic liquid together leaves some of the silica groups exposed to the analytes. This results in misshapen peaks for highly polar compounds and poor retention such as alcohols, carboxylic acids, and other carbonyl groups. One of the more interesting observations of this study concerned amines and nitrogen containing compounds such as dicyclohexylamine and 2,6-dimethylaniline. The values of k and α calculated after separation using the RTX-200 column showed that these two compounds had the best retention of any of the Grob components; however, when they were separated using the ionic liquid column, the results showed that these compounds had the worst retention of the 12 components. These compounds were observed to disappear and then reappear at random after performing multiple runs of the mixture. One of the reasons for this behavior is due to the structure of the cation of the ionic liquid which is known to consist of a quarternary amine or other nitrogen heterocyclic functional group[56]. The cation appears to interact so strongly with that of other nitrogen containing compounds that they becoming permanently "bonded" the ionic liquid cation and do not appear in the chromatogram.

The exact interaction mechanism occurring in this case is currently unknown and is beyond the scope of this thesis.

A notable observation for the calculated k values was seen for decane and undecane, both of which had k values equal to zero indicating that they have the same retention time as t_m resulting in coelution with the hold-up time. When alkanes are injected on an ionic liquid column with length typically used in a standard GC system, they also exhibit poor retention with values of k also less than 2, but greater than zero. This illustrates the well-known principle in gas chromatography that retention is proportional to the length of the column. One explanation for this principle is that a column with a longer length also results in a lower linear velocity for the carrier gas allowing the analyte more time to interact with the stationary phase. As stated previously, the short length of the second column in GCxGC results in a much higher linear velocity of the carrier gas and therefore results in poor retention of analytes on the column. Further, ionic liquids are considered to be the most polar stationary phases currently available for separation[56]. Therefore, a small nonpolar analyte such as decane or undecane exhibits little to no interaction with the ionic liquid stationary phase. Thus, the alkane is swept through the second column with the carrier gas and elutes from the column prior to the solvent peak. The values for N were generally lower than the values calculated using the RTX-200 column by a factor of 10. This is due to a combination of the poor retention times due to the high linear velocity of the column and the broad peak widths for each of the 12 components due to the multiple intermolecular forces occurring between the ionic liquid and the mixture components.

The results of the brief study of the ionic liquid show that although it was capable of eluting all 12 of the Grob components, all of them showed poor retention and poor efficiency. The column in general also showed poor selectivity toward all of the components. These observations show that the ionic liquid column shows worse chromatographic performance as the second column in GCxGC than the typical silica based polymer columns. Ultimately, since a majority of the compounds analyzed in the scope of this thesis all contain nitrogen, the ionic liquid column was rejected in favor of a silica polymer column in all work reported herein.

3.6 Conclusion

Throughout the study, it was observed that the linear velocity of the second column influenced k, N, and α. One of the most important effects is that it limits the retention of the analytes on the second column, but does generally does not appear to affect the selectivity of the column. However, the advantage of such a high linear velocity is that it allows the instrument to achieve two dimensional orthogonal separations without a loss of selectivity. The effect of the high linear velocity was clearly observed in the values determined for efficiency which were lower than normal compared to a typical capillary GC column due to the narrow peak widths after modulation and poor retention factors. Application of the Golay equation and a closer look at the partition coefficients demonstrated that the high linear velocity in the second column results in behavior similar to that of a packed column instead of a typical capillary column. Thus, it is possible to optimize the GCxGC method in order to achieve the best chromatographic performance of the second column.

CHAPTER 4 – ANALYSIS OF COCAINE IN US CURRENCY, WATER, AND URINE USING GC-MS AND GCXGC-TOFMS

4-1 Background

Cocaine is a solid, white crystalline tropane alkaloid that is derived from the *coca* plant. It is primarily a central nervous system(CNS) stimulant causing increased heart rate, tightness in the chest, heightened alertness, stroke, and death. In the 19th century, cocaine was used as a topical anesthetic for minor surgical procedures[57]. However, due to the highly addictive nature of the drug, it was abandoned for medical use and now considered a Class II controlled substance by the US Drug Enforcement Administration(DEA). The drug is normally administered into the body by nasal or oral inhalation. Like many drugs upon entering the body, cocaine is metabolized in the liver and is converted into characteristic metabolites which can be readily identified using GC-MS or LC-MS[58-60]. However, these metabolites can also form and be identified using the same techniques as a result of degradation following dissolution of the drug in a common solvent such as methanol. These metabolites are specific to a certain drug and their presence indicates that the parent drug had recently been present in the sample. This is especially important for the analysis of salvinorin A and Yaba which will be discussed in Chapter 6 and 7, respectively. The structure of cocaine and these characteristic metabolites are shown in Figure 4-1.

For over 20 years, trace amounts of cocaine have been found of the surface of currency from all over the world[61-65]. When currency is brought into contact with cocaine or with the hands of someone that has been handling cocaine, trace amounts of the drug are transferred to the surface of the money. Since cocaine remains in its crystal state when it is transferred, it is very stable often allowing it to be detected on the surface of currency for several years. The number of times

cocaine

ecgonidine

ecgonine
Methyl ester
(EME)

benzoylecgonine(BZE)

ecgonine
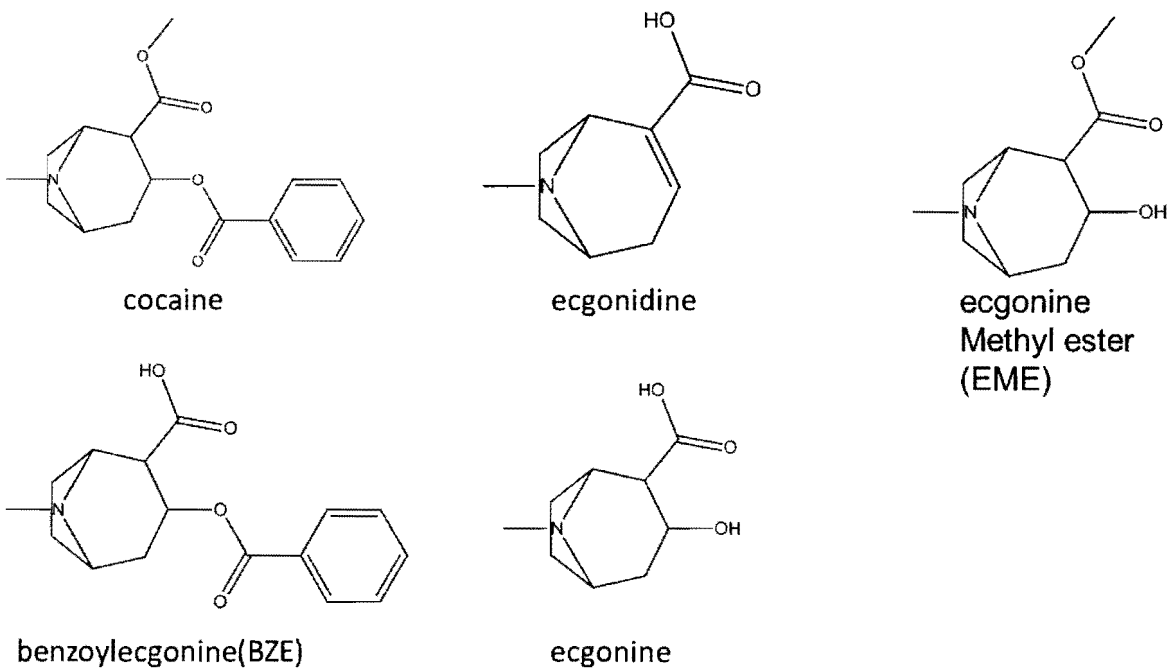
Figure 4-1 –Structure of cocaine and major metabolites.

cocaine can be transferred from banknote to banknote before cocaine is undetectable is limited by the sensitivity of the analytical technique used for analysis. During the course of this research, several samples of US currency were analyzed for the presence of cocaine and its metabolites.

4.2 Purpose of the experiment

In this work, the use of GC-MS and GCxGC-ToFMS were compared during the analysis of cocaine on the surface of US currency. Further, the use of SPME-GCxGC-ToFMS for the analysis of cocaine extracted from spiked deionized water and urine samples was also performed. The results from both experiments demonstrate that GCxGC-ToFMS is an effective tool for the trace analysis of drugs as well as the identification of their metabolites due to the orthogonal separation capability and high speed and sensitivity of the technique. Further, the high sensitivity and fully automated SPME method resulted in lower LODs and LOQs, higher recoveries of trace quantities, and better overall repeatability compared to results in the literature produced using SPE or LLE[62, 63].

4.3 Method Development and Optimization of the GC-MS method and GCxGC-ToFMS Method

A 1mg/ml cocaine standard was analyzed on each instrument prior to the analysis of the money extracts in order to determine the retention time and the mass spectra. The GC-MS instrumental method was optimized by changing the GC oven temperature programming rate and the final temperature hold time in order to get the shortest retention time and the shortest overall run time. The remaining method parameters were held constant during analysis by GC-MS, with the exception of the purge time.

126

The initial temperature program for the GC-MS covered the temperature range from 40°C to 300°C increasing at a rate of 10°C/min with hold times of 1 minute and 5 minutes at the initial and final temperatures, respectively. The initial chromatogram yielded a retention time of 18.3 minutes for cocaine, however the total run time was 30 minutes thereby showing a lot of empty space in the chromatogram. The program rate was increased to 20°C/min in order to shorten the overall run time and the retention time for cocaine. However, after two injections, no peak for cocaine was observed and temperature program rate was returned to 10°C/min which yielded an elution temperature of approximately 223°C for all subsequent injections of cocaine.

The initial column temperature was increased to 100°C and 150 °C which yielded overall run times of 24 minutes and 19 minutes, and retention times for cocaine of 13.3 minutes and 8.28 minutes, respectively. It was observed that the initial column temperature of 150°C eliminated most of the empty space on the chromatogram and this temperature was used for all subsequent analyses of cocaine. The final temperature and final hold time was decreased to 290°C and 1 minute, respectively. As expected, these changes had no effect on the retention time for cocaine, but they did reduce the overall run time to 12 minutes. Therefore, no further optimization was performed on this temperature ramp which was also used for the temperature program of the first column in GCxGC-ToFMS.

The GCxGC-ToFMS method was optimized by changing the modulation period, pulse time of the two hot nitrogen jets in the modulator, the temperature offset between the two ovens, and the scan rate of the ToFMS. All of the other method parameters were kept constant. The experiments and observations are summarized in Table 4-1.

Experiment	Modulation Period(sec)	Hot Pulse Time(sec)	Oven Temperature Offset(°C)	ToFMS acquisition rate(spectra/second)	Observation
Initial	5	0.6	5	20	wraparound of cocaine peak observed
1	6	0.6	5	20	no effect on wraparound of cocaine and no increase in cocaine retention on second column
2	6	0.9	5	20	slight reduction in wraparound of cocaine
3	5	0.9	5	20	wraparound of cocaine eliminated
4	5	0.9	10	20	increase in cocaine retention on 2nd column from 1.26 seconds to 1.94 seconds; no wraparound observed
5	5	0.9	10	100	reduction in background noise and increased S/N for cocaine

Table 4-1 - Summary of experiments for optimization of cocaine method using GCxGC-ToFMS

4.4 Detection and Confirmation of Cocaine

The money extracts were analyzed under the optimized conditions for each instrument as discussed in the previous section. Figure 4-2 compares the chromatograms obtained using GC-MS with the contour plots obtained using GCxGC-ToFMS for both the cocaine standard and a money extract. The retention time for cocaine from the standard and the money extract using both instruments was identical. The chromatograms in Figure 4-2 show the extracted ion chromatogram(EIC) at m/z: 82(the base peak for cocaine). The baseline of the chromatograms from the GCxGC plots for the cocaine standard were observed to be much smoother and show much less noise than the GC-MS chromatograms. The reduced background noise in the GCxGC chromatogram is due to the high sensitivity and rapid scan rate of the ToFMS system used with the GCxGC. Although the cocaine peak is clearly indicated in both GC-MS plots, the baseline is still very noisy due to the lower sensitivity and scan rate of the quadrupole system.

The identity of cocaine on the money was confirmed by comparing the mass spectra of cocaine from the standard, the NIST library, and the money extract. These spectra are shown in Figure 4-3 which also shows the fragmentation pattern of cocaine. The initial radical cation is formed by removing an electron from the nitrogen atom of the tertiary amine in the molecule resulting in the formation of the molecular ion at m/z: 303. The base peak for cocaine, at m/z: 82, is the result of the loss of the methyl ester and the benzyl ester moieties from the molecular ion via homolyic cleavages leaving only the pyridine ring with a positive charge on the nitrogen atom. Another significant peak in the MS for cocaine was at m/z: 182 which is the result of the loss of the benzyl ester group following formation of the M^+ ion. Other peaks present in the MS as a
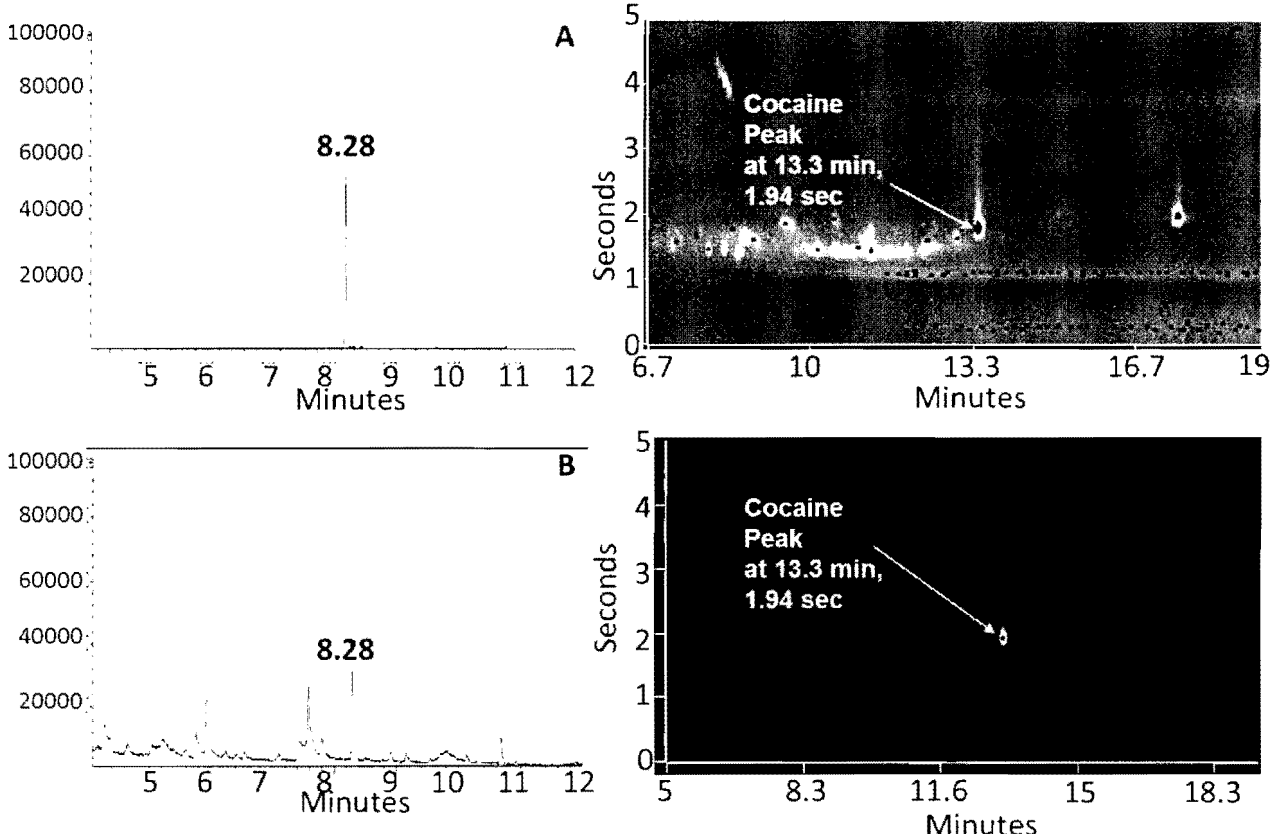
Figure 4-2- (A) GC-MS Chromatogram of 1mg/ml cocaine std.;(B) GC-MS chromatogram Of $1 bill extract;(C) GCxGC contour of 1 mg/ml cocaine std.;(D) GCxGC contour plot of $1 bill extract. All four chromatograms show the EIC at m/z: 82.
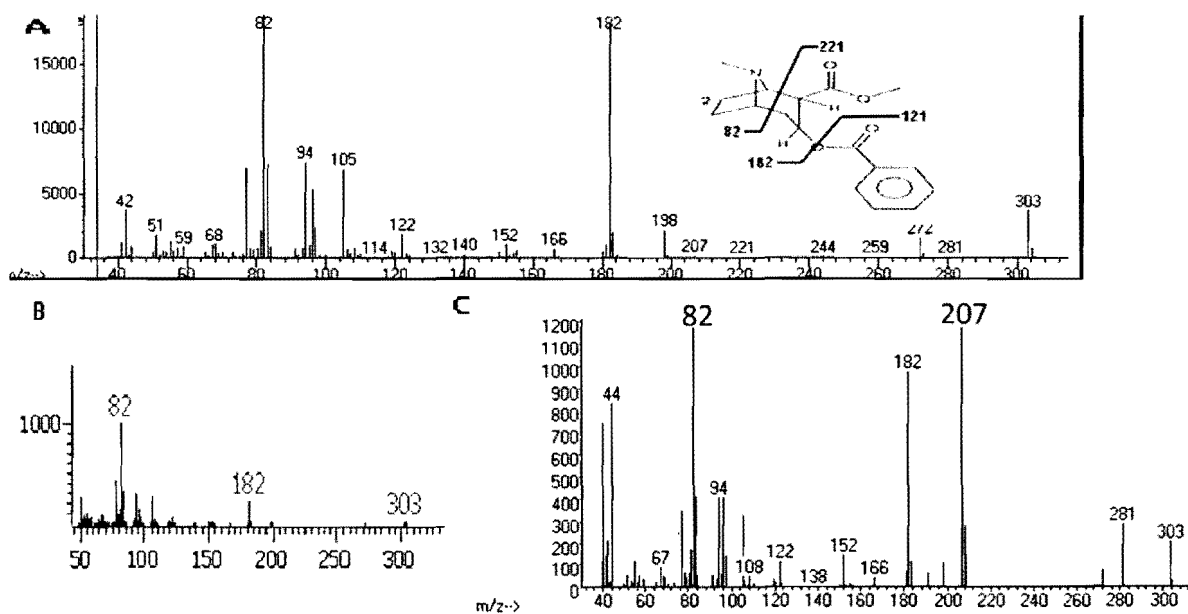
Figure 4-3 – Cocaine Mass Spectra: (A) NIST library MS of cocaine and cocaine
Fragmentation pattern;(B) ToFMS of cocaine;(C) GC-MS of cocaine

result of secondary fragmentation of the mass fragments at m/z: 82 and m/z: 182 were also observed, however these peaks were lacking in abundance in comparison to that of the molecular ion and base peak and were only observed in the quadrupole spectrum. They were not present in ToFMS spectrum due its higher sensitivity and the peak deconvolution algorithm built-in to the data analysis software. Therefore, further confirmation of cocaine using GC-MS was obtained for the money extract and the standard using SIM for m/z: 82, 182, and 303.

4.5 Calibration of the Cocaine Standard

Figure 4-4 shows a comparison of the calibration curves from the GC-MS and from the GCxGC-ToFMS both using m/z: 82 for the peak area calculation and plotted in the same linear range. The base peak for cocaine was used to calculate the peak area because of the minimal amount of background noise observed in the EIC for m/z: 82 as compared with the TIC following analysis on both instruments. Comparison of the curves in Figure 4-4 shows greater linearity below 100 ng using GCxGC-ToFMS indicating that it is better for the analysis of trace quantities of drugs primarily due to the higher sensitivity of the ToFMS. This observation is further supported by the comparing the baseline surrounding the cocaine peak for the EIC at m/z: 82 obtained using both instruments. The cocaine peak for GC-MS appears jagged and has a higher noise level in the baseline thereby resulting in poor linearity at trace quantities of cocaine. The cocaine peak for GCxGC-ToFMS appears much smoother and has a much lower nosie level in the baseline due to faster scan rate and higher sensitivity of the time-of-flight.
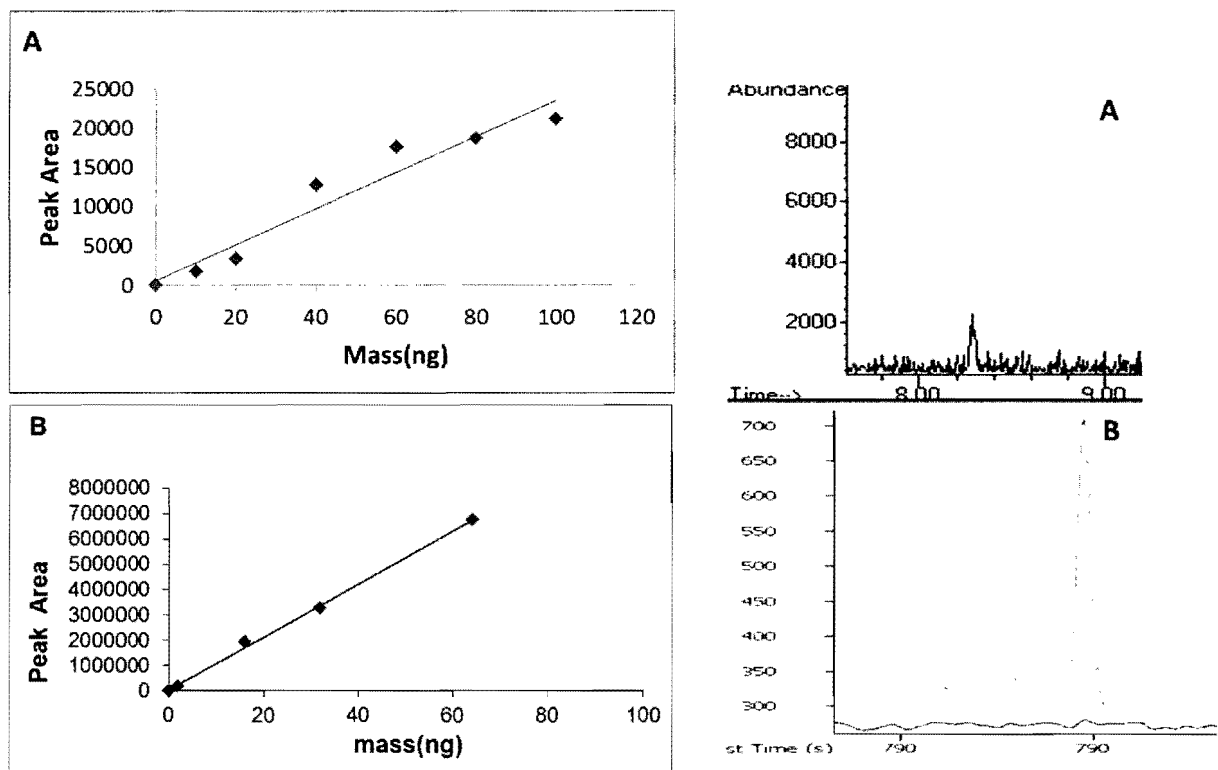
Figure 4-4 – Comparison of calibration curves for cocaine and cocaine signal:
(A) GC-MS; (B) GCxGC-ToFMS. Peak area calculated using m/z: 82.

4.6 Determination of Limit of Detection/Limit of Quantitation

LOD and LOQ of cocaine for both instruments was determined using the IUPAC method[55]. Table 4-2 shows the LOD and LOQ calculated for each instrument showing lower values for cocaine following analysis with GCxGC-ToFMS. As stated previously, the lower scan rate and lower sensitivity of the quadrupole results in a higher noise level in the baseline. This produces greater interference at the LOD where the S/N is between 2 and 3 thereby limiting the quadrupole to LODs in the low nanogram range. The rapid scan rates and higher sensitivity of the time of flight results in a lower noise level in the baseline. Thus, the interference at the LOD is greatly reduced; this results in an LOD in the low femtogram range.

The determination of the LOD and LOQ was repeated five times in order to determine the precision of the reported values for each instruments. The %RSDs calculated for the LOD determination using GC-MS and GCxGC-ToFMS were 10.03% and 36%, respectively. The lower precision obtained using the GCxGC-ToFMS was also due to the increased sensitivity of the ToFMS system. Further, since ToFMS is not a scanning technique, all of the masses are analyzed by the system. The result is that signals representing vial contaminations, column, septum, and SPME fiber bleed, etc. are detected and appear in as peaks in the chromatograms for a given sample. Although much of these signals are eliminated by instruments peak deconvolution algorithm, resulting in a smooth baseline, it often results in the elimination of the analyte signal and was noted to be more prevalent when very low concentrations of cocaine were analyzed. In this work, the scan rate was increased to 100 spectra/second, resulting in a lower overall noise level and a higher S/N for cocaine at the LOD, but no improvement in the precision for the LOD was observed.

	GC-MS	GCxGC-ToFMS
Low Conc.(ppm)	10	0.18
High Conc.(ppm)	100	64
Slope	231	1.05×10^5
R^2	0.9358	0.998
LOD	2.1 ng	8 fg
LOQ	30 ng	27 fg

Table 4-2 – Comparison of Linearity, LOD, and LOQ values determined for cocaine using GC-MS and GCxGC-ToFMS

4.7 Quantitation of Cocaine in Money Extracts

Table 4-3 compares the calculated masses for cocaine from the analysis using both instruments. The mass of cocaine on the money samples was determined using the observed peak area for cocaine determined using the EIC at m/z: 82 and the equation for the GCxGC-ToFMS calibration curve in Figure 4-4. Separate sets of money samples were used and prepared for analysis on each instrument. The same extraction procedure was repeated for both instruments to ensure complete extraction of the cocaine. All five new extracts of the $1 bill samples were run in triplicate on the GC-MS showing cocaine peaks in 60% of the samples analyzed. The second set of $1 extracts were run on the GCxGC-ToFMS showing a cocaine peak in all five samples. The calculated masses of cocaine are shown in Table 4-3 and reflect the total mass of cocaine detected after multiple extractions of the money samples analyzed using both instruments. The extraction was performed twice followed analysis with GC-MS in which the second extraction did not show a peak for cocaine. However, it was observed that it required four extractions before the mass corresponding to the cocaine detected using GCxGC-ToFMS fell below the calculated LOQ. Two blanks were run prior to the injection of the extracts to eliminate carryover of cocaine between samples. The analysis further demonstrates the increased sensitivity of the GCxGC-ToFMS instrument over the GC-MS instrument. In addition to cocaine, other drug substances such as amphetamines, opiates, sun screen, and ink dyes were also detected on the money samples when compared with the NIST library. It was further noted that some major metabolites of cocaine were also present on the money samples indicating that the drug also degrades upon prolonged exposure of the crystal form to an open environment. This aspect of cocaine was further investigated through a degradation study

(A)

Sample	t_R(min)	Peak Area	Mass(ng)
Extract 1	8.28	2.81×10^5	38
Extract 2	8.28	8.92×10^4	45
Extract 3	8.28	1.20×10^4	70
Extract 4	8.28	No cocaine detected	
Extract 5	8.28	No cocaine detected	

(B)

Sample	t_R(min)	Peak Area	Mass(ng)
Extract 1	790, 1.94	5.07×10^6	45
Extract 2	790, 1.88	6.28×10^5	5.3
Extract 3	790, 1.92	2.35×10^6	21
Extract 4	790, 1.96	5.62×10^6	51
Extract 5	790, 1.96	5.04×10^6	46

Table 4-3 – Mass of Cocaine extracted from $1 bills using:
(A) GC-MS; (B) GCxGC-ToFMS

of a cocaine standard in solution with methanol upon exposure to typical laboratory

conditions(e.g. room temperature and fluorescent lighting)

4.8 Thermal Degradation Study of the Cocaine Standard

One 1mL ampule of the cocaine standard was used to conduct the thermal degradation study.

The standard was left in the autosampler and injected in triplicate once a day until it had

completely evaporated. The goal of the study was to determine how the standards were affected

when they were exposed to typical laboratory conditions over an extended period of time. When

the study was conducted using GC-MS, the standard had completely degraded showing no peak

for cocaine after three days of exposure which was confirmed after multiple injections of the

standard. When this study was repeated using GCxGC-ToFMS, it was observed that both

multiple peaks for cocaine as well as peaks corresponding to some of the major metabolites of

cocaine were present. Figure 4-1 shows the structure of the major metabolites of cocaine

identified during the study. The identity of the metabolites was confirmed by comparison of their

mass spectra obtained from the ToFMS to their mass spectra in the NIST library. Their

fragmentation pattern of each metabolite was observed to be similar to that of cocaine. Each of

the metabolites contained the same azo-bicyclic ring structure which is unique to tropane

alkaloids. The base peak at m/z: 82 corresponding to the methyl pyrrolidine ion was also present

for all the metabolites detected. The only difference observed between the structures of the

metabolites were the identities of the functional groups bound to the azobicylic ring. Figure 4-1

shows that these functional groups were carboxylic acids, methyl esters, benzoyl esters, and

hydroxyl groups. Each of these functional groups shows a unique fragmentation pattern in their

mass spectra[44].

Three of the metabolites contain carboxylic acid moieties which exhibit a very specific fragmentation pattern consisting of four peaks. The first peak is the molecular ion, M^+, which was unique for each metabolite. The second peak has a m/z ratio of $[M^+ - 17]$ which corresponds to a loss of the hydroxyl group present in carboxylic acid. This peak is often coupled to a peak corresponding $[M^+ -18]$ which indicates a loss of water which is commonly observed for the carboxylic acid and alcohol functional groups. The fourth peak has the highest abundance of and has an m/z ratio of $[M^+ - 45]$ corresponding to the loss of the whole carboxylic acid moiety. The three metabolites with this moiety in their structure are ecgonine, ecgonidine, and benzoylecgonine(BZE) where their molecular ions at m/z: 184, 167, and 291, respectively. Loss of the carboxylic acid moiety for ecgonine yielded peaks at m/zs: 167 and 166 for the loss of the hydroxyl group and water. The peak at m/z: 139 was identified as the loss of the whole acid moiety. This same fragmentation pattern was also observed for ecgonidine and BZE peaks in which the loss of the hydroxyl and water corresponded to m/zs: 150 and 149 and m/z: 274 and 273 for ecgonidine and BZE, respectively. The loss of the whole acid moiety occurred at m/z: 122 and m/z: 246 for ecgonidine and BZE, respectively. Thus, the identity of these metabolites was confirmed by the identity of their respective molecular ions as well as the m/z ratios corresponding to loss of carboxylic acid.

The fourth compound identified was ecgonine methyl ester(EME). This compound is distinguished from the other metabolites by the presence of the hydroxyl and methyl esters functional group attached to the azo-bicyclic ring. The molecular ion for this metabolite is located at m/z: 187. Loss of the hydroxyl group and water occurs at m/z: 170 and m/z: 169. The other functional group in the molecule is methyl ester which produces peaks at m/z: 156 and m/z:

59. Esters form fragments on either side of the carbonyl group where the formation of the ion on the side with smaller fragment is favored[43]. The peak at m/z: 156 corresponds to the loss of the methoxy group [M^+-17]. The peak at m/z: 59 corresponds to the loss of the fragment on the left side of the carbonyl, at [M^+-128]. Therefore, the identity of this metabolite was confirmed by the identity of the M^+ ion and the characteristic fragmentation pattern of the ester. Figure 4-5 shows the GCxGC contour plot obtained from Day 5 of the degradation study where the locations of the four major metabolites discussed have been indicated. It was observed throughout the study that the peak areas of the metabolites increased as the peak area for cocaine decreased. Thus, the results indicate that cocaine was converted into its metabolites upon prolonged exposure of a 1 mg/mL cocaine standard to normal laboratory conditions.

4.9 Optimization of the SPME method for cocaine

The SPME method for cocaine was optimized by changing the following variables: fiber coating, extraction time, desorption time, and pH of the matrix. Carboxen-PDMS, carbowax-DVB, PDMS and polyacrylate fiber coatings were tested for the extraction of cocaine. PDMS and polyacrylate were the only two coatings that showed absorption of cocaine where polyacrylate produced the higher peak area for cocaine due to its higher polarity. Thus, polyacrylate was used for the initial extraction of cocaine from water as well as the validation of the SPME method. However, carryover of cocaine between extractions and degradation of the fiber at basic pHs was noted using polyacrylate. Based on these results, PDMS was used for the extraction of cocaine from urine. Although the coating show less absorption of cocaine, carryover between extractions was not observed showing good precision for repeated extractions of cocaine at the same concentration. PDMS fibers were also found to be more resistant toward very basic pHs
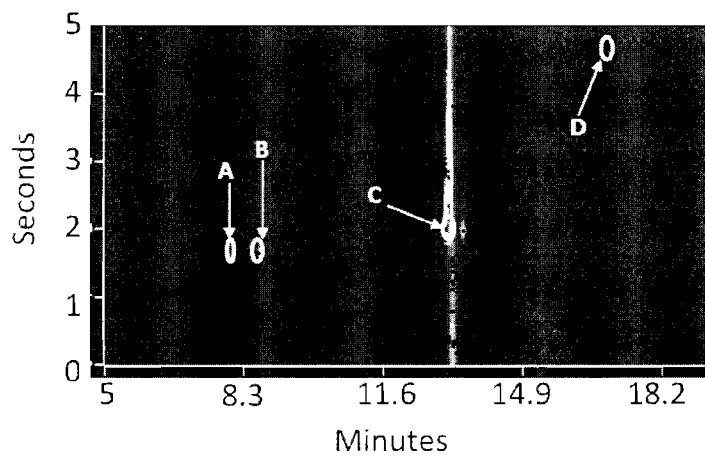
Figure 4-5- GCxGC contour plot of cocaine standard after 5 days of degradation
A-Ecgonidine (8 minutes, 1.80 seconds)
B-Ecgonine methyl ester (8.5 minutes, 1.80 seconds)
C-Cocaine (13.3 minutes, 1.94 seconds)
D-Benzoylecgonine (16 minutes, 4.70 seconds) was not present day 4

following an initial extraction of cocaine from urine at pH 14.0 which exceeded the pH limit, but did not degrade the fiber[17].

The extraction time for the SPME was optimized by extracting cocaine from water at 20 min, 30 min, 40 min, and 60 min. The peak area for cocaine after a 30 minute extraction time was the highest compared to all the other times and was chosen as the optimal extraction time for cocaine. The desorption time of the fiber was optimized by changing the purge time of the GC inlet to 15 seconds, 30 seconds, 45 seconds, 1 minutes, and 2 minutes with the highest peak area at a purge time of 1 minute. Therefore, the optimal desorption/purge time for the extraction was 1 minute.

4.10 Linearity study for SPME of cocaine from urine and water

Figure 4-6 shows the calibration curves for the SPME analysis of cocaine in water and urine. The linearity of the curve for cocaine in water is much better than that of the urine over the same concentration range of cocaine. This is indicated by the higher R^2 and better overall linear behavior of the individual points on the curve for the water extraction compared to the urine extraction. Further, %RSDs of the slopes of the calibration curves were 7.44% and 58% for deionized water and urine, respectively. Despite the low %RSD and high R^2 for the water extraction, the small deviations in the curve indicate that some of the cocaine may have been converted into its ionized state. Because it was suspected that the behavior was due to the sensitivity of the polyacrylate fiber towards basic pHs, water was not pH adjusted. The %RSD of slope for the urine curve further indicates poor linearity in conjunction with the R^2 value of 0.9673. This was not surprising due to the lower polarity of PDMS coating resulting less
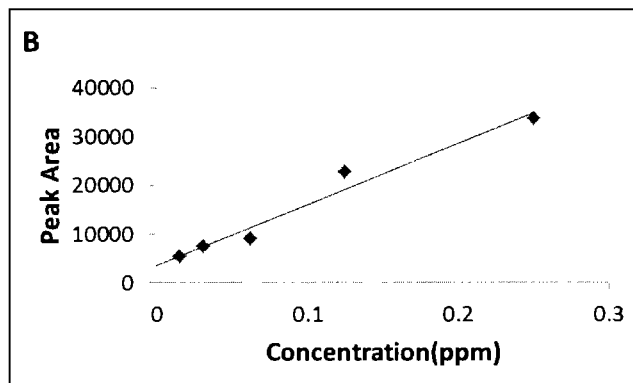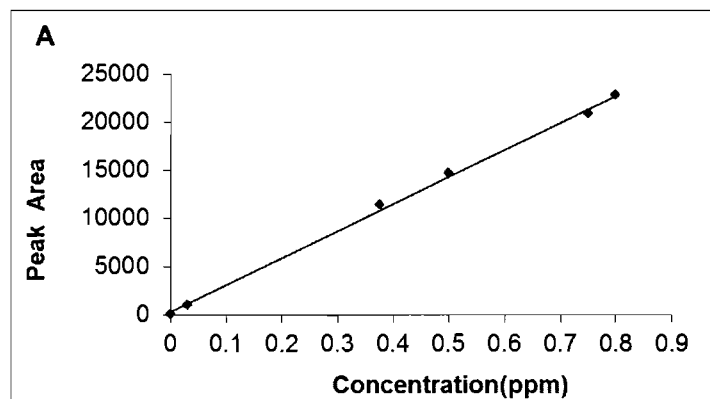
Figure 4-6 – Comparison of calibration curves for SPME of cocaine from: (A) water; (B) Urine. Peak area calculated using m/z: 82.

adsorption of cocaine in comparison to the more polar polyacrylate coating. The initial extraction

of the drug from urine using the PDMS fiber was performed without pH adjustment resulting in a

very low recovery of cocaine. Thus, the pH of the urine was adjusted to 14.0 which exceeded the

recommendation of the vendor resulting in degradation of the fiber after several extractions.

However, extraction at this pH resulted a higher recovery of cocaine. Therefore, the poor

linearity of the urine calibration curve was the result of using both a fiber coating of dissimilar

polarity compared to cocaine as well as exposing the fiber to a very basic pH.

4.11 LOD and LOQ for SPME of cocaine from water and urine

The LOD and LOQ for cocaine using liquid injection were determined to be 2.71 ng and 9.05 ng.

The LOD and LOQ for cocaine in water were 15 pg/mL and 50 pg/mL, respectively using

SPME. The LOD and LOQ for cocaine in urine were 25 pg/mL and 82 pg/mL. Water and urine

samples spiked with the LOD and LOQ of cocaine were analyzed three times with %RSDs

determined to be 18% and 20% for water and urine, respectively. The high values for the %RSDs

would normally indicate poor precision, however this is another example of the limitation of the

peak deconvolution alrgorithm of the ChromaTOF software as well as one major drawback to the

high sensitivity of the ToFMS.

4.12 Validation of the SPME method

Linearity, accuracy, and precision for the SPME method were validated for the extraction of

cocaine from water where a polyacrylate fiber was used for the extraction. Water was chosen for

the validation experiments because it is a much simpler matrix than urine and it served to

minimize matrix effects that resulted in a low recovery of cocaine and variability between

extractions. As discussed above, the pH of the water was not adjusted due to the sensitivity of the

polyacrylate fiber to basic pHs. Table 4-4 compares the results of the validation experiments to the quantitative parameters determined for the optimized curve

4.12.1 Linearity

The high and low values of the linear range are compared for the optimized and validated calibration curves in Table 4-4. The linear ranges for both curves were the same with the exception of the point at 800 ng/mL which was the upper limit of the linear range for the water extraction. This same concentration was plotted as a projected point on the validated curve where the expected peak area for 800 ng/mL was determined using the equation determined for the validated curve. Although the resulting R^2 value was similar for the two curves, the %RSD calculated for the slopes between the adjacent points of each curve showed some deviation indicating a difference in the linearity between the two curves. Therefore, the projected point at 800 ng/mL was eliminated from the validated curve where the true linear range of cocaine was determined to be 31 ng/mL to 500 ng/mL. The R^2 values and the %RSDs of the slopes for both curves are compared in Table 4-4 and showed that linearity for the validated curve was slightly better. Despite the subtle differences between the linear ranges of the two curves, the results for both show good linearity for trace concentrations of cocaine without having to adjust the pH of the water.

4.12.2 Precision

The validation of precision of the SPME method was performed at a high level and low level in order to determine repeatability of the method over the whole linear range. Precision was determined following the extraction of 62 ng/mL and 250 ng/mL cocaine from separate spiked water samples. Cocaine was extracted from the spiked water samples at both concentrations in

	Optimized Curve	Validated Curve
Linearity		
Low Value(ppb)	31	31
High Value(ppb)	800	500
R^2	0.998	0.9986
Precision	5.75%	4.52%
Accuracy(ppb)	N/A	149 ± 5.2
LOD(ppt)	15.00	88
LOQ(ppt)	50	294

Table 4-4– Comparison of Quantitative Parameters for optimized calibration curve and Validated calibration curve using SPME-GCxGC-ToFMS

triplicate and the %RSD for the peak area calculated for each concentration using the base peak for cocaine. Table 4-4 shows the precision determined for extraction of 250 ng/mL cocaine. The %RSD for the extraction of 62 ng/mL cocaine was determined to be 15.68%. These values indicate that the extraction method shows better precision at higher concentrations than at lower concentrations of cocaine which was not surprising since the S/N ratio at low concentrations of the drug was greater. As previously discussed, this same problem also affected the repeatability of the LOD and was determined to be due to both the limitation of the peak deconvolution algorithm in the data processing software and the high sensitivity of the ToFMS. This was not observed for the precision determined for the extraction of 250 ng/mL cocaine. In this case, the signal for cocaine at the high concentration is much greater than that of the noise resulting in much less interference between them. When peak deconvolution is performed, a majority of the noise is eliminated resulting in a much better precision at the high concentration of cocaine. It was determined that peak deconvolution is more effective during the analysis of higher analyte concentrations due to the minimal interference between the analyte signal and the noise.

4.12.3 Accuracy

Accuracy was determined from the %error of cocaine following the extraction of three water samples spiked with 150 ng/mL of the drug. The %error was determined by comparing the spiked concentration of 150 ng/mL cocaine to the extracted concentration. The extracted concentration of cocaine was determined using the equation for the validated calibration curve. The average %error after the three extractions was determined to be 2.57% indicating high accuracy for the extraction of cocaine from water. The values for accuracy reported in Table 4-4 show the average and the standard deviation for the extracted concentration following the three runs. Therefore, values in Table 4-4 show the SPME method was both accurate and precise for

the extraction of trace concentrations of cocaine. The %recovery of cocaine was also determined in order to confirm the results from the accuracy study and to determine if any significant matrix effects were present during extraction. Thus, the average %recovery for cocaine was determined to be 99.7% thereby confirming that the SPME method was accurate and that no significant matrix effects had occurred during extraction of cocaine. Thus, the results of the validation studies show that the SPME method was both accurate and precise for the extraction of trace concentrations cocaine from water despite the lack of pH adjustment.

4.13 Conclusions

The main conclusion from this study was that SPME-GCxGC-ToFMS is better suited for performing trace analysis of cocaine in comparison to liquid-liquid extraction techniques and/or GC-MS. The analysis of cocaine on the surface of US currency using GCxGC-ToFMS produced more linear calibration curves as well as an LOD and LOQ two orders of magnitude lower than what was determined using GC-MS. It was observed during the degradation study that the orthogonal separations of GCxGC-ToFMS, showed the presence of four major metabolites of the drug after extended exposure. Further, the results from the extraction of cocaine from water and urine using SPME showed a lower linear range as well as a lower LOD and LOQ than using LLE with GCxGC-ToFMS. The study also identified some of the limitations in the data processing software used by the GCxGC-ToFMS which were found to be caused by the high sensitivity of the ToFMS. However, the study shows that the benefits of SPME-GCxGC-ToFMS such as automation, high sensitivity, rapid analysis, and increased separation power make it better suited for trace analysis of drugs despite the limitations of the software.

CHAPTER 5 – ANALYSIS OF SALVINORIN A IN SAGE PLANTS, WATER, AND URINE

5.1 Background on Designer Drugs

In addition to cocaine, two designer drugs were studied using GCxGC-ToFMS. Designer drugs are normally chemically modified or synthetic versions of typical drugs of abuse that are meant to achieve a more potent euphoric effect[66]. In the US, these drugs have recently become a growing problem for law enforcement officials since they are not regulated or prohibited by existing laws[68]. Since the starting materials for these drugs are normally over-the-counter drugs and/or common household products, several laws in the US have been passed regulating the sale of these products[68, 69]. In this work, the two designer drugs studied were salvinorin A and Yaba and these will be discussed in the following two chapters. The work on salvinorin A was previously published by the author of this thesis[70]

5.2 Background on Salvinorin A

Salvia divinorum is a type of sage plant known to contain a psychoactive hallucinogenic drug known as salvinorin A[70-77]. The plant is used by the Mazatec in Mexico for curing and divination rituals. Recently, the plant has become popular in the United States as an alternative to marijuana and lysergic acid diethylamide (LSD). Prizinzano studied the pharmacology of salvinorin A, a neoclerodane diterpene, and discovered three main features about salvinorin A that distinguish it from typical hallucinogens: it is entirely natural whereas LSD is purely synthetic; it contains no nitrogen in its structure; it targets the κ opioid receptors whereas LSD targets serotonin receptors [70, 71, 73]. These features also make salvinorin A an excellent

149

candidate for a designer drug. Figure 5-1 shows the structure of salvinorin A and its common analogs.

In the United States, salvinorin A is not listed as a controlled substance by the Drug Enforcement Administration, nor is there any federal regulation prohibiting use of the drug [78]. Some states have classified this drug as illegal or have implemented regulations on the use of this drug. Previous work on salvinorin A has shown that the drug can be analyzed using both LC-MS and GC-MS [73, 78, 79]. However, these studies were mainly qualitative focusing on the biochemistry of the drug with no discussion of the quantitative figures of merit. LLE with GC-MS has been employed in previous studies of salvinorin A as the primary extraction technique for screening of biological samples and elucidation of analogs of salvinorin A [80].

Several papers have claimed that Salvinorin A can only be found in *S.divinorum* specifically, and no other sages[71-77]. In this work, three types of sage were chosen to determine whether or not they contained Salvinorin A; three sage species were *Salvia officinalis*, *Salvia dorii*, and *Salvia apiana*. *S.officinalis* is ordinary cooking sage commonly used as an herb to enhance flavors of meats due to the essential oils the sage contains[81]. *S.dorii* is known as desert sage and is often chewed or smoked as a substitute for tobacco producing a mild hallucinogenic effect on the user[82]. *S.apiana* is known as white sage and can be made into a tea to treat sinus, lung, and throat infections[83].
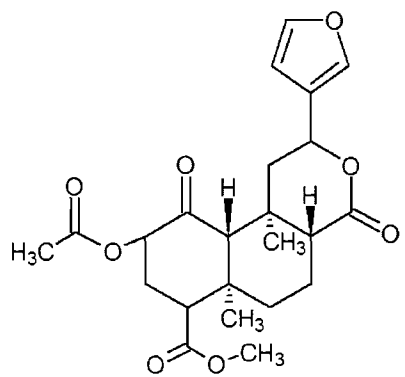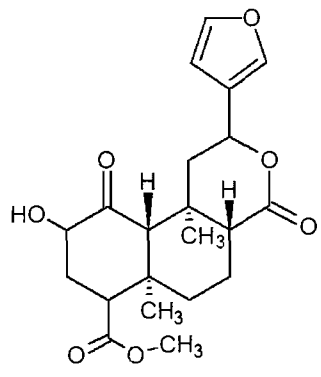
Salvinorin A   **Salvinorin B**   **Salvinorin C**
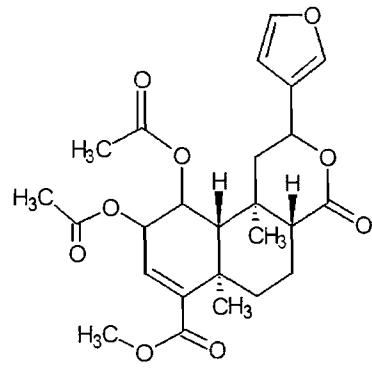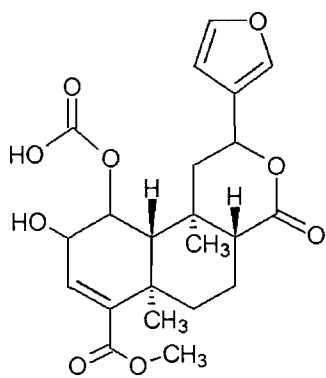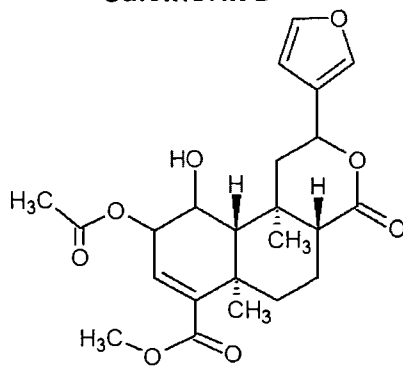
Salvinorin D   **Salvinorin E**

Figure 5-1 – Structure of Salvinorin A and Major Analogues.

5.3 – Purpose of the Experiment

In this work, LLE and solid phase microextraction (SPME) were used to extract salvinorin A from plants and spiked aqueous and human urine samples. *Salvia divinorum* leaves, stems and roots were extracted with traditional solvents, qualitatively and semi-quantitatively analyzed, while water and urine samples spiked with salvinorin A were extracted with both liquid-liquid-extraction and automated SPME for quantitation. GCxGC-ToFMS was used for the separation and detection of salvinorin A in all extracts in order to demonstrate the use of the technique for the qualitative and quantitative analysis of a designer drug.

5.4 - Analysis of Sage Plants

The three sage species previously mentioned were analyzed using GCxGC-ToFMS to confirm or deny the claims from the literature that salvinorin A was specific to *S.divinorum*. Figures 5-2 shows a comparison of the GCxGC contour plots from each sage following extraction with chloroform. The extraction of the plants was also conducted using methanol; however, it was observed that chloroform was capable of extracting more of the volatile and highly polar compounds in the extracts thereby providing a more detailed chemical profile for each sage. Although a majority of the compounds detected were essential oils and other odorants, some rare compound were detected such as cyanogen chloride[84], cannabinol[85], and cotinine[86]. However, the presence of each of these compounds was considered negilible due to the low S/N and the low peak areas determined. Subsequent instrumental analysis of each of these samples did not detect the presence of any of the aforementioned rare compounds. However, this experiment demonstrates that the orthogonal separations performed by the GCxGC and the rapid, high sensitivity of the ToFMS can be used to produce unique chemical profiles for complex, biological samples. It is most important to note that salvinorin A was not detected in any of these

(A) | **(B)** | **(C)**

S.Officinalis
A- Thujone
B- Borneol
C- Carophylene
D- Ledol
E- Pthalates
F- Steroids

S.Dorii
A- Benzoic Acid Derivatives
B- Pthalates
C- Aromadendrene

S.Apiana
A- Pthalates
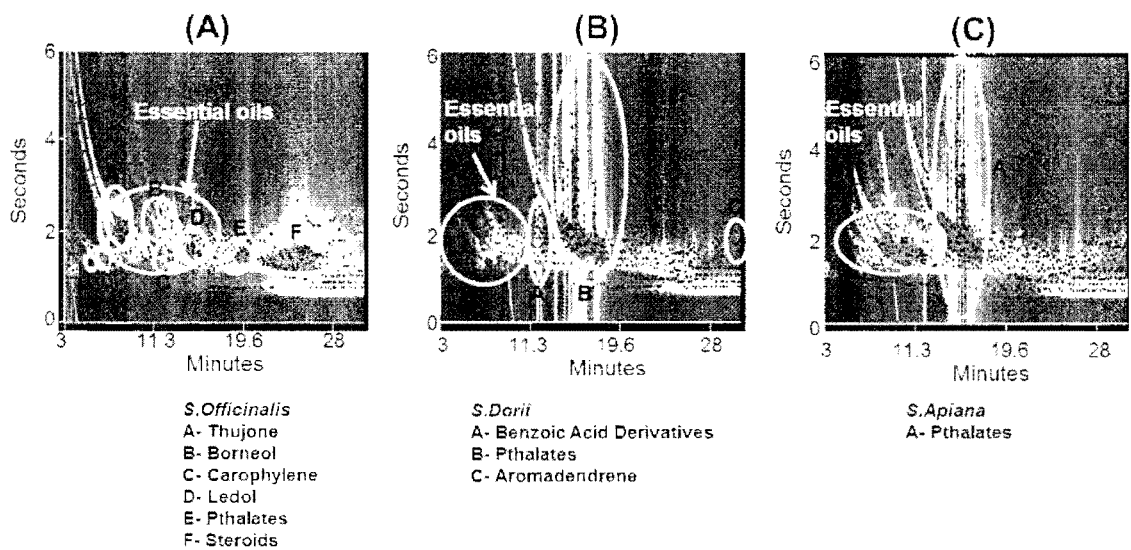
Figure 5-2 – Comparison of GCxGC contour plots and compounds detected in 3 sage species following chloroform extraction: (A) *S.officinalis*;(B) *S.dorii*; (C) *S.apiana*

sages regardless of the extraction solvent used. Thus, this confirms the claims in the literature that salvinorin A is only present in the *S.divinorum* sage plant.

5.5 Initial Confirmation of Salvinorin A

Prior to GCxGC-ToFMS analysis, a 1 mg/ml standard of salvinorin A was analyzed using traditional 1-dimensional quadrupole GC-MS according to the method of Giroud [74]. The mass spectrum provided by Giroud was used as the reference spectrum. Peak for peak matching between the two spectra was performed in order to confirm the presence of salvinorin A in the standard. Figure 5-3 shows a mass spectrum for salvinorin A from this work. The major peaks in the reference mass spectrum were at m/z: 94, m/z: 166, m/z: 273, and m/z: 432. The peak at m/z: 94 was the base peak and the peak at m/z: 432 was the peak for the molecular ion of Salvinorin A. The fragmentation pattern for each of the major peaks is discussed briefly by Giroud. The fragment for the base peak of salvinorin A contains the THF present in the parent indicating that the positive charge on the initial radical cation, and the molecular ion would be at the oxygen in the lactone ring located adjacent to the bond connecting the THF ring to the structure. Therefore, as the molecule begins to fragment in the ion source, it must open the lactone ring via hydrogen rearrangements and or homolytic α- cleavages. This appears to result in the breaking both bonds attaching the THF ring to the rest of the molecule.

5.6 Optimization of the GCxGC-ToFMS Method

The GCxGC method was optimized by identifying the following critical parameters affecting retention and the S/N of salvinorin A peak: the stationary phase of the second column, temperature ramp rate for both columns, the temperature offset between the primary and secondary ovens, the modulation period, and the MS scan rate. Each variable was changed one at
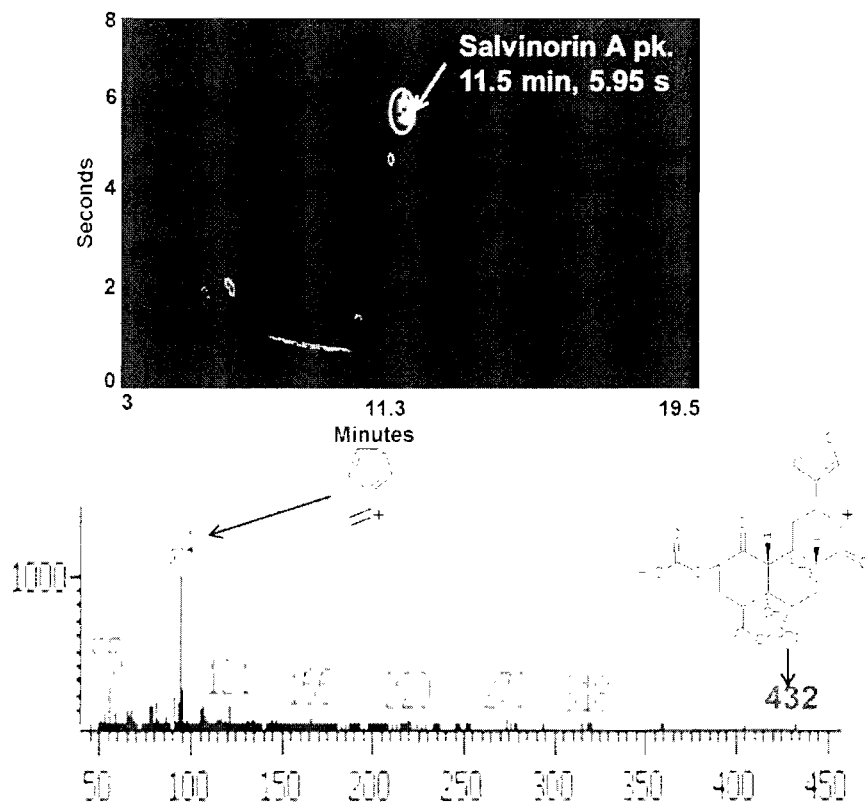
Figure 5-3 – GCxGC contour plot and ToFMS for salvinorin A
obtained under optimized conditions

a time while the other parameters were held constant to assess the effect of each variable. The 5% phenyl polydimethyl siloxane first dimension column is very common in drug analysis and is effective for wide ranges of analytes. RTX-200, a perfluoropolydimethyl siloxane derivative and DB-17, 50% phenyl polydimethyl siloxane, were evaluated for the second dimension, with DB-17 showing much stronger retention of the salvinorin A; thus it was chosen for further studies. With a single target analyte, a rapid, 30°C/min, temperature program in the first dimension ensures a rapid overall analysis. The offset between the ovens was increased from 5°C to 15°C to decrease second dimension retention and reduce wraparound, since salvinorin A and possible analogs are highly polar and may likely be retained on the second dimension column. The modulation time was also primarily increased to eliminate wraparound. The initial time was 5 seconds resulting in wraparound even with the higher oven offset, so it was increased to 8 seconds, yielding no wraparound and only a slight increase on the second dimension retention time. The MS scan rate was increased in order to produce smoother peaks and less noise in the mass spectra resulting in a higher S/N for salvinorin A. The initial rate of 20 spectra per second yielded noisy mass spectra and a jagged appearing peak on the chromatogram for salvinorin A. The final scan rate was 100 spectra/second. These conditions produced 1st dimension and 2nd dimension retention times for Salvinorin A of 11.5 min and 5.59 seconds, respectively, giving an elution temperature of 300°C. The GCxGC contour plot of a salvinorin A standard at 1000 ng/mL in chloroform, injected by liquid injection, indicating the peak for salvinorin A is shown in Figure 5-3. This demonstrates effective separation of the peak of interest from interferences such as column bleed, a strength of GCxGC.

5.7 Extraction from salvia divinorum plants

Salvinorin A was extracted from the roots, stems, and leaves of *S.divinorum* plants using LLE with chloroform. In order to estimate the amount of salvinorin A in each part of the plant, a calibration curve for salvinorin A was constructed using the external standard method. The curve had a linear range from 120-8000 ng/g with an R^2 value of 0.9998. During the method development phase, other solvents such as water, methanol, and acetonitrile were also tested, but chloroform provided the best linear range and correlation coefficient. Since chloroform is a strongly polar aprotic and hydrophobic solvent, it was able to dissolve salvinorin A without the risk of degradation. Salvinorin A was in solution with chloroform for the duration of this research and no degradation due to chloroform was observed.

The highest quantity of salvinorin A was found in the leaves of the plants, consistent with literature results, which indicate that the leaves are the primary part of the plant used for recreational use [71, 73]. However, after performing an exhaustive extraction of salvinorin A from the leaves, only approximately 60 ng/g of salvinorin A were observed, well below the lowest point on the calibration curve. The typical dose of salvinorin A necessary to achieve an euphoric effect is between 200 µg and 500 µg [71]. Therefore, a large quantity of our leaves would have been needed to generate the powerful euphoric effect that the drug is said to produce. It is likely that the cultivation conditions in our laboratory which were not optimized in any way, affected the plants performance. The literature also states that the leaves of the plant are often treated with additional salvinorin A in order to make them more concentrated, and thereby enhances the euphoric effect[71, 73]. Wide variation in both cultivation and extraction may offer

one explanation as to why the pre-concentration of salvinorin A in the leaves is often necessary to achieve a powerful effect. The stems and roots were also extracted using the same procedure. A detectable amount of salvinorin A was found in the stems, but salvinorin A was not detected in the roots.

Figure 5-4 shows a GCxGC contour plot from one of the *S.divinorum* leaf extracts indicating the presence of salvinorin A and analogs. The most prevalent of the analogs found were salvinorin B and C, although pharmacology studies of the salvinorin analogues have shown that only salvinorin A provides a hallucinogenic effect. Salvinorin A, B and C were identified by manually comparing their mass spectra to examples from Giroud [73]. Note that these are very closely related structures, as seen in Figure 5-1, so their first and second dimension retention times are similar, but both peaks are fully resolved. They would be much more difficult to fully resolve with traditional one-dimensional GC. Due to the unavailability of salvinorin B or C standards, the-amounts detected in the plant extracts were not quantified. However, by simple comparison of the peak areas, peak heights, and S/N ratios, it is expected that Salvinorin A is more prevalent than the other two analogues in all parts of the plant.

5.8 Extraction from spiked urine and water samples

Salvinorin A was extracted from spiked samples of urine and deionized water using both LLE and SPME. In this part of the study, the linear range, limit of detection, precision and accuracy were determined from water and urine, using external standard calibration. Analysis of spiked
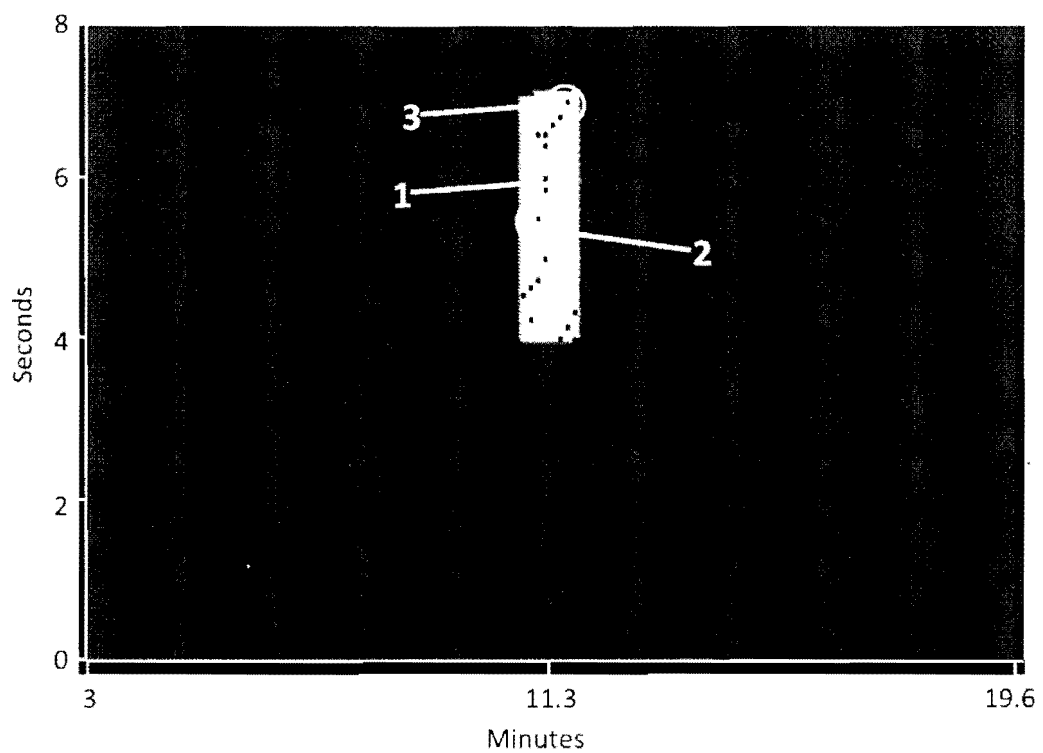
Figure 5-4 – GCxGC contour plot of *S.divinorum* leaf extract after 48 hours of degradation in methanol: 1) Salvinorin A at 11.6 min, 6.10 sec; 2) Salvinorin B at 11.3 min, 5.85 sec; 3) Salvinorin C at 12 minutes, 6.90 sec

samples for testing the feasibility of extraction techniques for salvinorin A is appropriate as salvinorin A appears unmetabolized as the parent compound in human urine. The conditions for SPME were optimized by changing the type of fiber and the extraction time, all of the other parameters were kept constant. The agitation speed was kept at 250 rpm which is the default speed for the autosampler, which agitates by moving the vial in a circular pattern around the needle. It was observed that increasing the agitation speed higher than the default setting often resulted in damage to the fiber. The incubation temperature was 30°C; higher temperatures produced no increase in peak area. Polydimethylsiloxane (PDMS), carboxen-divinylbenzene (CAR-DVB) and carbowax-divinylbenzene (CW-DVB) all showed little or no response for salvinorin A, so polyacrylate (PA) was chosen as the fiber coating. In general, polyacrylate has proven effective for extracting polar analytes from polar sample matrices. The optimal extraction time was determined to be 40 min by varying the extraction time and measuring the peak area response. Longer times gave no significant improvement.

Figure 5-5 shows TIC and EIC at m/z 94 GCxGC-ToFMS contour plots for the SPME extraction of salvinorin A from spiked urine samples at the 500 ng/mL level. The top figure is a total ion chromatogram, showing full detail of the separation of both the target compound from matrix and analysis interferences. The bottom plot is an extracted ion chromatogram at m/z 94, the base peak for salvinorin A, showing a more selective viewing of salvinorin A response. In both cases, the peak is clearly separated from interferences and readily quantifiable.
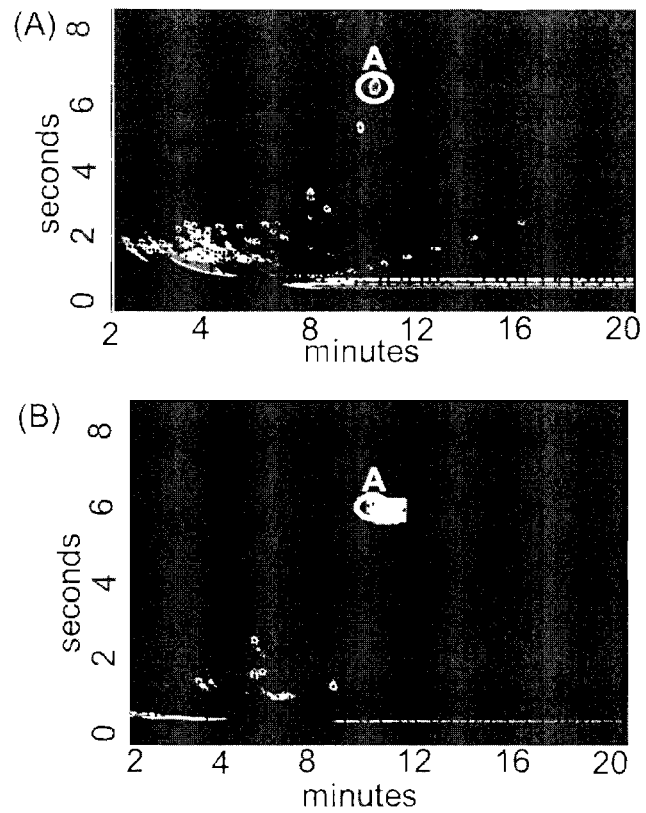
Figure 5-5 – GCxGC contour plots of Salvinorin A in urine at
retention times of 11.5 minutes and 5.95 minutes
(A) TIC (B) EIC at m/z: 94

5.9 Quantitation Results

Table 5-1 summarizes the analytical figures of merit for the LLE and SPME extractions from both water and urine. The limit of detection (LOD) for salvinorin A was determined using the IUPAC method with k = 3[55]. SPME showed a LOD at least one order of magnitude lower than LLE. The small volume of the SPME fiber coating (approximately 1 microliter) provides a potential concentration of up to 4 orders of magnitude with the 20 mL samples that were used in this work. This is significantly greater than the concentration achieved with the LLE method. Further, there is much less opportunity with the SPME technique for sample losses during sample transfer steps.

Precision was evaluated by analyzing spiked samples at the indicated concentration level (about in the middle of the expected calibration ranges) in triplicate for both LLE and SPME. For both urine and water extractions, the precision obtained by SPME was significantly better. This result was not surprising since the SPME method involves far fewer steps than the LLE method and is automated, reducing opportunities for experimental errors.

The calibration curve for the water extraction shows better linear behavior than that of the urine for concentration ranges plotted for both LLE and SPME. This is not surprising, due to matrix effects in urine. For both urine and water, SPME provided better linearity at lower concentrations, also as expected. The higher concentrations seen in the LLE curve are more typical of extractions that may be performed on plant material, while the SPME concentrations are more typical of those expected in clinical or drug testing analyses. Extraction of

	Water	Water	Urine	Urine
	LLE	SPME	LLE	SPME
LOD (ppb)	230	6	200	4
Precision (RSD)	16%	2%	24%	6%
Linear Range				
Low (ppb)	300	8	300	8
High (ppb)	5000	500	5000	500
R^2	0.9960	0.9906	0.9587	0.9857
Recovery (%)	102	105	83	88
Accuracy (125ppb)	ND	110 −/- 2	ND	114 −/1 2
Accuracy (620ppb)	520 −/-100	ND	620 −/- 150	ND

Table 5-1 – Comparison of Analytical Figures of Merit for salvinorin A

concentrations higher than 1000 ng/mL using SPME was not attempted due to the risk of exceeding fiber capacity. When the calibration curves for salvinorin A were plotted using LLE at the same low concentration range as SPME, salvinorin A was detected, but linear behavior was not observed for the extraction from both the water and urine. Therefore, SPME is better suited for trace analysis of salvinorin A, while LLE is better suited to the higher concentrations that may be found in extractions of plants or other salvinorin A containing products. In the case of urine extraction, a significant decrease in the matrix effects on salvinorin A extraction using SPME was observed, indicated by better precision from both water and urine and by the elimination of several sample handling steps in the LLE method that are directly attributable to the complexity of the matrix. These three factors helped to minimize sample loss between steps and variability between extractions.

Accuracy was evaluated by preparing five replicate spiked samples in water and urine at the indicated concentrations. It should be noted that in both the LLE and SPME determinations, the external standard method was used for quantitation. While the internal standard method is commonly used as a means for reporting improved precision, it was not chosen for this work. An appropriate internal standard with similar chemistry to salvinorin A, but not present in any samples and readily available at low cost, could not easily be obtained.

5.10 Conclusions

Salvinorin A, an up and coming hallucinogen, was extracted from plants, water and urine using LLE and SPME and determined in the extracts using GCxGC-ToFMS. Semi-quantitative studies

164

of leaves and stems of *s. divinorum* produced ppb quantities of salvinorin A, far below expected levels due to variation in cultivation and extraction methods. Salvinorin A was not detected in the roots. Salvinorin B and C were also detected in the leaves. Samples of water and urine spiked with salvinorin A were determined using SPME and LLE with SPME providing superior quantitative performance. Detection limits using SPME were approximately 5 ng/mL, with a linear range-from 8-500 ng/mL and precision of approximately +/- 10% using external standard quantitation. This range is appropriate for clinical or physiological samples. LLE was found more effective for higher concentrations that may be found in plant material or products containing salvinorin A. GCxGC-ToFMS provided chromatographic separation of the closely related salvinorin analogs and separation from chromatographic and matrix interferences.

CHAPTER 6 – ANALYSIS OF YABA IN WATER AND URINE USING SPME-GCxGC-ToFMS

6.1 - Background

Yaba is a designer drug consisting of a combination of caffeine, MDMA, methamphetamine, and ketamine. The structures for each drug are shown in Figure 6-1. Yaba has gained popularity in Thailand as a "club drug", but has also started to appear in the United States[87]. Aside from the drugs contained in Yaba, very little is known regarding the concentrations of the individual drugs in the mixture. Moreover, the interaction between each of the drugs as well as their total effect on the body is also unknown. Each drug acts on a specifc set of receptors in the brain which results in a euphoric effect that is unique to each drug. Thus, the combined effect of all four of the drugs acting on multiple receptors simultaneously greatly intensifies the overall euphoric effect as well as amplifying the amount stress on the user's body[87-90]. The following discussion will describe the mechanism of each drug once inside the body as well as commonalities in their chemical and physical properties.

Methamphetamine is a basic white crystalline solid with a pKa of around 9-10[66, 91]. It is fat-soluble allowing it to rapidly cross the blood-brain barrier. When the drug is of high purity, the crystals appear similar to that of ice chips or shards of glass. Methamphetamine gained notariety as a designer drug in the US in the 1980s as a less expensive alternative to cocaine[91]. Since that time, methamphetamine has grown in popularity in the US and is commonly used by a wide variety of people including truck drivers, college students, overweight people, etc. Two main reasons that make methamphetamine so attractive is that it causes a suppressed appetite resulting

Methamphetamine

3,4-Methylenedioxymethamphetamine(MDMA)

Ketamine

Caffeine
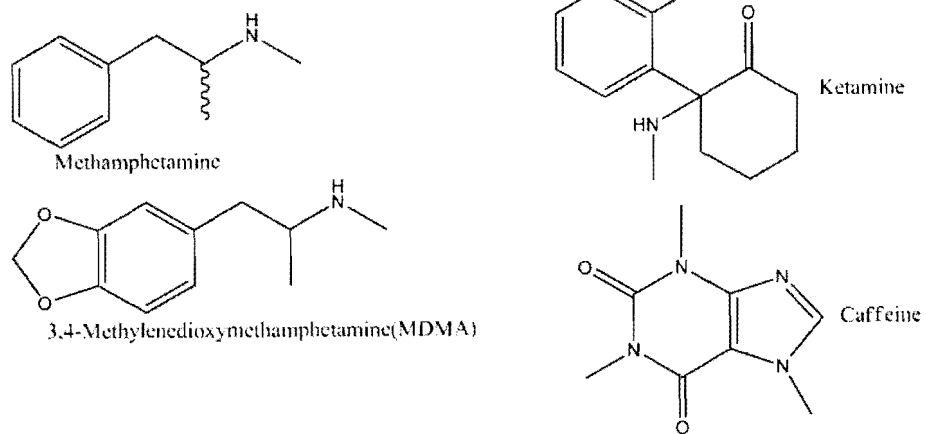
Figure 6-1 – Structures of four drugs contained in Yaba.

in rapid weight-loss and prolonged wakefulness that allows a user to remain awake for days at a time. It is also highly addictive due to the massive amount of dopamine released from the brain. The most common methods of administering methamphetamine include inhalation from smoking the drug or direct intravenous injection[92]. The drug then travels through the bloodstream, crossing the blood-brain barrier, and targeting the dopamine receptors. Unlike other drugs of abuse, methamphetamine actually interacts very strongly with these receptors resulting a more powerful and longer lasting period of euphoria as well as a greater depletion of dopamine in the body[66, 89, 91]. Other effects of using methamphetamine include a raise in body core temperature, restlessness, increased heartrate, heightened alterness, shortness of breath, nervousness, and death by stroke or cardiac arrest.

Like methamphetamine, MDMA is also a basic, white crystalline solid with a pKa of around 9-10[66, 93]. It is also fat-soluble and crosses the blood-brain barrier, however the rate at which MDMA crosses the barrier is slower than that of methamphetamine due to its structure. Figure 6-1 shows that the only difference between the structures of MDMA and methamphetamine is additional dioxymethylene functional group at the 3 and 4 position of the aromatic ring making it slightly more polar[94]. Due to structural similarity with methamphetamine, MDMA targets both dopamine *and* serotonin receptors in the brain. The most common form of adminsitration of MDMA is that of a powder compressed into a tablet that, when ingested, causes increased sexual awareness and arousal in addition to the stimulatory and long-lasting euphoric effect associated with methamphetamine.

The added euphoric effects of MDMA come from the interaction of the drug with serotonin receptors in the brain which control sleep regulation, anxiety relief, sexual behavior/awareness,

mood regulation, and also hallucinations [58, 94]. MDMA binds to a specifc serotonin receptor known as $5\text{-}HT_{2B}$ in the prefrontal cortex of the brain resulting in a conformational change in the receptor and release of serotonin[94]. The binding of MDMA releases a massive amount of serotonin from the brain which opens an ion channel adjacent to the $5\text{-}HT_{2B}$ receptor triggering a release of ions into the body. This is the typical mechanism observed for serotonin receptors which are part of a larger family of receptors known as G-protein coupled receptors(GPCRs)[58].

MDMA and methamphetamine are considered as Class I Controlled Substances by DEA since have no medicinal value and also has a very high potential for abuse much greater than that of most conventional drugs[95]. The structural differences between these two drugs give each one unique chemical properties implying that each drug would also yield unique metabolites formed upon interaction with the human body. Previous studies of the metabolites and impurities of each drug are available in the literature, however very little information is available regarding the profiles produced due to the combined interaction of these drugs[87-94].

Ketamine was originally developed in the 1960s, as a less potent alternative for general anesthesia and sedation instead of PCP[96]. It is currently used by veterinarians in conjunction was other sedatives such as diazepam (Valium) to induce general anesthesia in small mammals[66, 96]. It is classified by the DEA as a Class III Controlled Substance due to its high medicinal value and low potential for abuse[95]. The drug is most stable as a hydrochloride salt and can exist as either a white powder or clear liquid[88]. The hydrochloride acts similarly to a

buffer minimizing ionization of the drug when in the presence of slightly basic media such as the human body.

The most commons routes of administration are oral or through intramuscular injection. Like the two amphetamines, ketamine is fat-soluble and crosses the blood-brain barrier targeting the NMDA receptors in the brain. The NMDA receptors are calcium ion channels that are responsible for regulating memory and pain response[88, 95-97]. Unlike MDMA, ketamine binds *directly* to the ion channel acting as an antagonist meaning it prevents the flow of calcium and deactivates the receptor thereby preventing the brain from regulating memory and registering pain felt by the body[58]. This action is called "dissociative amnesia" which occurs when an individual is placed under general anesthesia prior to surgery[88]. However, in the case of ketamine usage, the individual is awake, but may have little or no recollection of the events that occurred while ketamine was bound to the NMDA receptors.

It should be noted that ketamine is the only one of the drugs contained in Yaba that does not target dopamine receptors. It is suspected that the role of ketamine in Yaba appears to be as a means to offset the powerful stimulatory effects of the two amphetamines. The amphetamines are known as receptor agonists since they both drastically increase the function of the receptors resulting in a massive release of dopamine and serotonin. Therefore, the combined actions of all three of these drugs occurring in the body at once gives the user both the powerful stimulatory and euphoric effect caused by the action of the two amphetamines as well as the "dissociative amnesia" effects caused by the action of ketamine[87, 97-99].

The fourth drug present in Yaba is caffeine which is one of the most widely used stimulants throughout the world since it is found in a wide variety of beverages including coffee, tea, cola products, etc. Use of caffeine can be traced back to the Stone Age, when primitive man discovered that eating specific beans or plants gave them "energetic, feelings of well-being"[100]. The drug itself is a basic, bitter, white, crystalline substance with a pKa of approximately 10[101]. Like the other drugs in Yaba, caffeine is fat-soluble allowing passage through the blood-brain barrier. However, it targets the adenosine receptors which are another type of GPCR that control a calcium ion gated channel. These receptors regulate dopamine release from the brain, suppress neural activity, and regulate blood flow to the brain[102]. Caffeine acts as an antagonist for this receptor resulting in reduced blood flow to the brain causing increased heart rate, alterness, and wakefulness.

When used in conjunction with methamphetamine, caffeine prevents the release of dopamine from the adenosine receptors ultimately resulting in a build-up of the neurotransmitter in the brain[87, 103]. This build-up provides methamphetamine with more dopamine that it can force out of the brain ultimately prolonging the euphoric effect experienced by the drug. The primary function of caffeine in Yaba is to act as cutting agent of methamphetamine. A cutting agent reduces the concentration a specific illicit drug in a single dose thereby reducing the potency of the euphoric effect. Although most cutting agents reduce both the potency and length of the euphoric effect for an illicit drug, caffeine reduces the *potency* of the euphoric effect of methamphetamine, but also prolongs the *length* of the euphoric effect. This behavior is atypical for a typical cutting agent and makes the interaction between caffeine and methamphetamine unique.

6.2- Purpose of the Experiment

The discussion above establishes the following similarities between the four drugs: they are fat-soluble and cross the blood-brain barrier; they target receptors in the brain which act on both the central and peripheral nervous systems; they share a common route of administration; they are excreted in the urine; and their respective pKa's reveal that are weak bases and therefore partially ionize in water. In this work, these properties were investigated in order to develop a extraction and analysis method for a full Yaba mixture from water and urine using solid phase microextraction(SPME) followed by analysis with GCxGC-ToFMS. The mixture was evaluated using a full-factorial design of experiments(DOE), which was explained in Chapter 2, providing insight regarding the interactions between the drugs following extraction for each matrix which could be useful for establishing a preliminary impurity profile of the Yaba mixture.

6.3- Analysis of Individual Drugs in Yaba

6.3.1- GCxGC-ToFMS Method Development and Optimization

Method development and optimization of the GCxGC-ToFMS method was conducted for all four of the drugs in Yaba using a 1 mg/mL non-extracted certified reference standard of each drug in ethanol. The goals for each analysis was to achieve the shortest retention time in the first dimension, the most orthogonal separation with no wraparound, the highest S/N ratio, and shortest overall run time. This was achieved by optimizing the conditions of the temperature programs for both columns, the temperature offset between the two programs, the modulation period, the hot pulse time of the modulator, and the scan rate of the ToFMS. The remaining method parameters were kept constant throughout the analysis. The same parameters were also changed during method optimization for the three remaining drugs in Yaba.

A wide temperature program from 40°C to 300°C and 45°C to 305°C were used for the first and second columns, respectively, to determine the initial retention times of each drug on each column. The program rate was 10°C/min and the hold times at the initial and final temperature were 1 minute and 5 minutes, respectively. These parameters were the same for both columns. The initial modulation period was 5 seconds with a hot pulse time of 0.60 seconds and cold pulse time of 1.90 seconds in order to optimize the orthogonal separation of each drug as well as determine the initial amount of wraparound on the contour plots. The scan rate of the ToFMS was changed in order to increase the S/N ratio of each drug. The initial rate was 20 spectra/second which produced jagged peaks as well as a very noisy baseline for the chromatogram and the mass spectra. The optimized instrumental conditions for each drug were described in Chapter 2.

6.3.1.1 - Caffeine

The initial retention time for caffeine in the first dimension was 14 minutes which corresponded to an elution temperature of 170°C and a run time of 32 minutes. The final temperature of the temperature programs was decreased to 200°C and 205°C for the first and second columns, respectively. This resulted in no change for the retention time in the first dimension, but reduced the overall run time to 22 minutes. The temperature program rate was increased to 15°C/min and the hold time at the final temperature was reduced from 5 minutes to 2 minutes resulting in a further reduction in the run time to 14 minutes and first dimension retention time of 9.67 minutes. The rate was also increased to 20°C/min which proved to be too fast yielding no peak for caffeine in repeated runs. However, the rate of 15°C/min was not determined to repeatable since the elution of the caffeine peak was not consistent and appeared to elute sporadically. Thus,

the program rate was returned to 10°C/min yielding the optimized retention time in the first dimension and run time of 14 minutes and 19 minutes, respectively.

The initial contour plot for caffeine under the initial modulator conditions yielded a second dimension retention time of 1.80 seconds with some wraparound present. The modulation period was increased to 6 seconds and 8 seconds in order to increase the retention of caffeine on the second column. No change in the retention time was observed at 6 seconds, however the retention time significantly increased to 2.49 seconds using an 8 second period, but also resulted in a greater amount of wraparound observed on the contour plot. The hot pulse time of the modulator was then increased to 0.90 seconds and 1.20 seconds, however no noticeable decrease in the amount of wraparound was observed. Therefore, the temperature offset between the ovens was then increased 5°C to 15°C which resulted in eliminating most of the wraparound and produced a better orthogonal separation. It was also observed that the higher offset did not further increase the retention time of caffeine on the second column indicating that 2.49 seconds was the optimal retention time for caffeine using the RTX-200 column.

The scan rate of the MS was increased to 50 spectra/second and 100 spectra/second. Both scan rates served to reduce the background noise level of the instrument, however since a higher S/N ratio and smoother peak for caffeine was observed at 50 spectra/second, it was determined to be the optimized scan rate. Figure 6-2 shows a GCxGC contour plot of caffeine analyzed under the optimized conditions.
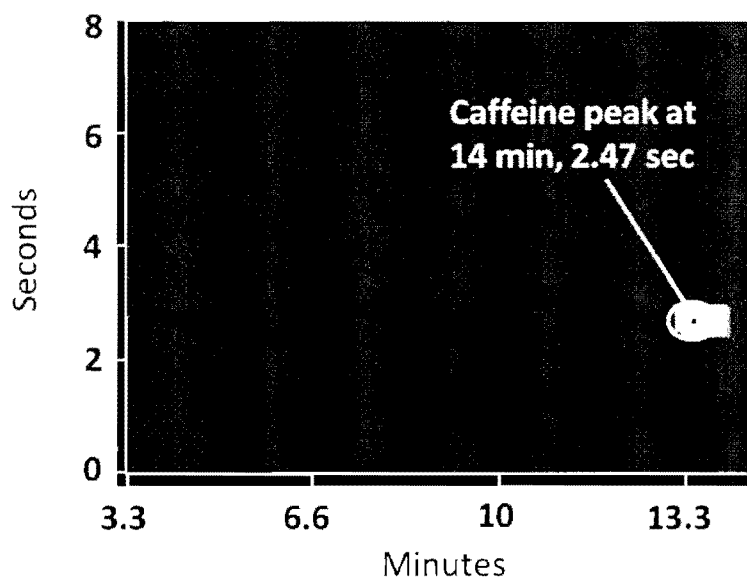
Figure 6-2 – GCxGC contour plot for 1 µg/mL of caffeine analyzed under optimized instrumental conditions. Plot shows EIC for m/z: 194.

6.3.1.2 - Methamphetamine

Initial analysis of methamphetamine under these conditions yielded retention times for

methamphetamine of 12.25 minutes and 2.26 seconds for the first and second column,

respectively, where the overall run time was 54 minutes. The initial GCxGC contour plot showed

a good orthogonal separation for methamphetamine and also had little wraparound present.

Therefore, the only change necessary to optimize the instrumental method was to shorten the

overall run time by changing the initial and final temperatures for the temperature programs

corresponding to both columns. The initial temperatures were increased from 40°C and 50°C to

70°C and 80°C for the first and second columns, respectively. Since the elution temperature of

methamphetamine was determined to be 102°C, the final temperatures of both programs were

decreased from 290°C and 300°C to 190°C and 200°C for the first and second column,

respectively. This reduced the run time to 27 minutes. The rates for both temperature programs

were increased to 10°C/min to further reduce the run time; however, due to high volatility of

methamphetamine, no peak was observed at this rate and it was returned to 6°C/min. These

changes to the temperature programs resulted the retention times of 6.25 minutes and 2.26

seconds in the first and second dimensions, respectively, and a run time of 27 minutes. Figure 6-

3 shows the GCxGC contour plot obtained for methamphetamine using the optimized

instrumental conditions.

6.3.1.3 - MDMA

The difference in structure shown in Figure 6-1 suggests that MDMA has a higher molecular

weight and thus a higher vapor pressure than methamphetamine. This indicates that MDMA

should have a longer retention time and higher elution temperature on the first column than

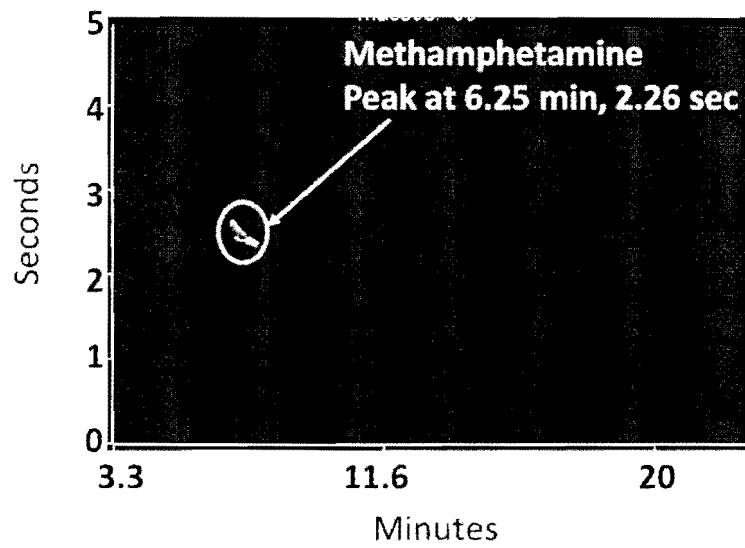methamphetamine. The first dimension retention time for MDMA was determined to be 18.5

Figure 6-3 – GCxGC contour plot for 1 µg/mL of methamphetamine analyzed under optimized instrumental conditions.
Plot shows EIC for m/z: 58.

minutes using the same instrumental conditions used for methamphetamine. The elution temperature was determined to be 175°C, which was approximately 70°C higher than that of methamphetamine. The temperature program rates for both columns was increased to 10°C/min resulting in a first dimension retention time for MDMA of 11.5 minutes and run time of 19 minutes. However, the peak for MDMA was not present in repeated runs at this rate and it was determined to be too fast and not repeatable for MDMA. The final temperatures were increased to 220°C and 235°C for the first and second columns, respectively. These temperatures did not affect the retention of MDMA on the first column and were found to be repeatable for MDMA. The second dimension retention time for MDMA was observed to be 2.26 seconds. Since the contour plot showed good orthogonal separation and minimal wraparound, no changes to the modulator conditions or temperature offset were made. Thus, the optimized retention times for MDMA were determined to be 11.5 minutes and 2.26 seconds whereas overall run time was 21 minutes. The remaining parameters of the instrumental method were not changed. Figure 6-4 shows a GCxGC contour plot for MDMA analyzed under the optimized method.

6.3.1.4 - Ketamine

Under the initial conditions described above, the first dimension retention time for ketamine of 14.5 minutes which corresponded to an elution temperature of 195°C and an overall run time of 30 minutes. The initial temperature of the first dimension temperature program was increased to 80°C and 85°C for the first and second column, respectively, resulting in an overall run time of 27 minutes and a first dimension retention time of 12 minutes. However, multiple peaks for ketamine were observed under this temperature program resulting in different retention times on both columns between runs. This variation was also observed following changes to both the final temperatures and program rates. Thus, since none of the other programs were determined to
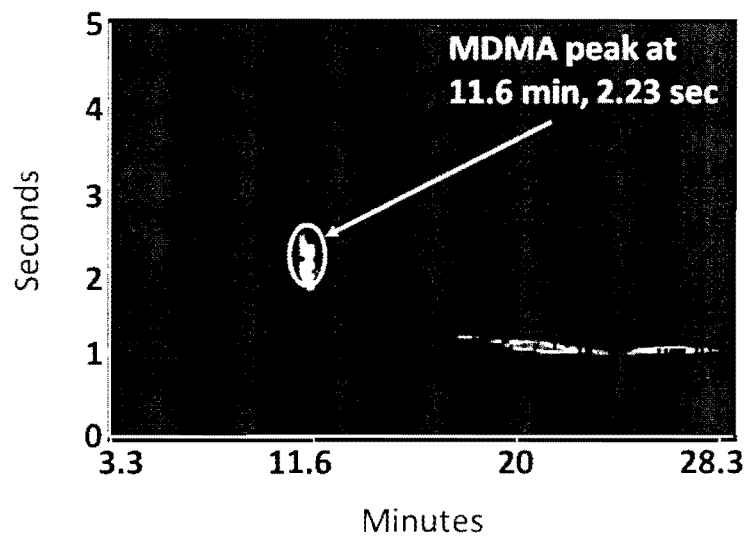
Figure 6-4 – GCxGC contour plot for 500 ng/mL of MDMA
analyzed under optimized instrumental conditions.
Plot shows EIC for m/z: 58.

be repeatable, the initial temperature programs used for ketamine were used as the optimized

conditions. The structure of ketamine, shown in Figure 6-1, contains a benzyl chloride

functional group as well as a ketone functional group thereby indicating that it should be more

polar than either of the two amphetamines. However, not only was wraparound of ketamine on

the second column observed on the contour plot following analysis under these conditions, but

the second dimension retention time was approximately one second lower than the

amphetamines at 1.25 seconds. Therefore, the temperature offset between the temperature

programs was increased from 5°C to 15°C in order to improve the orthogonal separation of

ketamine and to increase its second dimension retention time to 2.25 seconds; however, this did

not eliminate the wraparound present in the contour plot. Thus, the hot pulse time of the

modulator was increased from 0.90 seconds to 1.20 seconds which served to eliminate the

wraparound. Further, overload in the second dimension was also observed in the ketamine peak;

thus, when the initial modulator temperature was increased from 100°C to 110°C, no overload

was observed in the second dimension. The remaining instrumental parameters were not changed

from the initial conditions. The GCxGC contour plot for ketamine under the optimized

conditions is shown in Figure 6-5.

6.3.2- Development and Optimization of the SPME Method

A PDMS-DVB fiber was chosen to extract all four of the drugs in Yaba from both matrices

based on reports in the literature than this type of fiber was selective towards amines and

amphetamine compounds[13, 14, 48]. The main parameter that was changed during method

development was the extraction time in order to maximize the recovery of each drug from both

matrices. The general procedure for optimizing extraction time in SPME was described in

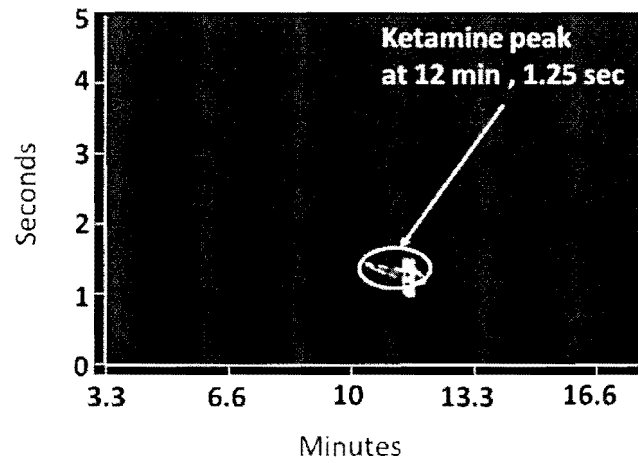Chapter 1. The remainder of the extraction conditions were kept the same for each of the four

Figure 6-5 – GCxGC contour plot for 1 µg/mL of ketamine
analyzed under optimized instrumental conditions.
Plot shows EIC for m/z: 180.

drugs. In order to minimize matrix effects normally associated with extraction procedures, deionized water was used as the matrix for extraction during method development.

6.3.2.1 - Caffeine

Extraction of the 1 μg/mL caffeine standard under the initial SPME conditions did not yield a peak following GCxGC-ToFMS analysis. This extraction was repeated under the same conditions using the same concentration for caffeine yielding the same results. One of the requirements in order for SPME to work properly is that the sample containing the analyte to be extracted must be brought to equilibrium which occurs during the incubation period of the sample immediately prior to extraction. As discussed in chapter 1, equilibrium in SPME is dependent on the temperature and agitation speed of the sample. Since the agitation speed could not be increased without damaging the fiber, the temperature during incubation and extraction was increased from 30°C to 35°C and 40°C. Caffeine was extracted in either case indicating that either temperature resulted in the equilibration of the sample. The optimized incubation temperature was determined to be 40°C since it was later determined that concentrations of caffeine below 62 ng/mL could not be extracted when a lower incubation temperature was used. This point will be discussed further later in the chapter. Caffeine was extracted at 30 minutes, 40 minutes, 50 minutes, and 60 minutes to determine the optimal extraction time. Figure 6-6 shows that the peak area for caffeine steadily increased up to an extraction time of 60 minutes. Although caffeine was also extracted using an extraction time of 70 minutes, it did not show a significant further increase in the peak area and was also not included in Figure 6-6. Therefore, the optimized extraction time for caffeine was determined to be 60 minutes. Further, carryover of the drug was observed between extractions and was eliminated by baking out the fiber for 20 minutes between extractions.
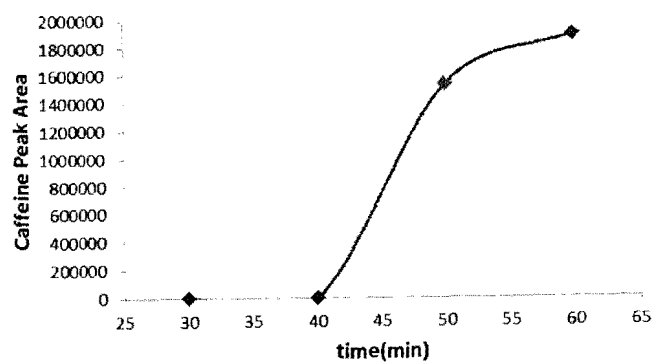
Figure 6-6 – Extraction time analysis curve for caffeine

6.3.2.2 - Methamphetamine, MDMA, and ketamine

The peak for methamphetamine produced under the same SPME conditions used for caffeine

showed a strong signal and high peak area for the drug indicating that the same SPME method

can be applied to both caffeine and methamphetamine. The incubation and extraction

temperatures were lowered from 40°C to 30°C due to the higher volatility of methamphetamine

and also to prevent it from degrading. Figure 6-7 shows the extraction time analysis curve for

methamphetamine which shows similar peak areas for 40 minute, 50 minute, and 60 minute

extraction times. Therefore, the optimized extraction time for methamphetamine was determined

to be 40 minutes. The same protocol was also used to develop the method for both MDMA and

ketamine which extraction time analysis curves similar to that of methamphetamine. This

demonstrated that a single SPME method could be used for the extraction of all four drugs

contained in a single mixture.

6.3.3 – Confirmation by ToFMS

The identity of each drug in Yaba was confirmed by comparison of the ToFMS spectrum

obtained following analysis to the respective spectrum in the NIST library. Further confirmation

was determined by analysis of the fragmentation pattern corresponding to each drug.

6.3.3.1 - Caffeine

Figure 6-8 shows the comparison between the ToFMS obtained for caffeine and the NIST library

spectrum. The major peaks common to both spectra in Figure 6-8 were at m/z: 55, 109, and 194.

The peak at m/z: 194 corresponds to both the base peak and the M^+ ion for caffeine. The

fragment corresponding to m/z: 109 forms as the result of a loss of a methyl-isothiocyanate

radical via a heterolytic cleavage followed quickly by the loss of carbon monoxide. The peak
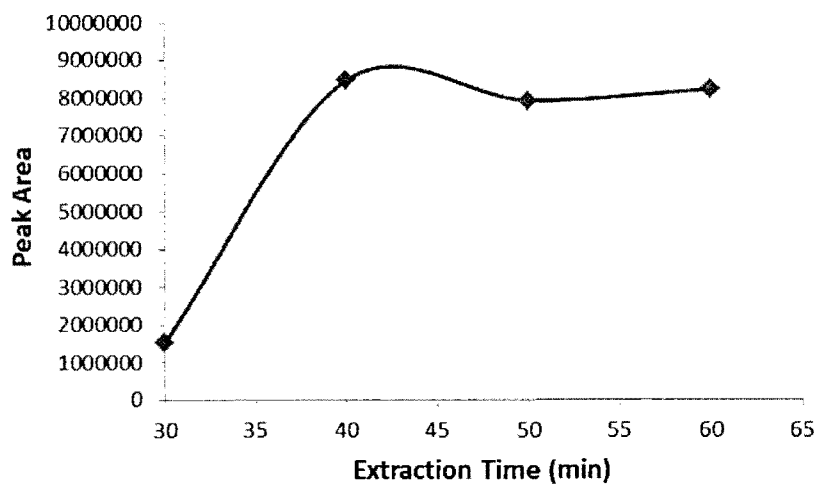
Figure 6-7 – Extraction Time Analysis
Curve for Methamphetamine
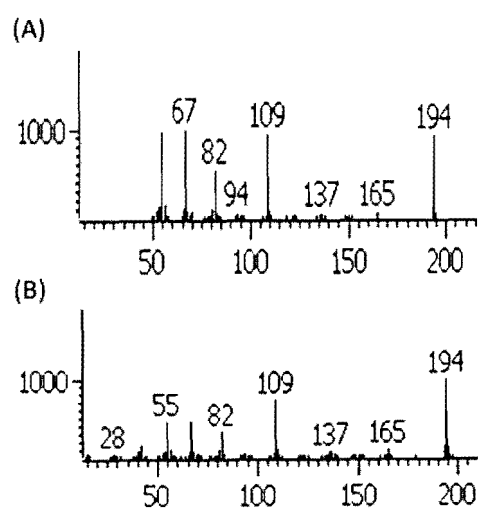
Figure 6-8 – Comparison of mass spectrum for caffeine from (A) ToFMS
To (B) NIST Library

corresponding to m/z: 55 is formed via two heterolytic cleavages and hydrogen rearrangements resulting in the loss of two hydrogen cyanide moieties.

6.3.3.2 - Methamphetamine

Figure 6-9 shows the comparison between the ToFMS obtained for methamphetamine and the NIST library spectrum. The major peaks in both spectra were at m/z: 58, 91, and 149 where the base peak for methamphetamine is at m/z: 58 and the M^+ Ion is at m/z: 149. The low abundance of the molecular ion is due to the low ionization energy of primary and secondary amines and is characteristic for these compounds[44]. Although the ionization energy of amines is relatively low, the abundance of the M^+ Ion is very low and is often negligible for primary and secondary amines[114]. Fragmentation of the M^+ ion occurs thru homolytic α-cleavage resulting in the loss of the phenyl methyl group in methamphetamine(see Figure 6-1). The fragment at m/z: 91 also forms as a result of heterocyclic cleavage resulting in the loss of alkyl amine corresponding to the base peak. The low abundance of the fragment at m/z: 91 in comparison to the base peak is due to the rules governing fragmentation in EI mass spectrometry described by McLafferty[44]. The fragmentation pattern observed for methamphetamine is typical of secondary amines as well as amphetamine compounds[42-44, 66].

6.3.3.3 - MDMA

Figure 6-10 shows a comparison of the mass spectra for MDMA obtained from the ToFMS and the NIST library spectrum. The major peaks in both spectra were observed at m/z: 58, 135, and 193 where m/z: 58 is the base peak and m/z: 193 is the M^+ ion. The base peak at m/z: 58 corresponds to the mass fragment bearing the same structure as the base peak for methamphetamine. Due to the similar structures of methamphetamine and MDMA, the
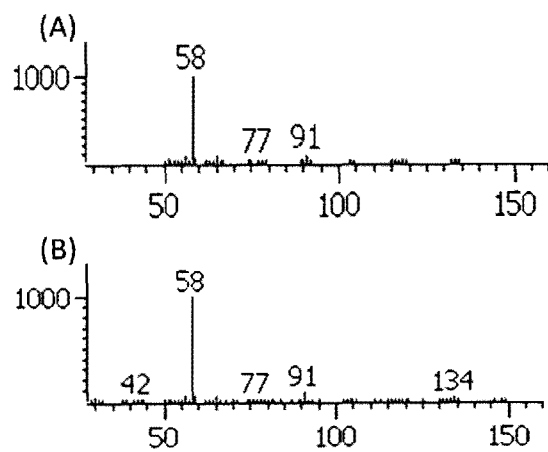
Figure 6-9 – Comparison of mass spectra for methamphetamine obtained from (A) ToFMS and (B) NIST Library
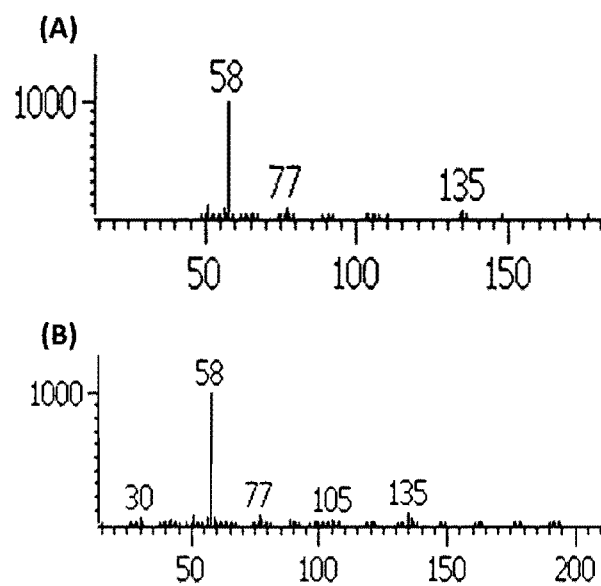
Figure 6-10 – Comparison of mass spectra for MDMA
Obtained from (A) ToFMS and (B) NIST Library

formation of the fragment corresponding to the base peak in MDMA follows the same

mechanism as previously described for methamphetamine. The peak at m/z: 135 in the mass

spectrum of MDMA is formed via heterolytic cleavage resulting the formation of a fragment

bearing the 3,4-methylenedioxy moiety which can be used to distinguish it from other

amphetamines not bearing this moiety. It must also be noted that the same fragmentation

mechanism described for formation of the m/z: 91 mass fragment of methamphetamine is

followed for the formation of the m/z: 135 mass fragment of MDMA. Thus, these unique masses

used to differentiate between amphetamines contained in the a single sample since they typically

follow the same fragmentation pattern. This point will be discussed further during the analysis of

the full Yaba mixture in which a variety of amphetamines were identified.

6.3.3.4 - Ketamine

Figures 6-11 shows a comparison of the mass spectrum for ketamine obtained from the ToFMS

and the NIST library spectrum. The major peaks similar to both mass spectra were identified at

m/z: 237, m/z: 209, and m/z: 180 where m/z: 237 corresponds to the molecular ion and m/z: 180

corresponds to the base peak. The low abundance of the molecular ion is due to the low

ionization energy and instability of secondary amines[44]. The base peak in the mass spectrum

at m/z: 180 is formed following the loss of an ethyl ketone radical with a mass of 57 amu via

homolytic α-cleavage and hydrogen re-arrangement. Formation of the peak at m/z: 209 is

formed following the opening of the cyclohexanone ring and the loss of the ketone group via

homolytic α-cleavage and hydrogen re-arrangement.
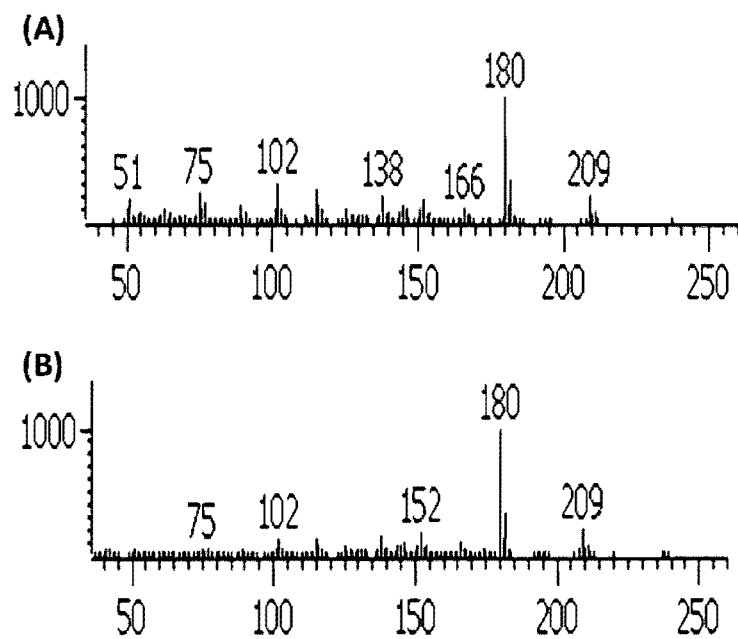
Figure 6-11 – Comparison of mass spectra for ketamine obtained
From (A) ToFMS and (B) NIST Library

191

6.3.4- Quantitation results from spiked water and urine samples

Table 6-1 summarizes the analytical figures of merit (linearity, LOD, LOQ, accuracy, recovery, and precision) determined for each drug in Yaba and are discussed below in the following sections.

6.3.4.1- Linearity

Calibration curves for the extraction of each drug from spiked water and urine samples are compared in Figure 6-12 and Figure 6-13 where the range plotted for each curve is reported in Table 6-1. The peak areas used to plot each curve were calculated using the extracted ion chromatogram (EIC) for the base peak corresponding to each drug. It was observed that the EIC showed less interference from the background noise and greater S/N for each drug ultimately resulting in better linearity in comparison to the total ion chromatogram(TIC).

Due to the slightly acidic nature of both the water(pH~6.5) and urine(pH~6.0), the pH of both matrices was adjusted to 8.0 prior to extraction. The pH value was based on the pKa values for each of the drugs(see Table 1-1). A second set of calibration curves were produced without performing pH adjustment to either matrix and compared to the curves in Figure 6-12 and Figure 6-13. Since no significant change in the linearity between the two sets of curves corresponding to the water extraction, only the pH of the urine was adjusted. The most common trend noted in Figure 6-12 and Figure 6-13 was that the urine curves showed slightly better linearity than those of the water curves produced both with and without pH adjustment. Thus, these results indicate that both the pH of the matrix and type of matrix are critical factors affecting the linearity of the trace quantities of basic drugs. The linearity study was repeated using water as the matrix in order to validate all four of the SPME methods developed and optimized for the drugs in Yaba.

WATER	Precision(%RSD)	Linear Range(ng/mL)	LOD(pg/mL)	LOQ(pg/mL)	%Recovery	Accuracy(%Error)
Caffeine	11.60%	31 - 1000	5.21	14	101%	8.60%
Methamphetamine	9.12%	31 - 500	1.25	4.16	78%	22.60%
MDMA	11.66%	31 - 1000	0.62	2.08	96%	9.44%
Ketamine	11.39%	8 - 250	0.58	1.9	106%	10.36%
URINE pH 8.0	Precision(%RSD)	Linear Range(ng/mL)	LOD(pg/mL)	LOQ(pg/mL)	%Recovery	Accuracy(%Error)
Caffeine	6.87%	31 - 500	1.57	5.2	94%	7.07%
Methamphetamine	2.68%	31 - 500	2.71	9.03	90%	9.72%
MDMA	6.99%	31 - 1000	40	135	92%	8.49%
Ketamine	12%	8 - 250	2.94	9.81	72%	28.32%

Table 6-1 - Summary of Analytical Figures of Merit for all four drugs in Yaba

Caffeine

$y = 23.083x + 1012.7$
$R^2 = 0.9876$

Methamphetamine

$y = 7779.3x - 41302$
$R^2 = 0.9891$

MDMA

$y = 4572.7x - 352505$
$R^2 = 0.991$

Ketamine
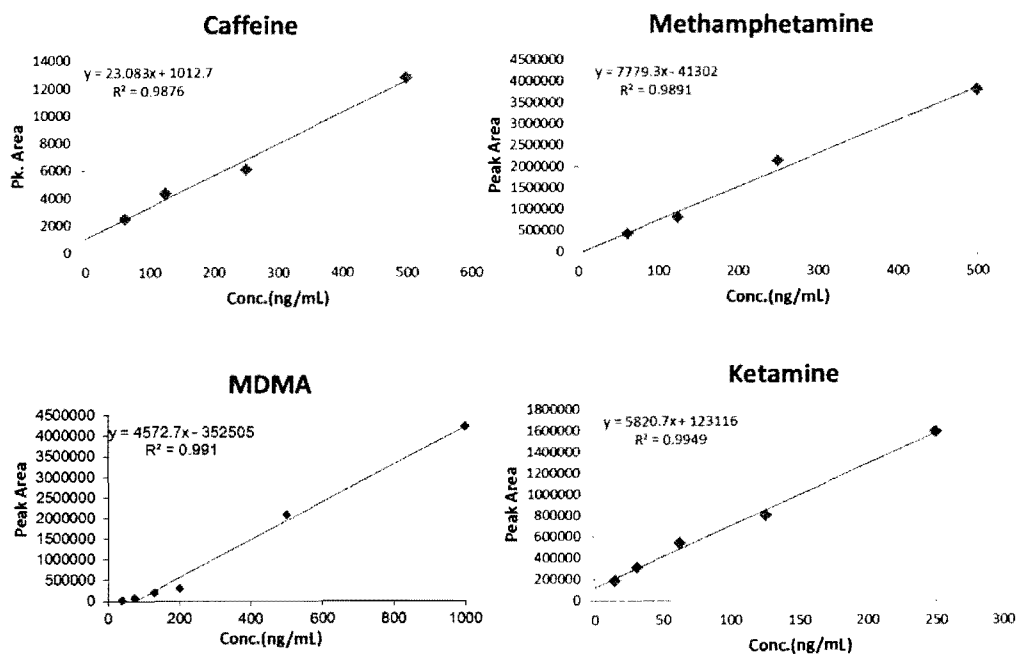
$y = 5820.7x + 123116$
$R^2 = 0.9949$

Figure 6- 12 - Comparison of Calibration Curves for all four drugs in Yaba extracted from water
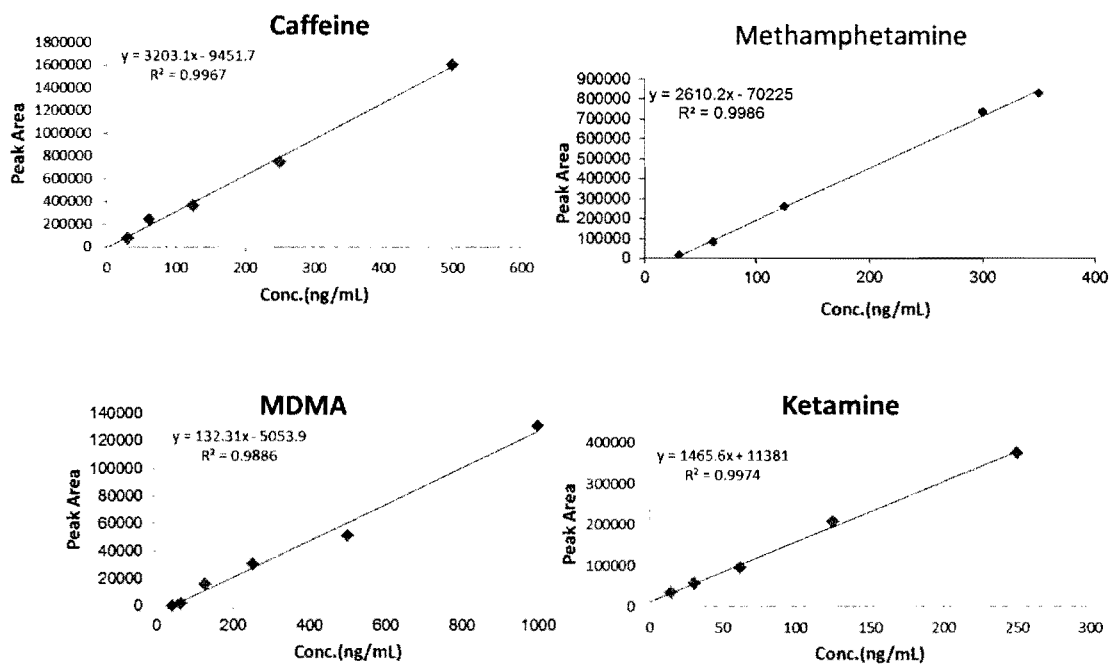
Figure 6-13 - Comparison of calibration curves for all four drugs in Yaba extracted from urine at pH 8.0

The range tested was the same range reported in both Tables 6-1 and 6-2 in which the calibration curves from the validation study showed slightly greater R^2 values and as well as smaller values for the %RSDs for the slopes between each segment on the curve. Therefore, the results showed that the linearity of all four drugs was repeatable and that all four SPME methods were valid.

6.3.4.2- Determination of the LOD and LOQ

The LOD and LOQ for each drug are reported in Table 6-1 and was determined using the IUPAC method[55]. The values were much lower than any values previously reported in the literature which was expected based on the high sensitivity and rapid scan rate of the ToFMS. However, the values for the %RSDs determined after performing the experiment three time were above 20% for all four drugs following extraction from both matrices indicating the LOD and LOQ values were not repeatable. This observation was not surprising since the LOD and LOQ values correspond to low S/N ratios which is subject to greater interference from the background noise. It should also be noted that the high sensitivity not only allows detection of analytes quantities in the low ppt range, it also detects the very weak signals from column bleed, septum contaminants, matrix contaminants, etc. This results in greater interference with the analyte signal at the LOD and LOQ. The data processing has a built-in peak deconvolution algorithm allowing it to eliminate most of the noise from the various contaminants, but often results in the elimination of the analyte signal at the LOD and LOQ as well as poor repeatability. This was a common limitation of the data processing software that was a frequent challenge observed during the determination of the LOD and LOQ of each drug discussed in this work. It must also be noted that this limitation of the software was independent of the extraction and instrumental conditions and was only corrected by adjusting the S/N and peak width thresholds in the data

WATER	Precision(%RSD)	Linear Range(ng/mL)	LOD(pg/mL)	LOQ(pg/mL)	%Recovery	Accuracy(%Error)
Caffeine	6.72%	31 -500	104	347	104%	11%
Methamphetamine	6.62%	31 - 250	0.15	0.5	98%	5.34%
MDMA	10.76%	75 - 500	0.29	0.98	90%	11%
Ketamine	2.38%	8 - 200	1.05	3.52	109%	16%

Table 6-2 – Summary of validated analytical figures of merit
for all four drugs in Yaba

processing method parameters. The LOD and LOQ study was repeated in order to validate the SPME methods developed and optimized for all four drugs in Yaba. The results are shown in Table 6-2 which noted to be lower than the LODs and LOQs reported in Table 6-1 with the exception of caffeine. However, these values were still within the low par per trillion range which was lower than the LODs and LOQs reported for the other drugs studied in this thesis. Thus, the results show not only are the SPME methods developed for all four drugs valid, but also that the LODs and LOQs were repeatable.

6.3.4.3- Recovery and Accuracy

The values determined for %Recovery and accuracy for each drug are also reported in Table 6-1. Accuracy was determined as the %error between the extracted and a spiked concentration of 125 ng/mL. The %Recovery of water was higher than that of urine indicating that the nature of the matrix is also contributes the matrix effects affecting the recovery of trace concentrations from each matrix. Therefore, since water is the simpler matrix, less interference was observed during extraction resulting in a slightly higher %recovery of caffeine compared to urine. This implies that the %error between the extracted concentration and the spiked concentration of each would be lower in water than urine indicating higher accuracy upon extraction of caffeine from the simpler matrix. However, the values in Table 6-1 show a slightly lower %error for the extraction of each drug from urine than water. Therefore, this not only further demonstrates that the pH of the matrix is a critical factor affecting the extraction of trace concentrations of drugs, but also that the nature of the matrix affects the accuracy of the extraction. The only exception noted for the trend observed in the accuracy of the drugs in Yaba was ketamine which showed a much lower recovery and higher %error following extraction from urine. It was suspected that was due to the close proximity of the pKa value to the adjusted pH of the urine resulting in greater

ionization of the neutral ketamine. As discussed previously, the ketamine standard used was the more stable salt form resulting in a lower pKa compared to the other drugs in Yaba and making the drug more resistant to pH adjustment of the matrix. This observation indicates that extraction of drugs in their salt form result in higher recoveries without the need for pH adjustment due to its increased stability. The accuracy study was repeated using water as the matrix in order to validate the SPME methods developed and optimized for all four drugs in Yaba. These results are shown in Table 6-2 which were noted to be similar to accuracy results reported in Table 6-1 indicating that all four SPME methods were repeatable.

6.3.4.4 – Precision of the Extraction Method

Precision was determined from %RSD calculated after three extractions of three samples spiked with 250 ng/mL each drug. The results are also shown in Table 6-1 and follow the same trend observed following the accuracy study. Thus, these results further demonstrate that pH of the matrix and the nature of matrix are critical factors affecting the extraction of trace quantities of basic drugs. The precision study was repeated at 31 ng/mL in order to determine if the extraction method was precise at a lower concentration which showed greater interference from the background noise. Although the results showed lower precision at the lower concentration, the %RSD for all four drugs was less than 20% indicating the SPME method was determined to precise. The precision study was repeated using water as the matrix in order to validate the SPME method. The results are shown in Table 6-2 which reflect the precision at the high concentration of 250 ng/mL and also show that are much lower than precision reported in 6-1 for the same concentration level. Further, the validation study also showed %RSD values less than 15% at the low levels for all four of the drugs in Yaba, with the exception of ketamine. However,

the %RSD for ketamine was less than 20% at the low level, indicating the SPME methods developed and optimized for all four drugs was repeatable.

6.4 – Analysis of Full Yaba Mixture Using Full-Factorial DOE

6.4.1 – Development and Optimization of the GCxGC-ToFMS Method

The initial instrumental method for the analysis of the full Yaba mixture was developed based on the results from the individual analysis each drug. The instrumental conditions used for the analysis of each drug were compiled and then combined in order to elute all four drugs spiked into water and urine samples using a single method yielding a run time of 30 minutes. The same temperature program conditions for ketamine was also used for the analysis of the full Yaba mixture because it covered the widest temperature range neccesary to elute all four drugs in single run. A temperature offset of 15°C was used since it was observed to yield the best orthogonal separation for the individual analysis of all four drugs. A modulation period of 6 seconds with a hot pulse time of 0.90 seconds was observed to maximize the orthogonal separation of each drug as well as minimize the amount of wraparound observed on the contour plot. The remaining instrumental conditions were previously described in Chapter 2. A contour plot of the full Yaba mixture extracted from urine is shown in Figure 6-14 in which the locations of each drug in Yaba have been identified on the plot along with the location of some of the major degradation products. The identity of each drug and degradation product was confirmed following comparison of the mass spectra of each drug in the mixture to its NIST Library mass spectrum. The clear separation of these compounds as well as the high response corresponding to each of four drugs demonstrates the orthogonal separation capability of the GCxGC and high sensitivity of the ToFMS.
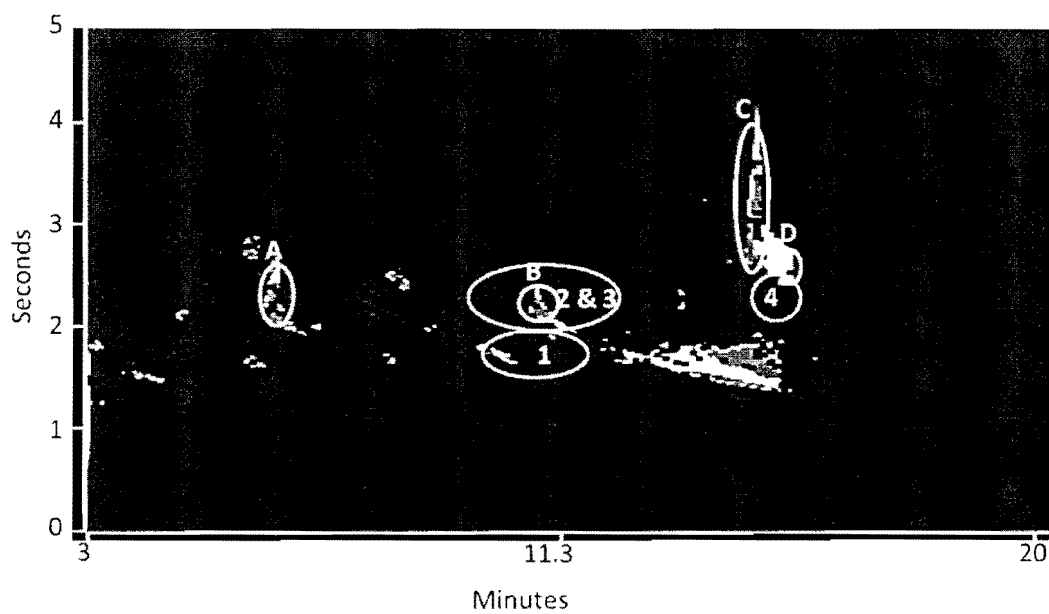
Figure 6-14 - GCxGC Contour Plot of TIC for Yaba extracted
from Urine at pH 8.0
Parent Drugs:
(A) 750 ppb Methamphetamine 6.25 min, 2.26 sec; (B) 500 ppb MDMA 10. 8 min, 2.32 sec
(C) 500 ppb Ketamine 14.6 min, 2.82 sec; (D) 31 ppb Caffeine 15 min, 2.47 sec
Degradation Products:
1) ephedrine and pseudoephedrine; 2) amphetamines; 3)3,4-methylenedioxy-Amphetamines
4) aziridines

6.4.2 – Development and Optimization of the SPME Method

The optimized SPME methods used for the analysis of each drug were compiled in order to develop the initial SPME for the extraction of the full Yaba mixture. Since the type of fiber, extraction temperature, incubation time, desorption time and temperature, and agitation speed were the same for all four drugs, the only parameter of the SPME method changed during optimization was the extraction time. The extraction time was optimized to be 40 minutes which was average of the optimized extraction times previously determined for each drug. A water sample spiked with 500 ng/mL of each drug was also used for the optimization of the SPME method. The SPME and GCxGC-ToFMS methods were repeated two more times in order to ensure repeatability.

6.4.3 – Comparison of the Yaba extracts from water and urine

A full-factorial DOE was used to extract the full Yaba mixture from both water and urine and was discussed in Chapter 2. The pH of *both* the water and the urine was adjusted to 8.0 since the greater intereferences expected to be present due to the interactions between the drugs in the Yaba mixtures. The precision and accuracy for each drug in the mixtures was determined which followed the same trend discussed above for the analysis of each individual drug. However, despite the pH adjustment of both matrices, all four drugs showed very poor precision and accuracy following three runs of the DOE in comparison to the precision and accuracy determined during the quantitative analysis of each drug above. It was suspected that competition between the drugs for absorption into the SPME fiber was occurring during extraction resulting in poor recoveries of each drug in the full mixture. Further, the identification of the degradation products shown in Figure 6-14 indicate interactions between the drugs in the mixture were prevalent which may have resulted in additional matrix effects resulting in poor precision. It was

also noted that the identity of the degradation products was dependent on the type of matrix from which Yaba was extracted thereby producing a unique profile of the drug mixture from water and urine. Tables 6-3 and 6-4 show the major degradation products identified from both matrices along with their base peaks and M^+ Ions.

The group 1 compounds are ephedrine and ephedrine related compounds which are often used as the starting material for the synthesis of methamphetamine[68,69,91,92]. The %peak area of the ephedrine related compounds was determined to be 3.50% indicating that these compounds were present at low levels. This is not surprising since the drugs used for this work were certified reference standards, however this demonstrates that the high acquisition rate and sensitivity of the ToFMS allows it to detect unique compounds that can be used to identify possible synthetic routes for illicit drugs. Group 2 compounds are known metabolites of methamphetamine which also stimulate the central nervous system(CNS) causing a large release of dopamine and adrenaline from the brain[68,69,92,93]. These compounds are often present following analysis of the drug regardless of its purity and regardless of the media from which it is extracted during the quantitative analysis of methamphetamine. The peak area% determined for these compounds was considerably low in comparison to methamphetamine, but provide a further demonstration of the capabilities of the ToFMS to detect trace levels of illicit drugs even when extracted from a complex matrix such as urine. It should be noted that these compounds made up a majority of the the degradation products detected in both matrices which was not surprising since the PDMS-DVB fiber used is known to be selective toward amphetamine compounds[12-14]. The compounds in Group 3 contain the 3,4-methylenedioxyphenyl moiety in their structure which is the defining structural feature of MDMA indicating that these compounds could be major

Group 1-Ephedrine compounds	Base peak	M$^+$ Ion
(-)-Ephedrine (m/z: 77, 105)	58	N/A
Norephedrine (m/z: 77, 91, 133, 134)	44	N/A
Norepinephrine (m/z: 65, 93, 169)	139	N/A
Pseudoephedrine, (+)- (m/z: 77, 105)	58	N/A
Group 2-Amphetamines	**Base peak**	**M$^+$ Ion**
3,5-Dimethoxyamphetamine (m/z: 152)	44	196
4-Benzyloxy-N-methylamphetamine (m/z: 91, 198)	58	N/A
Methamphetamine acetylated (m/z: 100)	58	191
N-Ethylamphetamine (m/z: 91, 148)	72	N/A
N-Formylmethamphetamine (m/z: 58, 118)	86	N/A
N-Methyl-4-ethoxyamphetamine (m/z: 122, 180)	58	N/A
Group 3-Methylenedioxyamphetamines	**Base peak**	**M$^+$ Ion**
MDEA (m/z: 135)	72	207
3,4-Methylenedioxyphenyl acetone (m/z: 43, 77)	135	178
3,4-Methylenedioxyphenylacetic acid (m/z: 45, 50, 77)	135	180
N-methyl-N-formyl-3,4-methylenedioxyamphetamine (m/z: 86, 135, 162, 221)	58	N/A
Group 4-Aziridines	**Base peak**	**M$^+$ Ion**
Aziridine, 1-methyl- (m/z: 15, 28)	42	57
Aziridine, 2,2,3,3-tetramethyl- (m/z: 42, 84)	58	99
Aziridine, 2-methyl- (m/z: 28)	42	57

Table 6-3 – Base Peaks, M$^+$ Ions, and major ions present in mass spectra of Major Metabolites and Degradation Products Identified following Yaba extraction from water at pH 8.0.

Group 1	Base Peak	M^+ Ion
(-)-Ephedrine (m/z: 77, 105)	58	N/A
Ephedrone (m/z: 77, 105)	58	N/A
Norephedrine (m/z: 77, 91, 133, 134)	44	N/A
Norepinephrine (m/z: 65, 93, 169)	139	N/A
Pseudoephedrine, (+)- (m/z: 77, 105)	58	N/A
Group 2	**Base Peak**	**M^+ Ion**
1,7-Dimethylxanthine (m/z: 68, 123)	180	180
Group 3	**Base Peak**	**M^+ Ion**
2,3-Dimethylamphetamine (m/z: 65, 77, 91, 119, 131)	44	163
3,5-Dimethylamphetamine (m/z: 152)	44	163
4-Benzyloxy-N-methylamphetamine (m/z: 91, 198)	58	N/A
Amphetamine (m/z: 91, 105)	44	N/A
Dextroamphetamine (m/z: 91, 105)	44	N/A
Hmma (m/z: 137, 164, 177)	58	195
N-Formylmethamphetamine (m/z: 58, 118)	86	N/A
N-Methyl-4-ethoxyamphetamine (m/z: 122, 180)	58	N/A
Group 4	**Base Peak**	**M^+ Ion**
N-methyl-N-formyl-3,4-methylendioxyamphetamine (m/z: 86, 135, 162, 221)	58	N/A
MDEA (m/z: 135)	72	207
Group 5	**Base Peak**	**M^+ Ion**
Aziridine, 1-(methoxymethyl)- (m/z: 42)	57	87
Aziridine, 1-methyl- (m/z: 15, 28)	42	57

Table 6-4 – Base Peaks, M^+ Ions, and major ions present in mass spectra of
 Major Metabolites and Degradation Products Identified
following Yaba extraction from urine at pH 8.0.

metabolites of MDMA. The %peak area for this Group was also very low further demonstrating the capability of the GCxGC-ToFMS to separate and detect low level compounds in complex mixtures. The compounds in Group 4 are compounds containing the aziridine moiety which are known impurities that form as a result of methamphetamine synthesis from pseudoephedrine[68, 69, 92, 93]. Thus, this further supports that the methamphetamine spiked into the samples was most likely synthesized using a method that required pseudoephedrine.

The critical difference between the degradation products observed in the water and urine extracts was the identification of the caffeine metabolite, 1,7-dimethylxanthine[104]. This compound was only observed in the urine extract and is listed as Group 2 in Table 6-4. This indicates that a more complex matrix, such as urine, is required to cause a very stable compound, like caffeine, to degrade. Therefore, the results of the DOE show that the type of matrix was more critical than the pH of the matrix for determining a unique chemical profile for each Yaba mixture. The DOE was repeated without adjusting the pH of either matrix in order to confirm this observation. As expected, the results showed much lower recoveries for each drug at both the high and low concentrations, but no change in the degradation products identified was observed between the extractions performed with or without pH adjustment. Therefore, the study demonstrated the pH of matrix primarily affects the recoveries of each drugs whereas the type of matrix affects the degradation products themselves. It should be noted that this was a preliminary study in which the urine and water samples were known to be blank and were spiked with known concentrations of each drug. Thus, the results in this study could be used as a control group for law enforcement personnel to develop a more detail impurity profile of Yaba.

6.5 – Conclusions

The overall results show that a simple SPME-GCxGC-ToFMS method was developed for the analysis of a full mixture of Yaba. During the quantitative analysis, it was noted that the pH of the matrix was indentified as the dominant source of matrix effects affecting the accuracy and precision for the extraction of each drug. However, the results of the DOE showed that additional matrix effects were caused by the interactions between the four drugs in Yaba as well as competition and selectivity of the PDMS-DVB SPME fiber resulted in poor recovery and poor precision for the extraction of each drug from the mixture. It was also noted that these affects were still prevalent despite adjusting the pH of both the water and urine to 8.0. Comparison of the extraction of Yaba from water and urine indicated that the nature of the matrix is also a critical factor affecting the types of degradation products formed and identified. This work demonstrates that orthogonal separation capability, high sensitivity, and rapid full-spectrum acquisition of the GCxGC-ToFMS can be very useful not only to thoroughly separate mixtures of multiple illicit drugs and also provide unique chemical profiles following their extraction from complex matrices.

CHAPTER 7 – ANALYSIS OF BP DEEPWATER HORIZON OIL SPILL SAMPLES

7.1 - Background

On April 20, 2010, there was an explosion at the BP Deepwater Horizon oil rig off the coast of the Gulf of Mexico due to improper installation of a blowout preventer[105]. The explosion broke the main pipe protruding into the oil well beneath the sea floor ultimately causing the rig to sink into the gulf on April 22, 2010[105-107]. Oil was released from the broken pipe in at average rate of 57,000 gallons/day and then traveled approximately 2 miles to the surface of water[107]. The difference in the density and the solubility between the salt water and the oil resulted in the separation of the oil as it traveled to the surface thereby making the Gulf of Mexico act like a giant extractor. This observation was confirmed following analysis of oil samples taken from five different depths in the Gulf of Mexico.

Crude oil is primarily made-up of two types of volatile compounds, straight and branched chain alkanes and polycyclic aromatic hydrocarbons(PAHs)[108]. The straight chain alkanes range in size from methane to triacontanes, alkanes with a chain of 40 carbons. Crude oil also contains a plethora of branched chain alkanes and cycloalkanes which are virtually impossible to distinguish without the use of GCxGC-ToFMS[109-112]. The PAHs range in size from benzene, with one aromatic ring to pyrenes and chrysene, with four aromatic rings. Several substituted PAHs with one through 4 substitutions on the base structure and various isomers of alkanes and PAHs are also contained in crude oil sample[110].

The density of pure water is 1.00 g/mL, the density of sea water is greater than that or pure water (around 1.02 g/mL to 1.29 g/mL) due to the high salt concentration. Therefore, some compounds

that have densities in the range stated above for salt water will sink in pure water, but float in sea water. Thus, since all the straight chain alkanes commonly found in crude oil have densities less than 1 g/mL, they will float on both pure water and sea water. PAHs with two or more aromatic rings sink in pure water and seawater because the density is greater than that of either pure water or sea water. This information provides an effective tool to characterize the oil at different depths based upon the most prevalent compounds detected.

7.2 – Purpose of the Experiment

The primary purpose of this study was to use the separating power of GCxGC-ToFMS to characterize oil samples taken from the Deepwater Horizon oil spill at different depths in the Gulf of Mexico. Comprehensive Two Dimensional Gas Chromatography(GCxGC) has been well-established in the literature as the preferred technique for the analysis of oil samples over GC-MS[110-113]. When GCxGC is coupled to ToFMS, it produces rapid identification of the multitude of peaks produced after a single separation thereby creating a unique chemical profile for each oil sample. The chemical profile of each sample were observed to be dependent upon the depth at which it was taken thereby allowing characterization of the oil as it traveled to the surface of the water.

7.3 Development and Optimization of the Instrumental Method

Prior to analysis using GCxGC-ToFMS, the oil sample was analyzed using GC-MS. The initial data from both instruments produced the typical "humpogram" that is observed for most petrochemical samples such as crude oil and gasoline. The GC-MS provided mass spectra for only the aliphatic series of alkanes ranging from C_8 to C_{24} whose mass spectra and retention

times were verified following comparison to a standard alkane mixture. It also provided mass

spectral data for PAHs such as naphthalene, anthracene, and phenanthrene. The GCxGC-ToFMS

also showed this same aliphatic alkane series up to C_{34} as well as a variety of other types of

hydrocarbons, the most notable being polyaromatic hydrocarbons(PAHs). The PAHs were both

substituted and unsubstituted ranging in size from one aromatic ring to five aromatic rings. Upon

further analysis of the GCxGC data, many of the compounds had similar retention times in both

dimensions and appeared to be coeluting. Therefore, in order to further separate these

compounds, the temperature programming rate was lowered from $10^{o}C/min$ to $5^{o}C/min$ which

increased the run time to approximately one hour.

The GCxGC plot did not show any wraparound following analysis of the oil sample using the

optimized temperature program; however, poor separation and a lack of retention in the second

dimension was observed between the aliphatic series of alkanes and the PAHs. The modulation

period was increased from 5 seconds to 8 seconds and hot pulse time was increased from 0.90

sec to 1.50 sec in order to increase the separation between the nonpolar and polar compounds in

the oil ultimately resulting in better retention on the second column. These changes provided a

slight improvement in the separation between the alkanes and the PAHs and a negligible

difference in the second dimension times following the analysis at the higher modulation period.

The temperature offset between the ovens was also increased to $15^{o}C$; however, no improvement

in the separation between the alkanes and PAHs was observed nor was any increase in retention

on the second column observed. Since neither increasing the modulation period, the hot pulse

time, nor the offset between the ovens had any significant effect on the separation or retention in

the second dimension, it was clear that a more polar stationary phase was necessary in order to increase both the separation and the retention in the second dimension.

The second column was changed to a DB-17 stationary phase that consists of 50% poly-phenyl-methylsiloxane and 50%-PDMS. The original second column was an RTX-200 stationary phase consisting of trifluoropropyl-methyl-polysiloxane. Figure 7-1 shows a contour plot for the TIC of a surface oil sample following separation using the DB-17 stationary phase. The high percentage of the phenyl polymer in the DB-17 phase significantly increases the polarity of the column, thereby resulting in increased pi-pi interactions between the PAH compounds and the phenyl groups of DB-17. This resulted in better overall retention of these compounds on the column.

7.4 Selection of the extraction solvent

The oil was extracted using a simple liquid-liquid extraction which is described in Chapter 2. During the development of the extraction method, dichloromethane and pentane were used to extract the hydrocarbon compounds from the oil samples. Both solvents are compatible with GC systems and are commonly used in GC analysis due to their high vapor pressure and low boiling points. The oil sample represented by contour plot shown in Figure 7-1 was extracted using dichloromethane. These plots show that a majority of the compounds extracted by the dichloromethane were PAHs instead of the alkanes. Pentane had the opposite effect when it was used as the extraction solvent. The difference in the selectivity observed between the two solvents is due to the difference in their solubility toward PAHs and alkanes. Pentane is non-polar making the alkanes in the oil samples more soluble allowing pentane to extract more of the alkanes than the PAHs. Dichloromethane is more polar making the PAHs in the oil sample more soluble in it resulting in dichloromethane extracting more PAHs than alkanes. Thus, the results
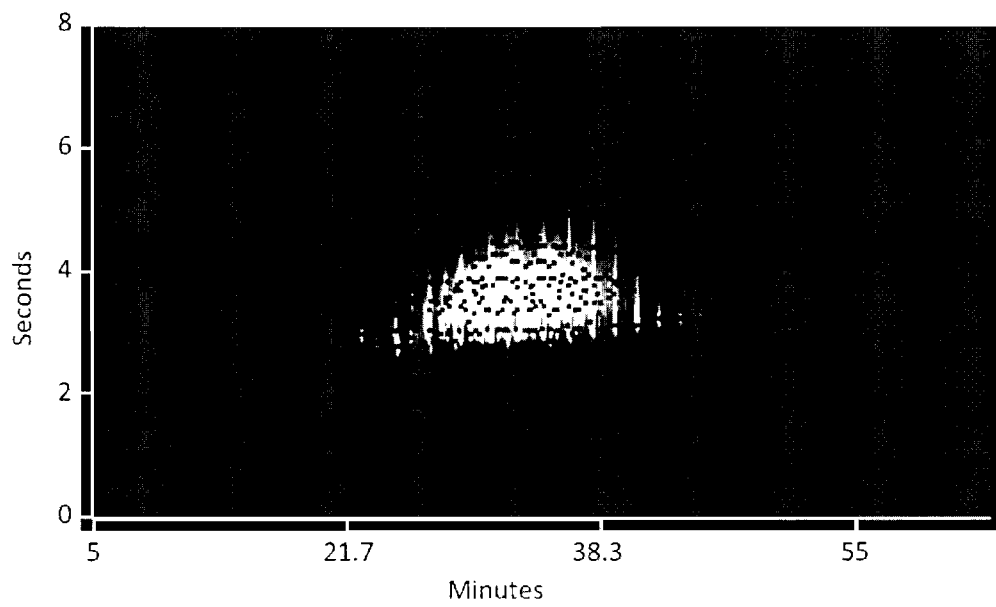
Figure 7-1 – GCxGC Contour Plot of surface oil sample
obtained under optimized conditions

show the dominant type of compounds extracted from the oil samples was dependent on their solubility in each solvent. While the chemical composition of the PAHs was distinctive in each oil sample whereas the alkanes showed little variation from sample to sample.

7.5 Deepwater Samples

Figure 7-2 shows the contour plots for the two deepwater oil samples analyzed. Figure 7-2A is the oil sample taken directly from the well located beneath the ocean floor. Figure 7-2B is the oil sample taken from the well head approximately 2 miles below the surface of the Gulf. Gaines and Frysinger describe a method to characterize an oil sample based on the peak area ratios determined for several key alkanes and PAHs usually prevalent in oil samples and was applied to the BP Oil Samples[109-112]. Figures 7-3 and 7-4 show the distribution of selected PAHs and alkanes based on the peak area ratios computed for the pre-spill and deepwater samples, respectively.

The distribution of the PAHs shown in Figures 7-3 and 7-4 indicate that chemical composition of the two deepwater oil samples are different from each other. The results show that the PAHs were generally higher in the pre-spill sample to the other deepwater sample. This indicates that these smaller PAHs are susceptible to degradation upon exposure to the sea water of the gulf resulting in a higher abundance of PAHs in the pre-spill sample than the other deepwater sample. The aromatic properties of these compounds make them very stable and resistant to weathering effects and degradation. Further, PAHs are more polar allowing them to be easily distinguished from other hydrocarbons present in petroleum products such as alkanes or cycloalkanes and give the oil samples a unique "fingerprint" that can be used to distinguish
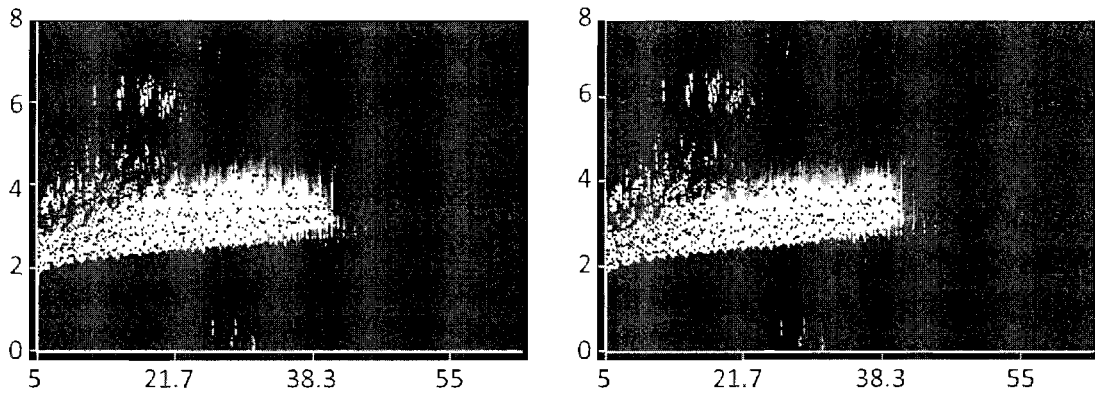
Figure 7-2 – GCxGC contour plots of pre-spill and deepwater
Oil samples where x-axis is time in minutes and y-axis is time
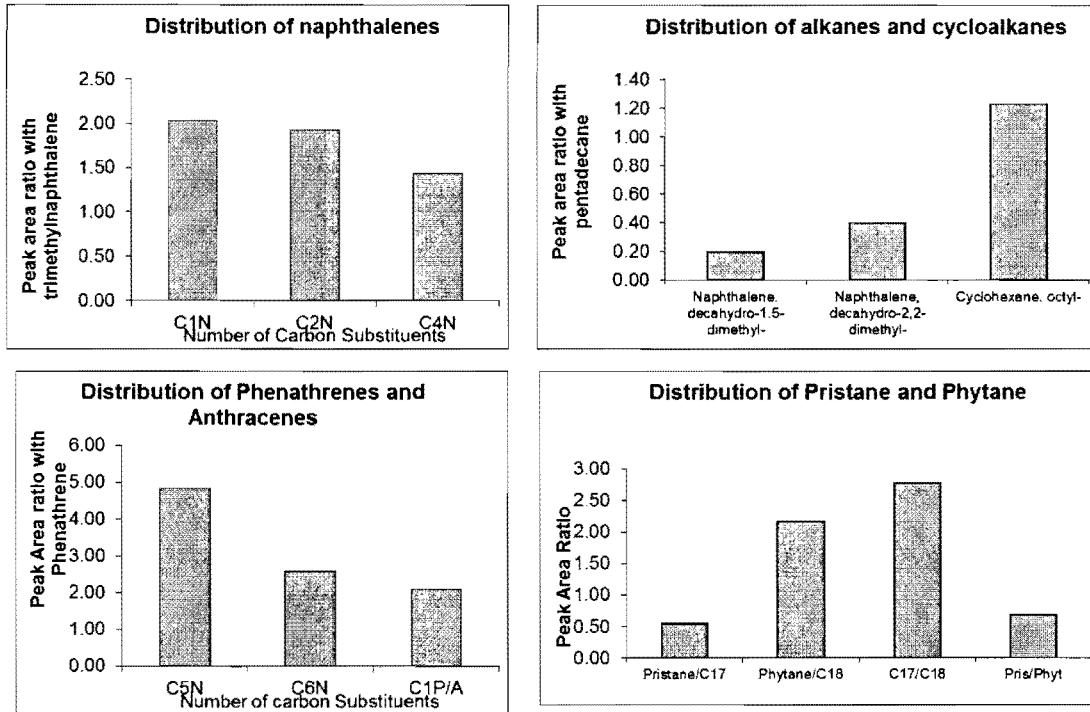In seconds: (A) Pre-spill Oil Sample; (B) Deepwater Oil Sample

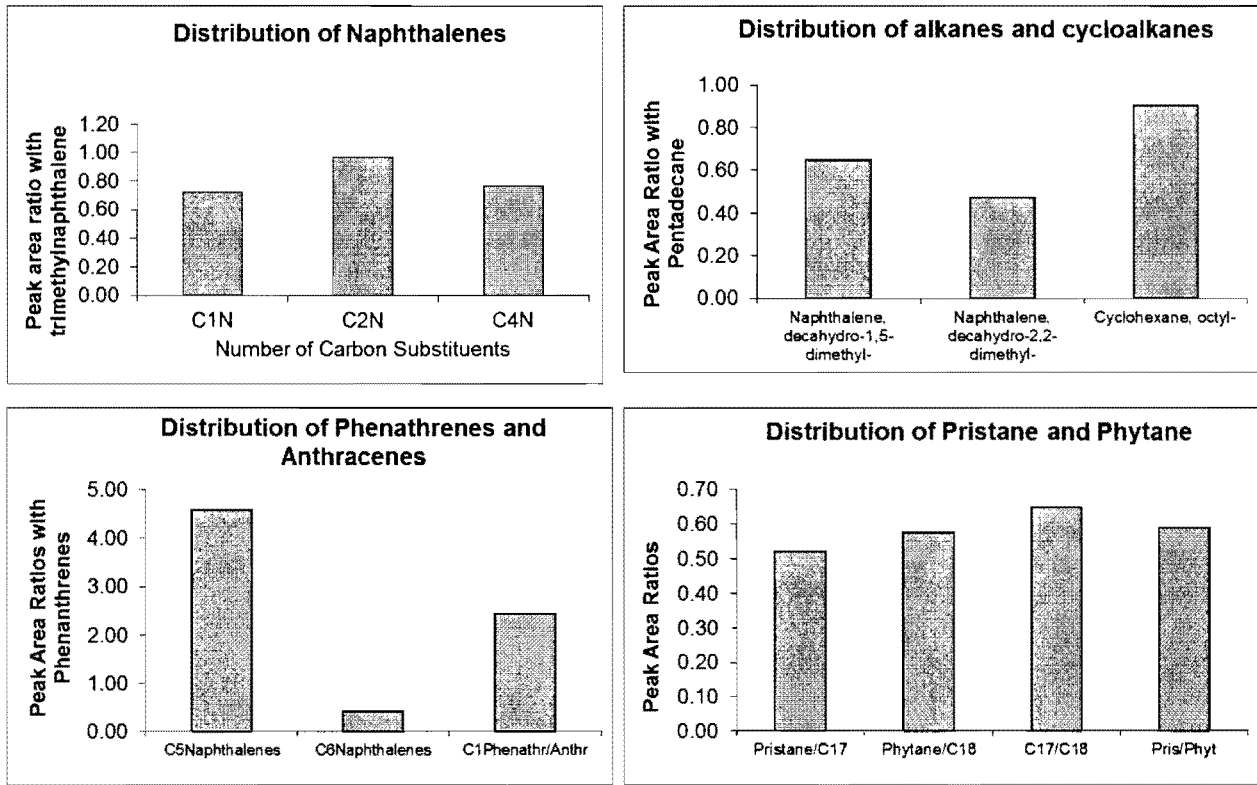Figure 7-3 Peak Area Ratios for Pre-Spill Sample

Figure 7-4 – Peak Area Ratios for Deepwater Oil Sample

between oil coming from different samples. The most notable of the substituted alkanes in the oil samples were pristane and phytane which are used as "biomarkers" since their ratio is specific to a particular source of oil. The data in Figure 7-3 and 7-4 showed a decrease in two biomarkers between the pre-spill sample and the deepwater sample. This is the same general trend observed with the PAHs indicating that these biomarkers degrade upon exposure to the sea water.

The observed differences in the PAHs and the alkanes between the two deepwater samples can be related to the difference between the density of the sea water and the components of the oil. Since the density of the sea water is greater than that of pure water allowing more organic substances in the oil to rise to the surface thereby resulting in a lower abundance for the PAHs and alkanes in the deepwater sample. Although the data suggest that the lower abundance may be due to degradation or to an increase in the volatility of the compounds, it may only be due to the difference in the density between the oil compounds and the seawater. This could provide an explanation for the marked difference between the chemical composition of the two deepwater samples shown in Figures 7-3 and 7-4.

7.6 Surface Samples

Two oil samples taken from the surface were also analyzed. One sample was taken from a brown colored mousse patty floating on the surface. The other sample was a slightly more viscous black colored sample collected closer to the coastline. Figure 7-5 shows the GCxGC contour plots for both of the surface samples. The intensity of the contour plot for the black surface sample is clearly higher than that of the brown mousse patty sample. A majority of the compound detected in the mousse patty are various PAHs. Further, the contour plot of the mousse patty shows a clearer separation between the PAHs and the alkanes in comparison to the black surface sample.
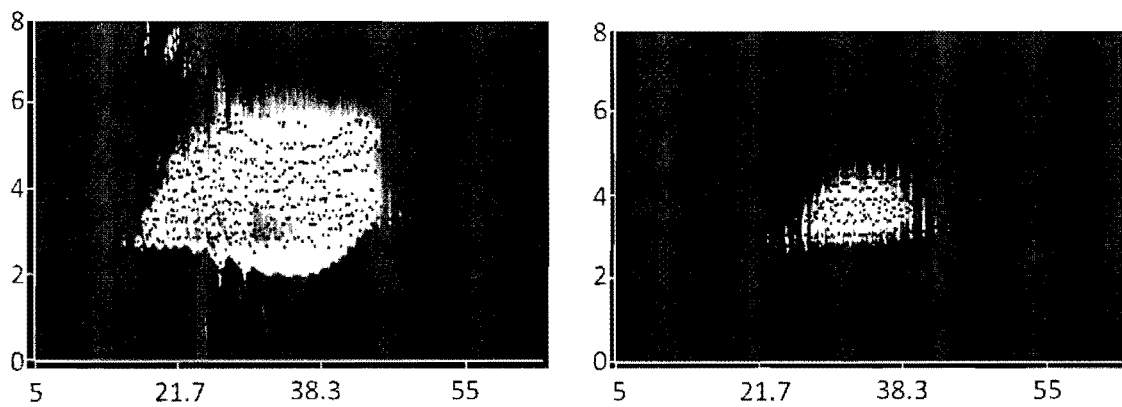
Figure 7-5 – GCxGC Contour Plots of Surface BP Oil Samples where
X-axis is in time in minutes and y-axis is time in seconds:
(A) Black Tar Surface Sample; (B) Mousse Patty Surface Sample

The same peak area ratio calculations performed on the two deepwater samples were also performed on the two surface samples. The results of the calculations for the brown samples are shown in Figures 7-6.

In comparison to the deepwater samples, the surface samples showed a higher abundance of the substituted naphthalenes and anthracenes/phenathrenes. The most notable observation was that these PAHs appeared to decrease in abundance between the pre-spill sample and deepwater sample, but then significantly increased in abundance between the deepwater sample and the mousse patty surface sample. The difference between the abundances of the PAHs between the pre-spill and deepwater samples was discussed in the previous section, however the same reasoning can be applied to the difference between the deepwater and mousse patty samples. Thus, since the PAHs studied are generally less dense than that of the seawater, they float to the surface resulting in a higher much abundance for these compounds in the mousse sample in comparison to the deepwater sample. This data further implies that the differences in the abundances of the PAHs between the deepwater and surface samples are due to the difference in the density between the seawater and the compounds in the oil. The same trend was observed between the deepwater and mousse patty surface samples for the alkanes and cycloalkanes, as well as for the two biomarkers, which further supports the conclusion that the difference between the abundance of the compounds in the oil is primarily due to the difference in density with the seawater.

The black tar surface sample was also analyzed using the same peak area ratio calculations used to analyze the previous samples. The results are shown in Figure 7-7. The PAHs and the alkanes appeared to decrease in their abundances between the two surface samples suggesting that they
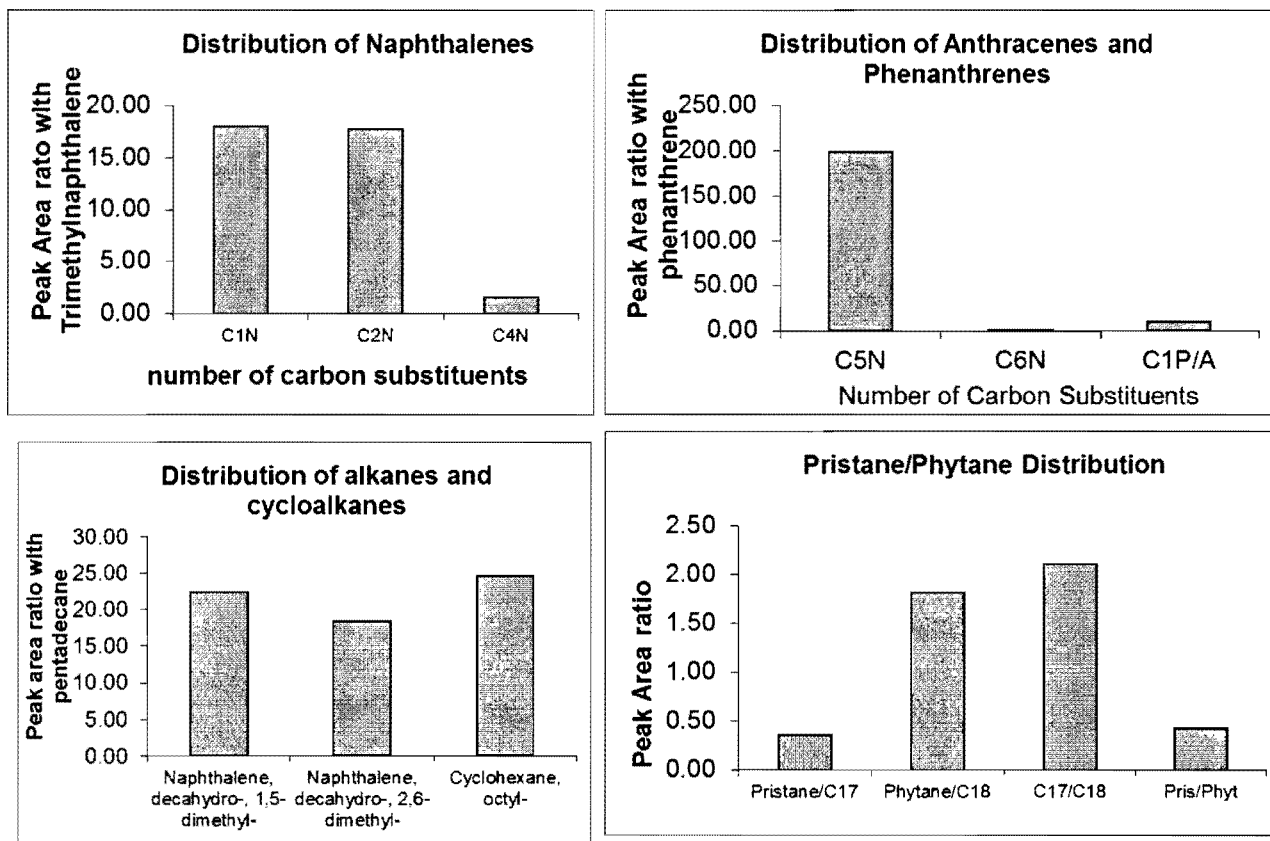
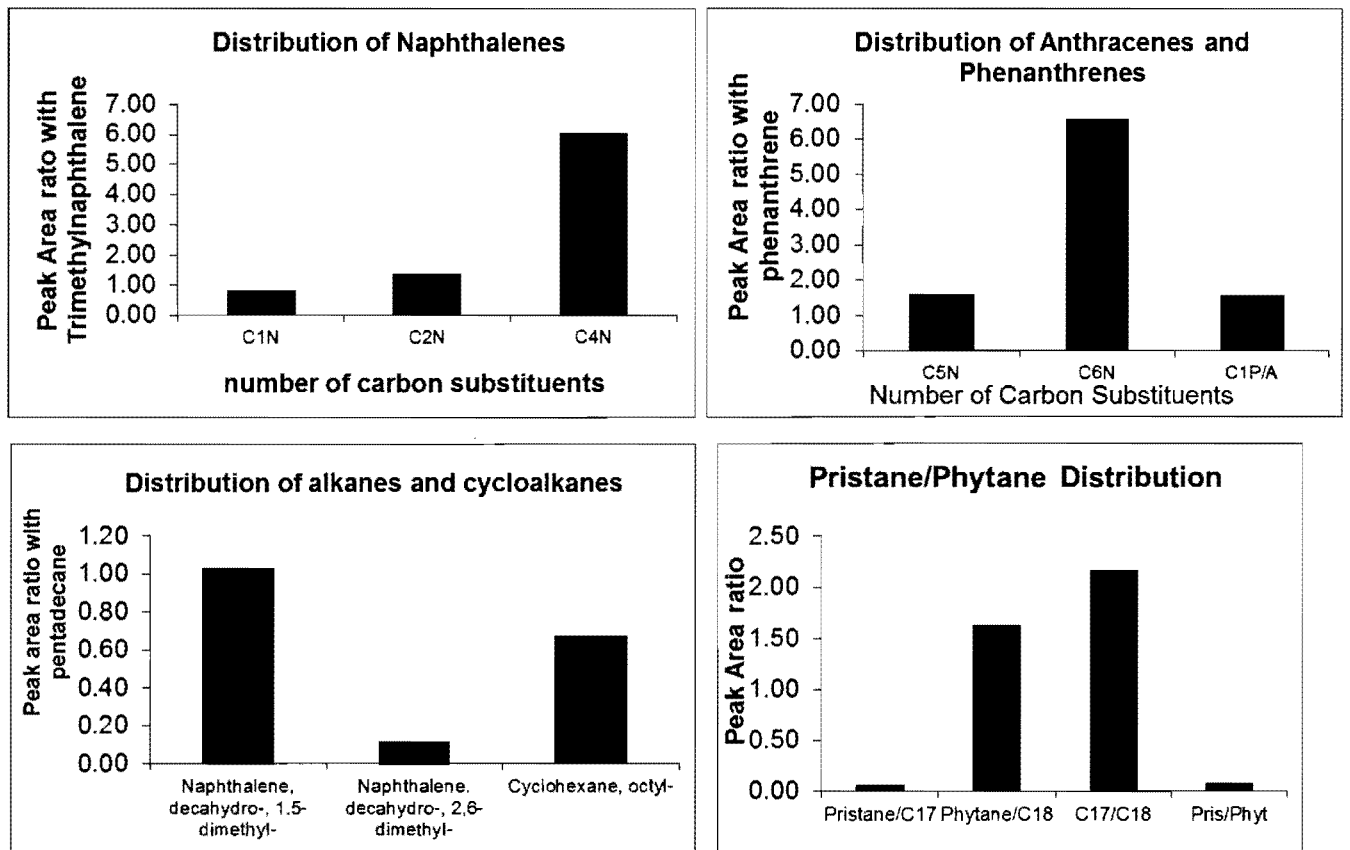Figure 7-6 –Peak Area Ratios of Mousse Patty Sample

Figure 7-7 – Peak Area Ratios for Black Tar Surface Sample

either degraded or evaporated as the oil drifted closer to the coastline. It was also observed that

the black tar surface sample contained more of the alkane isomers than any other sample

previously analyzed. This implies that a majority of the weathering effects and degradation occur

only after the oil has reached the surface. It was further observed that the separation between the

alkanes and the PAHs was more pronounced in the surface samples compared to the deepwater

sample and pre-spill sample. Therefore, the data suggest that the oil is separated into its larger

and smaller compounds as it travels through the seawater to the surface based on the difference

in density between the water and the compounds. They also suggest that a majority of the

weathering effects and degradation of the compounds in the oil occur only after the oil has

reached the surface.

7.7- Conclusions

This study demonstrates an effective environmental application for GCxGC-ToFMS, over GC-

MS. Not only do the results show that GCxGC is capable of producing thorough separations of

highly complex samples, but the incorporation of the ToFMS provides the identification of each

of each peak separated on the contour plots. Thus, this information was used to produce specific

chemical profiles for each of the oil samples samples. Figure 7-8 shows location of each of the

oil samples and its corresponding GCxGC contour plots. The results show that the deepwater

samples mainly contained larger, heavier hydrocarbons more dense than the seawater whereas

the surface oil samples contained smaller, lighter hydrocarbons less dense than the sea water.

The precise mechanism as to how the process occurs in not completely understood and must be

further studied; however, the data support this explanation providing an initial characterization of
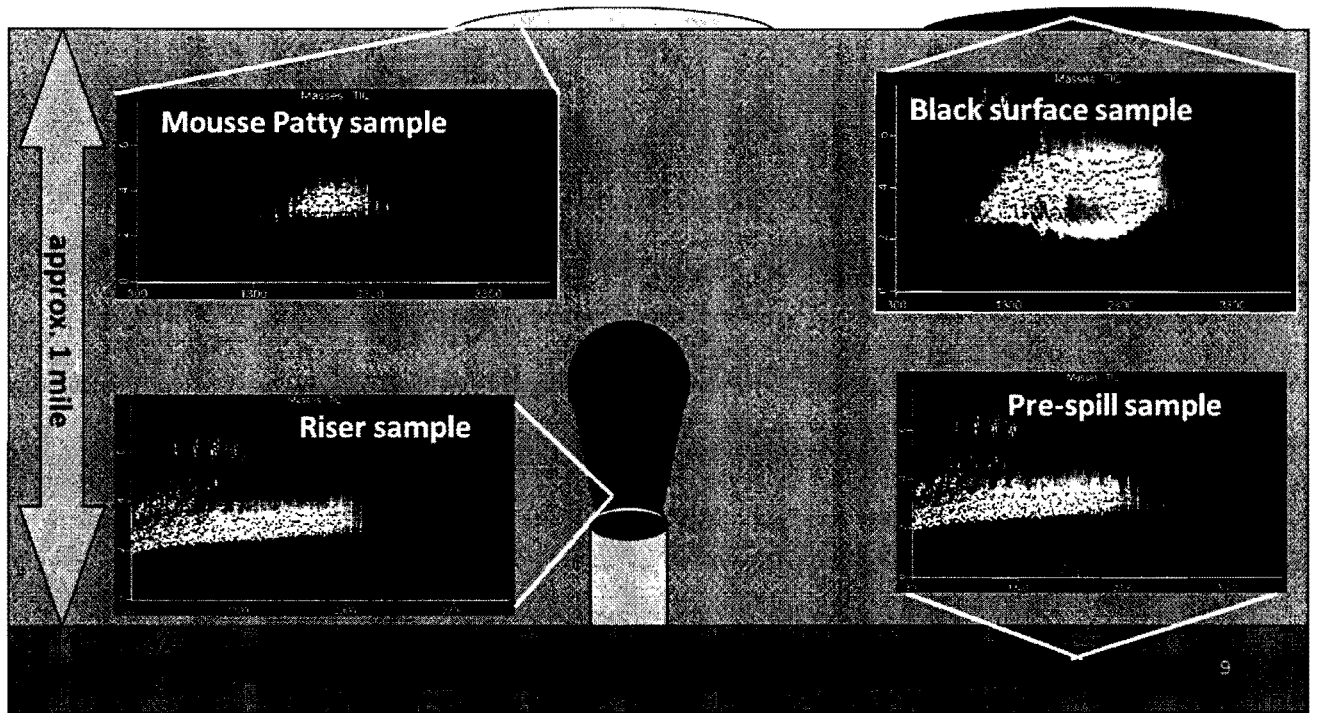
the oil as it travels to the surface.

Figure 7-8 Location and corresponding GCxGC contour plots of BP oil samples analyzed

CHAPTER 8 – CONCLUSIONS

Throughout the course of thesis, GCxGC-ToFMS was used as a powerful technique for the complete separation and analysis of various illicit drugs extracted from both water and urine. This is achieved by using two columns of different dimensions and with different stationary phases in order to separate complex samples by the respective vapor pressures and polarities of their volatile components. The use of a cryotrap modulator allow for the rapid comprehensive separation of the entire sample on both columns. The combined use of the two columns as well as the cryotrap modulator produces orthogonal separations for each sample which means that the sample undergoes independent separation on each column without interfering with each other. This more than doubles the peak capacity capable by any standard GC-MS system thereby allowing the separation of unique components in each sample during a single analysis. Some of these components include drug metabolites, various impurities, degradation products, and isomers. The ToFMS produces rapid, full-scan mass spectra for each of the peaks separated by the GCxGC allowing each peak to be identified resulting in complete chemical profile for each sample analyzed.

During the analysis of cocaine discussed in Chapter 4, GCxGC-ToFMS was compared to standard GC-MS and was shown to produce an LOD and LOQ that was at least one order of magnitude lower than the LOD and LOQ determined using GC-MS. During quantitative analysis of the drug, the high sensitivity of the ToFMS produced more linear calibration curves with less background noise, higher R^2 values, and less deviation in the slopes between adjacent points on the curves. Further, the orthogonal separation capability of the GCxGC enabled the identification of three major metabolites of cocaine that could not be detected using GC-MS following the exposure of a cocaine standard to typical laboratory conditions for three days. Therefore, the

analysis of cocaine showed that GCxGC-ToFMS can also be used as a forensic tool for the trace analysis of illicit drugs on surfaces.

In Chapter 3, the chromatographic performance of the second column in the GCxGC was analyzed using the Grob Test Mixture. Although the study showed the elution of all 12 of the Grob Mixture components, analysis of the retention factor, selectivity, and efficiency showed that the overall chromatographic performance was sacrificed in order to achieve rapid separation of samples on the second column. It was found that this behavior was mainly caused by the very high linear velocity of the carrier gas flowing through the second column. However, despite the low retention factors and low efficiencies determined for each of the 12 components, the selectivity determined for all 12 components was found to be between 1 and 2, indicating that the second column maintains selectivity despite the fast separation and high linear velocity of the carrier gas. The chromatographic performance of an ionic liquid stationary phase in the second column was also briefly studied in Chapter 3 as a possible candidate for the separation of the compounds in the Grob mixture. However, due to the poor values determined for the retention factors, selectivity, and efficiency as well as the inability of the ionic liquid to separate nitrogen containing compounds, it was determined to be unsuitable and was replaced with a more traditional stationary phase.

The initial analysis of cocaine and salvinorin A using GCxGC-ToFMS showed that technique was effective for trace analysis in that it yielded a lower LOD and LOQ as well as more linear calibration curves. However, it was observed that the accuracy and precision of the results showed some deviation following liquid-liquid extraction(LLE) of salvinorin A from both water

and urine as well as solid-liquid extraction of cocaine from the surface of money. Since this was determined to be related to the sample preparation techniques used, a variability study of the LLE method for salvinorin A from both matrices was performed. The results showed high deviation in both the recovery from sample to sample as well as in the extraction precision due to the tedious nature of the extraction method. The extraction was repeated using fully automated SPME and the results were compared to those obtained via LLE; these not only showed higher recoveries and much better extraction precision, but also yielded linear calibration curves for concentrations below 1 ppm as well as lower LOD values in the low ppb to high ppt range. Due to these results, it was concluded that SPME-GCxGC-ToFMS was the preferred method for the trace analysis of drugs extracted from biological matrices. SPME-GCxGC-ToFMS was repeated for the extraction of cocaine from both urine and water in order to confirm the effectiveness of SPME over LLE for trace analysis of other illicit drugs. The results also showed high recovery with minimal deviation between samples following extraction from both urine and water as well as good precision which was indicated by %RSD values that were determined to be less than 10%. The calibration curve following SPME of cocaine from both matrices also showed better linearity than the curve obtained for the non-extracted standard in which the concentration range plotted for cocaine was below 1 µg/mL. Although the curve following water extraction was much better than the curve following urine extraction due to the more complex nature of urine, the concentrations of cocaine plotted were well-below 1 µg/mL using SPME where the plot for the non-extracted standard obtained using liquid injection did detect cocaine at these same concentrations. Therefore, the results further support that SPME is the preferred technique for trace analysis of illicit drugs.

However, despite the high sensitivity of SPME, it was determined during the analysis of cocaine and the four drugs contained in Yaba that the critical factor affecting extraction of the drugs from both water and urine was the pH of the matrix. It was also observed that upon adjusting the pH of the matrix to be at least 2.0 pH units away from the pKa of each, the accuracy, precision, and linearity for the extraction of the drug greatly improved. Thus, this indicated that the pH of the matrix was the primary source of the matrix effects observed in both water and urine. However, during the validation studies for caffeine and cocaine, better results for accuracy, precision, and linearity were obtained when the pH of water was not adjusted indicating that the addition of a buffer to adjust the pH interfered with the adsorption of each drug onto the fiber even when the concentration of the buffer was reduced from 1.0M to 0.1M. This was not observed during the extraction of each drug from urine following proper pH adjustment indicating the adjusted pH prevents minimizes interferences from other components allowing the drug to be readily adsorbed onto the SPME fiber with better accuracy and precision. Thus, it was determined that the complexity or nature of the matrix is also a critical factor affecting the extraction of the drug.

The dependence on the nature of the matrix and the pH of the matrix when performing SPME was further confirmed from the results of the DOE performed for the analysis of the full Yaba mixture. As discussed in Chapter 6, the full Yaba mixture was extracted from water both with and without pH adjustment of the matrix to a pH of 8.0. The results showed better recovery and precision when pH adjustment was used. They showed a trend in which both the recovery and precision for each of the four drugs was slightly better when the drugs were present at the high concentration of 500 ng/mL. This trend was not observed nor was any trend observed for the results from the extraction conducted without pH adjustment of the matrix. Thus, these

observations further support the conclusion that the pH of the matrix is a critical factor affecting extraction. However, the results from the extraction of Yaba from urine also did not show any clear trend in the recovery or precision for the four drugs at either 500 ng/mL or 31 ng/mL despite adjusting the pH of the matrix to 8.0. Therefore, these results further support the conclusion that the nature of the matrix is also a critical factor affecting extraction. It is important to note that both of the critical factors affecting extraction were prevalent for both the analysis of the individual drugs as well as the analysis of drug mixtures despite the simplicity and higher sensitivity of SPME compared to LLE. Therefore, the properties of the matrix must be considered equally along with the properties of the analytes regardless of the extraction technique being performed.

Although it was determined the critical factors affecting the extractions of both the individual drugs and the drug mixtures were the same, the key difference between them were the values determined for the recovery and precision of each drug. It was noted in Chapter 6 that the recovery and precision of each drug extracted from the Yaba mixture using a single method was much worse than the recovery and precision of each drug extracted individually using a separate method. The reason was determined to be due to the interactions between the drugs themselves and between the drugs and the matrix resulting in competition between the drugs for adsorption onto the SPME fiber. These effects created greater interferences thereby increasing the matrix effects as well as severely affecting the accuracy and precision for the extraction. Although it was determined that both critical factors affecting extraction were present during the extraction of Yaba, the complexity of the matrix was more prevalent. It was concluded that the interactions between the drugs in Yaba resulted in the formation of drug metabolites and degradation

products following the extractions from both matrices. Since this observation was more prevalent following the urine extractions, it was determined that the complexity of the matrix was the greater factor affecting extractions of multiple drugs.

The metabolites and degradation products present in the Yaba mixtures demonstrate a key benefit of the orthogonal separations performed by the GCxGC as well as the high sensitivity and rapid, full scanning capability of the ToFMS. These two capabilities of the instrument were also demonstrated during the degradation of the cocaine standard and the analysis of salvinorin A in the leaves of the *S.divinorum* plant. Both of these analyses showed the presence of several key metabolites corresponding to each drug following analysis via GCxGC-ToFMS. It was found that the identification of these metabolites provides a unique chemical profile that can be used to build detailed impurity profiles for each drug. These impurity profiles can be used by forensic scientists as well as law enforcement officials to determine the route of synthesis, presence of cutting reagents, and even drug trafficking patterns over a specific geographical region. It should also be noted that the degradation study for cocaine was also performed using GC-MS, but only after three days did not detect a peak for any metabolite of the drug nor a peak for cocaine itself. It was therefore concluded that the data for cocaine, salvinorin A, and Yaba would not have been achieved, but due for the orthogonal separation capability of the GCxGC system used in conjunction with the high sensitivity and rapid scan capability of the ToFMS system.

The majority of this thesis has focused on forensic applications of GCxGC-ToFMS for both conventional and designer drugs. However, an environmental application of the instrument was demonstrated during the analysis of oil samples from the BP oil spill. It was discussed Chapter 8,

that the orthogonal separation capability of the GCxGC along with the capability of the ToFMS allowed the complete separation of oil samples as well as the identification of each peak detected in samples taken from various depths of the Gulf of Mexico. The results showed that specific patterns and compounds were present in each sample which were unique depending upon the location where each sample was taken. Thus, this established correspondence between each sample and the depth at which the sample was taken to allow their preliminary characterization. These results were observed to be superior to results obtained for the same samples using GC-MS which only showed the typical "humpogram" for a crude oil or petrochemical sample. The only discernible compounds identified were the homologues series of alkanes between decane and triacontane. The same "humpogram" was also produced following GCxGC analysis where not only was the same homologous series of alkanes observed, but also various branched chain and alkene isomers of the alkanes and various PAHs and substituted PAHs could also be identified. This not only further demonstrates the superior separation power of the GCxGC, but also demonstrates the versatility of the instrument for multiple applications.

However, despite the capabilities of SPME-GCxGC-ToFMS discussed throughout this thesis, the instrument does have some limitations. One of the major limitations of GCxGC-ToFMS was discussed in Chapter 3 during the evaluation of the chromatographic performance of the second column. It was concluded that the lack of retention and overall performance of the second column was primarily due to the high linear velocity of the carrier gas in the second column. It was also noted that smaller dimensions and the high linear velocity of the second column also result in an isothermal separation in the second dimension despite the use of a temperature

program. This is a clear demonstration of how good chromatographic performance inside the second column is sacrificed in order to achieve very fast separation within it.

The second limitation of the system was due to the peak integration algorithm and peak deconvolution algorithm used in the data processing software. This was found to be a frequent issue throughout the course of the research especially for the analysis of very low concentrations. It was also determined that this issue was related to both the high sensitivity of the ToFMS and the conditions of the modulator. It was previously discussed that the lack of accuracy and precision observed at very low concentrations was due to greater interference from the noise(e.g. column bleed, septum bleed, and matrix effects) resulting in low S/N ratio. Due to the high sensitivity of the ToFMS, peaks at these low concentrations were often detected. However, this feature of the ToFMS also detected all of the peaks corresponding to the noise. Although most of the noise was removed by the software using the peak deconvolution algorithm prior to processing the sample data, some of the noise was still present making challenging for the software to distinguish between the noise and the analyte peak which often resulted in no integration for the analyte peak during data processing. Another frequently observed challenge was that the analyte peak was often eliminated prior to integration during peak deconvolution of the raw data. This was especially prevalent during the determination and confirmation of the LOD and often resulted in poor precision. The peak deconvolution and the peak integration algorithm are based on the expected peak widths following separation in both the first and second dimension entered by the user. It must be noted that the expected peak widths entered do not correspond to a range of peak widths; they are specific numbers that the software compares to the actual peak widths of the first and second dimensions peaks appearing on the raw

chromatogram. Any raw peaks that do not match both of the expected peak widths are rejected by the software as actual peaks and the software does not assign a compound nor does it integrate the peak. Therefore, the software does not allow the user to perform manual integration, but it does allow the user to select a range of expected retention times for compounds in each sample. However, this cannot be considered manual integration since only the raw peaks whose actual retention times fall within the specified range entered for the expected retention times in both dimensions are assigned a compound name and integrated by the software.

The conditions of the modulator, specifically the modulation period, also affects both the peak integration and peak deconvolution algorithms of the data processing software. The modulation period determines the number of "slices", or second dimension peaks, comprising a single peak eluted in the first dimension. Ideally, each peak eluted in the first dimension should be a skewed Gaussian and should have the same peak width. In addition, the number of "slices" taken for each peak in the first dimension should be the same where their individual peak widths should also be the same. However, this rarely ever happens due to mass transfer effects occurring on both columns as well as variation in the linear velocity of the carrier gas as the sample passes from the first into the second column. As discussed in chapter 3, these effects are more prevalent in the second column due to the high linear velocity of the carrier gas and often result in a greater resistance to mass transfer between the analyte and the stationary phase and little retention in the second column. These effects result in peak width variations in the second dimension. Peak tailing was also prevalent for some compounds in the first dimension due to a lower linear velocity and lower resistance to mass transfer between the analyte and the non-polar stationary phase in comparison to the second column. This effect resulted in a variation in the number of

"slices" taken for these peaks during peak modulation. Therefore, the deviation between the expected and the actual second dimension peak widths compounded with the deviation between the modulation period and the actual number of "slices" resulted in both the incorrect grouping of "slices" and improper integration of the peaks during data processing. It was therefore concluded that the combined effects of the high sensitivity of the ToFMS and the modulation period cause limitations critical to the function of the peak deconvolution and the peak integration algorithms performed by the data processing software, thereby directly effecting the analytical figures of merit.

In addition to the limitations discussed above for the GCxGC-ToFMS system, two critical limitations were frequently observed when using SPME. One limitation was related to the conditioning requirements stated by the vendor. It was frequently observed that recovery following the first few extractions after conditioning a new fiber were lower than subsequent extractions using the same fiber regardless of the fiber coating. This indicates the requirements established by the vendor for conditioning of the fiber may not have been completely accurate. The purpose of conditioning the fiber is to ensure that the fiber is clean and free of any contaminants or impurities that may interfere with the adsorption of analytes onto the surface of the fiber. Thus, the low recovery and lack of precision of extraction analytes following initial use of a new fiber indicates that the some impurities and/or contaminants are present on the fiber despite application of the conditioning requirements. In order to maximize recover of a new fiber, the same samples would have to be run multiple times to ensure that the fiber was free of contaminants. However, it was observed that performing extraction of a blank vial followed by extraction of a vial containing only the matrix, but no analyte was necessary when using a new

fiber in order to maximize recovery of an analyte. It must also be noted that the fiber was baked out using the conditioning requirements of the vendor between each. Although this process was time consuming and may have shortened the lifetime of the fiber, it be became standard practice in order to maximize the performance of SPME. The second limitation when using SPME was observed following extraction of the full Yaba mixtures. As discussed in Chapter 6, the accuracy and precision for each of the drugs was much lower and was determined to be due to competition between the four drugs for adsorption onto the surface of the fiber. However, it was also observed that this competition also resulted in the formation and extraction of specific metabolites and degradation products for the amphetamines, that were not present when the drug was contained in a matrix by itself. Therefore, it was concluded that SPME could be not only be used for the screening of biological matrices for the presence of the parent drugs, but that it can also be used to produce a unique impurity profile of the drug when contained in a mixture with other drugs. It is believed that this information could greatly assist law enforcement officials and forensic scientists in establishing a database for new designer drugs and new drug mixtures.

However, despite the limitations of SPME-GCxGC-ToFMS, it has been demonstrated throughout this thesis to be the preferred technique for the trace analysis of drugs abuse. It is also been shown that it is also been an effective tool for characterizing complex samples and mixtures. This research provides an initial framework establishing SPME-GCxGC-ToFMS as an effective tool for both forensic and environmental applications which can benefit both law enforcement officials and environmental scientists. Therefore, the results presented in this thesis can be used to establish a detailed impurity profile for a complex designer drug such as Yaba or the specific chemical profile for a drug taken from a natural product such as sage. Further, this

research also provides some insight as to the chromatographic performance of the GCxGC-ToFMS system revealing some of the limitations of both the software used during data processing as well as the instrument itself. While SPME-GCxGC-ToFMS is a versatile technique with multiple applications, the theory and mechanism governing its operation must be studied and its limitations must be understood in order to exploit its advantages.

REFERENCES

[1] Wells, M. in; Mitra, S(Eds). Sample Preparation Techniques in Analytical Chemistry. John Wiley & Sons, Inc. New York. 2003. 37-57.

[2] Snow, N.; Slack, G. in; Grob, R.; Barry, E(Eds). Modern Practice of Gas Chromatography: 4th Ed. John Wiley & Sons, Inc. New York. 2004. 547-605.

[3] Lemke, T. Review of Organic Functional Groups: An Introduction to Medicinal Chemistry: 4th Ed. Lippincott, Williams, & Wilkins. New York. 2003.

[4] Fermi, E. Thermodynamics. Dover. 1937.

[5] Hill, Petrucci, McCreary, Perry. General Chemistry:4th Ed. Pearson Education, Ltd. 2005.

[6] Chen, Y.; Guo, Z.; Wang, X.; Qui, C. J. Chromatog. A. 2008. 1184: 191-219.

[7] Marchi, I.; Viette, V.; Badoud, F.; Fathi, M.; Saugy, M.; Rudaz, S.; Veuthey, J. J. Chromatog. A. 2010. 1217: 4071-4078.

[8] Suni, N.; Lindfors, P.; Laine, O.; Ostman, P. Ojanpara, I.; Koliacho, T.; Kauppita, T.; Kastanen, R. Anal. Chimica Acta. [In Press, Accepted Manuscript]. 2011.

[9] Franke, J.; DeZeeuw, R.; Wjisbeck, J. J. Pharmaco. Biomed. Anal. 1988. 6: 415-420.

[10] Dams, R.; Huestis, M.; Lambert, W.; Murphy, C. J. Am. Soc. Mass Spec. 2003. 14: 1290 -1294.

[11] McNair, H.; Miller, J. Basic Gas Chromatography: 2nd Ed. John Wiley and Sons, Inc. New York. 1998.

[12] de Koning, J.A. "Sample Preparation Techniques for Gas Chromatography". 2008. 34-40.

[13] Pawliszyn, J. SPME: Theory & Practice. Wiley-WCH. New York. 1997.

[14] Pawliszyn, J. Applications of SPME. Royal Society of Chemistry. 1999. 49-73.

[15] Stashenko, E.; Martinez, J. Trends in Anal. Chem. 2004. 23: 553-561.

[16] Junting, L.; Peng, C.; Suzuki, O. Forens. Sci. Internatl. 1998. 97: 93-100.

[17] Supelco SPME Fiber Conditioning, Operating Temperature Range, and pH Range Reccommendations. Bellefonte. 2011.

[18] Kataoka, H.; Saito, K. J. Pharmac. Biomed. Anal. 2011. 54: 926-950.

[19] Grob, R. in Grob, R.; Barry, E. Modern Practice of Gas Chromatography: 4th Ed. 2004. 25 -65.

[20] Martin, A.J.P.; Synge, R.L.M. *J. Biochem.* 1941. 35: 1358.

[21] James, A.T.; Martin, A.J.P. *J. Biochem.* 1952. 50: 679.

[22] van Deemter, J.; Zuiderweg, F.; Klinkenberg. *Chem. Engin.* 1956. 5: 271-289.

[23] Craig, L.; Post, O. *Anal. Chem.* 1949. 21: 500-504.

[24] Golay, M. *J. Chromatog. A.* 1965. 348: 316-320.

[25] van Es., A; Rijks, J.; Cramers, C.; Golay, M. *J. Chromatog. A.* 1990. 517: 143-159.

[26] Gas Chromatography Column Selection Guide. Agilent J&W. 2010.

[27] Snow, N. *J. Chem. Educ.* 1996. 73: 592-597.

[28] Giddings, J. *J. Chromatog. A.* 1962. 39: 569-573

[29] Grob, K. Split and Splitless Injection for Quantitation in Gas Chromatography: 4th Ed. Wiley-VCH. New York. 2001.

[30] "Aglient Split Liners". www.agilent.com

[31] Bartle, K.D. in Mondello, L.; Lewis, A.; Bartle, K.D. Multidimensional Chromatography. John Wiley & Sons, Inc. 2002. 6-12.

[32] Dalluge, J.; Beens, J.; Brinkman, U. *J. Chromatography A.* 2003. 1000: 69-108.

[33] Lewis, A.; Bartle, K.D. in Mondello, L.; Lewis, A.; Bartle, K.D. Multidimensional Chromatography. John Wiley & Sons, Inc. 2002. 47-72.

[34] Marriott, P. in Bartle, K.D. in Mondello, L.; Lewis, A.; Bartle, K.D. Multidimensional Chromatography. John Wiley & Sons, Inc. 2002. 77-106.

[35] Beens, J.; Brinkman, U. *Anal. Bioanal.Chem.* 2004. 378: 1939-1958.

[36] Pegasus 4D-GCxGC-ToFMS User's Manual. LECO Corp. 2008..

[37] Wilson, R.; Siegler, W.; Hoggard, J.; Fitz, B.; Nadeau, J.; Synovec, R. *J. Chromatog. A.* 2011. 218: 3130-3139.

[38] Firor, R.L. Agilent Application Note. Agilent Technologies. Wilmington, DE. 2011.

[39] Grob, Jr. K. *J. Chromatog. A.* 1983. 279: 225-232.

[40] Grob, Jr. K.; Grob, G.; Grob, K. *J. Chromatog. A.* 1978. 156: 1-20.

[41] Skoog, D.; Holler, F.; Nieman, T. Principles of Instrumental Analysis: 5th Ed.Principles of
   Instrumental Analysis: 5th Ed. Brooks-Coles-Thomson Learning. Chicago. 1998.

[42] de Hoffmann, E.; Stroobant, V. Mass Spectrometry: Principles and Applications: 3rd Ed.
   John Wiley and Sons, Inc. New York. 2007.

[43] Dass, C. Fundamentals of Contemporary Mass Spectrometry. John Wiley and Sons, Inc.
   New York. 2007. 17-20; 210-247.

[44] McLafferty, F. Turcek, F. Interpretation of Mass Spectra. University Science Books.
   Sausolito. 1998.

[45] Chapman, J. Practical Organic Mass Spectrometry: 2nd Ed. John Wiley & Sons, Inc. New
   York. 1993.

[46] Cotter, R. Time of Flight Mass Spectrometry. ACS Symposium. 1994.

[47] Song, S.; Marriott, P.; Wynne, P. *J. Chromatog A.* 2004. 1058: 223-232.

[48] Pugh, S.; Heim, Supplement to *J. Rapid Comm. Mass Spec.* 2009. S1-S9.

[49] Silva, Jr. A.; Pereira, H.; Casill, F.; Conceiano, F.; Neto, J. *J. Chromatog. A.* 2009. 1216:
   2913-2922.

[50] Christensen, K.; Jergensen, M.; Kotowska, D.; Petersen, K.; Kristiansen K.; Christensen,
   L. *Ethnopharmacology.* 2010. 132: 127-133.

[51] Ugland, H.; Krogh, M.; Rasmussen, K. *J. Pharmac.Biomed. Anal.* 1999. 19: 463-475

[52] Okajima, K.; Namera, N.; Yashiki, M.; Tsukue, I.; Kojima, T. *Forens. Sci. Internatl.* 2001.
   116: 15-22.

[53] Staerk, U.; Kulpmann, W.; *J. Chromatog. B: Biomed. Sci. Appl.* 2000. 745: 399-411.

[54] Gentili, S.; Torressi, A.; Marsili, R.; Chiarotti, M.; Macchia, T. *J. Chromatog. B.* 2002.
   780: 183-192.

[55] Long, G.; Winefordner, J. *Anal. Chem.*1983. 55: 712A-724A.

[56] Yao, C.; Anderson, J. *J. Chromatog. A.* 2009. 1216: 1658-1712.

[57] Petersen, R. *NIDA Research Monographs.* 1977. 13: 17-34.

[58] Fox, S. Human Physiology: 6th Ed. WCB-McGraw Hill. Boston. 1999. 197-198.

[59] Peterson, K.; Logan, B.; Christian, G. *Forens. Sci. Internatl.* 1995. 73: 183-196.

[60] Lin, S.; Walsh, S.; Moody, D.; Foltz, R. *Anal. Chem.* 2003. 75: 4335-4340.

[61] Ebejer, K.; Lloyd, G.; Berenton, R.; Carter, J.; Sleeman, R. *Forens. Sci. Internatl.* 2007. 171: 165-170.

[62] Esteve-Turrilla, F.; Armenta, S.; Moros, J.; Garrigues, S.; Pastor, A.; de la Guardia, M. *J. Chromatog. A.* 2005. 1065: 321-325.

[63] Armenta, D.; de la Guardia, M. *Trends in Anal. Chem.* 2008. 27: 344-351.

[64] Jenkins, A. *Forens. Sci. Internatl.* 2001. 121: 189-193.

[65] Carter, J.; Sleeman, R.; Parry, J. *Forens. Sci. Internatl.* 2003. 132: 106-112.

[66] Cole, M. Analysis of Controlled Substances. John Wiley & Sons, Inc. New York. 2003.

[67] Buchanan, J.; Brown, C. *Med. Toxicol. Adv. Drug Exp.* 1988. 3:1-17.

[68] Miller, M.; Kovel, N. *NIDA Research Monographs.* 1991. 115: 1-136.

[69] Lee, J.; Han, E.; Lee, S.; Kim, E.; Park, Y.; Lin, M.; Chang, M.; Park, J. *Forens. Sci. Internatl.* 2006. 161: 209-215.

[70] Barnes, B.; Snow, N. *J Chromatogr A.* 2012: 1226: 110-115.

[71] Prizinzano, T. *Life Sciences.* 2005. 78: 527-531.

[72] Gonzales, D.; Riba, J.; Bouso, J.; Gomez-Jacobs, G.; Barbanoj, M. *Drug & Alcohol Dep.* 2006. 85: 157-162.

[73] Giroud, C.; Felber, F.; Augsberger, M.; Horisberger, B.; Rivier, L.; Mangin, P. *Forens. Sci. Internatl.* 2000. 112: 143-150.

[74] Lozama, A.; Prizinzano, T. *Bioorg. & Med. Chem. Lett.* 2009. [Article in press]

[75] Tsujikawa, K.; Kuwayama, K.; Miyaguchi, M.; Kanamori, T.; Iwata, Y.; Inoue, H. *Xenobiotica.* 2004. 39: 391-398.

[76] Hagiwara, H.; Suka, Y.; Nojima, T.; Hoshi, T.; Suzuki, T. *Tetrahedron.* 2009. 65: 4820 -4825.

[77] Yan, F.; Roth, B. *Life Sciences.* 2004. 75: 2615-2619.

[78] Jermain, J.; Evans, H. *J. Forens. Sci.* 2009. 54: 612-616.

[79] Schmidt, M.; Prizinzano, T.; Tidgewell, K.; Harding, W.; Butelman, E.; Kreek, M.; Murry, D. *J. Chromatog. B.* 2005. 818: 221.

[80] Pichini, S.; Abandanes, S.; Farre, M.; Pellegrini, M.; Marhei, E.; Pacifici, R.; de la Torre, R.; Zuccaro, P. *Rapid Comm. In Mass Spec.* 2005. 19: 1649.

[81] Elidi, M.; Eidi, A.; Bahar, M. *Nutrition.* 2006. 22: 321-326.

[82] USDA Plant Profile. "Salvia dorii". www.plants.usda.gov

[83] Petit, G.; Klinger, H.; Jorgensen, N.; Occlowitz, J. *Phytochemistry.* 1966. 5: 301-309.

[84] US Army FM 3-11.9. Potential Military Chemical/Biological Agents and Compounds. Department of the Army. 1990. 27-28.

[85] Baer, A.; Holstege, C. in Wexler, P. Encyclopedia of Toxicology(2nd Ed). Elsevier, Inc. New York. 2005: 211-212.

[86] Chandra, S.; Mehendale, H. in Wexler, P. Encyclopedia of Toxicology(2nd Ed.) Elsevier, Inc. New York. 2005: 211-212.

[87] Substance Abuse Safety Newsletter. "Yaba-The New Street Buzz". July 2009.

[88] Kuwayama, K.; Inoue, H.; Kanamori, T.; Tsujikawa, K.; Hiyaguchi, H.; Iwata, Y.; Miyauchi, S.; Kumo, N.; Kishi, T. *Forens. Sci. Internatl.* 2007. 170: 183-188.

[89] Bialer, P. *Psych. In the Mentally Ill.* 2002. 25: 231-243.

[90] Maurer, H.; Bickboeller-Friedrich, J.; Kraemer, T.; Peters, F. *Toxicol. Letters.* 2000. 112: 133-142.

[91] Fisone, G.; Borgkvist, A.; Usiello, A. *Cell. Molec. Life Sci.* 2004. 61: 857-872.

[92] Volkow, N. *NIDA Research Report Series.* 1998. 1-8.

[93] Carn, M. "Methamphetamine: Intoxication, Detoxification, Withdrawal, and Treatment." Methamphetamine Summitt. 2005.

[94] Cheng, J.; Chan, M.; Chan, T.; Hung, M. *Forens. Sci. Internatl.* 2006. 162: 87-94.

[95] Lyles, J.; Cadet, J. *Brain Research Reviews.* 2003. 42: 155-168.

[96] Lowry, W.; Garriott, J. Forensic Toxicology. Plenum Press. New York. 1978.

[97] www.erowid.org/chemicals/ket/ket_timeline.php

[98] Smith, K.; Larive, L.; Romanelli, F. *Am. J. Health-Sys. Pharma.* 2002. 59:1067-1076.

[99] Herman, B.; Vocci, F.; Bridge, P. *Neuropsychopharmacology*. 1995. 13: 269-293.

[100] Eschotado, A.; Symington, K. A Brief History of Drugs from the Stone Age to the Stoned Age. Park Street Press. 1999.

[101] Wang, Y.; Lau, C. *Pharamco. Biochem. & Behav.*1998. 60: 271-278.

[102] Osgood, M.; Ocorr, K.; Nelson, D. Lehninger's Principles of Biochemistry. Macmillian. 2008.

[103] Kuribara, H. *Life S ciences*. 1994. 55: 933-940.

[104] Chilakapati, J.; Mehendale, H. in Wexler, P. Encyclopedia of Toxicology(2nd Ed). Elsevier, Inc. New York. 2005:205-207.

[105] Deep Water Horizon Accident Investigation Report. BP Executive Summary. 2010.

[106] USCG Deep Water Horizon Investigation Report Review. 2011.

[107] "The Amount and Fate of Oil." Draft of National Commission on BP Deep Water Horizon Oil Spill & Offshore Drilling. 2011

[108] Appendix 6A. Components of Crude Oil and Refined Products. www.epa.gov/region6/6en/xp/longhorn_nepa/lppapp6a.pdf

[109] Probstein, R.; Hicks, R. Synthetic Fuels. Dover Publication, Inc. Mineda. 2006. 309-327.

[110] Gaines, R.; Frysinger, G.; Hendrick-Smith, M.; Stuart, J. *Environ. Sci. Technol.* 1999. 33: 2106-2112.

[111] Reddy, C.; Eglinton, T.; Hounshell, A.; White, M.; Xu, L.; Gaines, R.; Frysinger, G. *Environ. Sci. Technol.* 2002. 36: 4754-4760.

[112] Frysinger, G.; Gaines, R.; Xu, L.; Reddy, C. *Environ. Sci. Technol.* 2003. 37: 1653-1662.

[113] Van De Weghe, H.; Vanermen, G.; Gemoets, J.; Lockman, R.; Bertels, D. *J. Chromatog. A.* 2006. 1137: 91-100.